

Monofunctional and dendritic Schiff base (N, N') ruthenium carbene complexes and (N, O) related ruthenium complexes: Synthesis, characterization and their catalytic activity in olefin metathesis reactions.

By

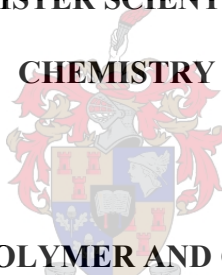
Yolanda Tancu

DISSERTATION

Submitted in fulfilment of the requirements for the degree

MAGISTER SCIENTIAE in

CHEMISTRY



**DEPARTMENT OF POLYMER AND CHEMICAL SCIENCE
STELLENBOSCH UNIVERSITY**

Supervisor: S.F Mapolie

December 2010

DECLARATION

I declare that the thesis titled *Monofunctional and dendritic Schiff base (N, N') ruthenium carbene complexes and (N, O) related ruthenium complexes: Synthesis, characterization and their catalytic activity in olefin metathesis reactions*, is my original study (work), and it has never been presented in any form at any other research group before. All the information sources that are used or quoted in this study have been acknowledged by means of complete references.

Name: Yolanda Tancu

Signature:.....

Date:

Copyright © 2010 Stellenbosch University

All rights reserved

ABSTRACT

The aim of the project was to synthesize ruthenium carbene complexes active in olefin metathesis reactions. Several ruthenium based olefin metathesis catalysts were synthesized. These complexes included the Grubbs-type complexes with the formula: $[\text{PCy}_3(\text{Cl})_2(\text{L})\text{Ru}(\text{CHPh})]$ where L is the 4-imino pyridine ligand. The other type was the $[p\text{-cymene}(\text{Cl})\text{Ru}(\text{L})]$ where L is the salicylaldimine ligand. Monofunctional as well as dendritic ligands were synthesized. Both the monofunctional and dendritic ligands and their complexes were fully characterized using a series of spectroscopic techniques and microanalysis. The *p*-cymene salicylaldimine ruthenium complexes were also analyzed for their thermal stability using TG.

The modified Grubbs-type complexes were tested for the self metathesis of 1-octene and in the ring-closing metathesis of diethyl diallylmalonate with some mononuclear complexes. The stability of the modified Grubbs G1 complexes in solution was monitored using ^1H NMR spectroscopy. The mononuclear **C1** $[\text{PCy}_3(\text{Cl})_2(\text{L})\text{Ru}(\text{CHPh})]$ where L is the 4-iminopropyl pyridine, was used as a model complex to study the stability as the dendritic complexes have low solubility in NMR solvents. **C1** was found to be highly unstable in solution and decomposed due to hydrolysis of both the carbene functionality and the imine group. This behavior is believed to be the major reason for the low activity these types of complexes portray. These catalytic reactions were performed without the use of the solvent and carried out under ambient conditions.

The *p*-cymene chloro ruthenium salicylaldimine complexes **C10** and **C12** were found to polymerize norbornene in ring-opening metathesis polymerization reactions. This catalytic reaction was facilitated by the use of a co-catalyst, *viz.* trimethylsilyldiazomethane (TMSD). The polynorbornenes formed were characterized by ^1H NMR, IR spectroscopy and GPC. They were found to be polydispersed due to an uncontrolled polymerization process.

OPSOMMING

The aim of the project was to synthesize ruthenium carbene complexes active in olefin metathesis reactions. Several ruthenium based olefin metathesis catalysts were synthesized. These complexes included the Grubbs-type complexes with the formula: $[\text{PCy}_3(\text{Cl})_2(\text{L})\text{Ru}(\text{CHPh})]$ where L is the 4-imino pyridine ligand. The other type was the $[p\text{-cymene}(\text{Cl})\text{Ru}(\text{L})]$ where L is the salicylaldimine ligand. Monofunctional as well as dendritic ligands were synthesized. Both the monofunctional and dendritic ligands and their complexes were fully characterized using a series of spectroscopic techniques and microanalysis. The *p*-cymene salicylaldimine ruthenium complexes were also analyzed for their thermal stability using TG.

The modified Grubbs-type complexes were tested for the self metathesis of 1-octene and in the ring-closing metathesis of diethyl diallylmalonate with some mononuclear complexes. The stability of the modified Grubbs G1 complexes in solution was monitored using ^1H NMR spectroscopy. The mononuclear **C1** $[\text{PCy}_3(\text{Cl})_2(\text{L})\text{Ru}(\text{CHPh})]$ where L is the 4-iminopropyl pyridine, was used as a model complex to study the stability as the dendritic complexes have low solubility in NMR solvents. **C1** was found to be highly unstable in solution and decomposed due to hydrolysis of both the carbene functionality and the imine group. This behavior is believed to be the major reason for the low activity these types of complexes portray. These catalytic reactions were performed without the use of the solvent and carried out under ambient conditions.

The *p*-cymene chloro ruthenium salicylaldimine complexes **C10** and **C12** were found to polymerize norbornene in ring-opening metathesis polymerization reactions. This catalytic reaction was facilitated by the use of a co-catalyst, *viz.* trimethylsilyldiazomethane (TMSD). The polynorbornenes formed were characterized by ^1H NMR, IR spectroscopy and GPC. They were found to be polydispersed due to an uncontrolled polymerization process.

ACKNOWLEDGEMENTS

To the Heavenly Father for his mercy and glory in protecting and loving me always. He knows the better and worst of me. I thank Him for the strength He has given me to endure whatever comes my way.

I also dedicate this work to my family for the ultimate support they gave me throughout my studies. Without your support, I would not have done this. To my loving mother, you are my rock.

To the organometallic research group lead by Prof. S.F. Mapolie, thank you guys for the suggestions and discussions we had. I have learnt a lot from each and everyone of you. A special thanks to Prof for his supervision and moral support. You have given me an opportunity to grow as a young scientist especially in handling synthetic work, the challenges it brings and how to overcome them.

Stellenbosch University has given me a chance to make use of its high technology equipment that has assisted me in my studies. A special thanks to the CAF group for their analytical techniques is due.

Last but not least, SASOL for financial support. Dr. Elzet Grobler, my Sasol mentor who has supported, inspired and dedicated her time in trying to make sure my interests were met. Thank you very much for your discussions, I really appreciated each and everyone of them.

CONFERENCE CONTRIBUTIONS

Poster presentation:

Yolanda Tancu and Selwyn Mapolie

Synthesis of Monomeric and Dendrimeric Schiff Base Ruthenium Carbene Complexes.

Cape Organometallic Symposium, Cape Town, South Africa, 2008.

Poster presentation:

Yolanda Tancu and Selwyn Mapolie

Dendrimeric Schiff Base Ruthenium Carbene Complexes: Application in Olefin Metathesis catalysis.

Catalysis Society of South Africa, Rawsonville, South Africa, 2009.

TABLE OF CONTENTS

Declaration		II
Abstract		III
Opsommig		IV
Acknowledgements		V
Conference Contributions		VI
List of Abbreviations		VII
List of Schemes		IX
List of Figures		XI
List of Tables		XV
Chapter One:	OLEFIN METATHESIS REVIEW	1
Chapter Two:	SYNTHESIS AND CHARACTERIZATION OF MONOFUNCTIONAL AND DENDRITIC (N,N') AND (N,O) SCHIFF BASE LIGANDS	42
Chapter Three:	SYNTHESIS AND CHARACTERIZATION OF MONONUCLEAR AND DENDRITIC RUTHENIUM COMPLEXES BASED ON 4-IMINO-PYRIDINE AND SALICYLALDIMINE/ <i>P</i> -CYMENE LIGANDS	72
Chapter Four:	PRELIMINARY TESTING OF SOME COMPLEXES IN OLEFIN METATHESIS REACTIONS	118
Chapter Five:	SUMMARY AND FUTURE WORK	150

LIST OF ABBREVIATION

ROP	Ring-opening polymerization
SHOP	Shell Higher Olefins Process
ROMP	Ring-opening metathesis polymerisation
CM	Cross metathesis
ROM	Ring-opening metathesis
ADMET	Acyclic diene metathesis
RCM	Ring-closing metathesis
AlMe ₃	Trimethylaluminium
CDCl ₃	Deuterated chloroform
L	Ligand
Mes	2,4,6-trimethylphenyl
NAr	2,6-diisopropylphenylimido ligand
NHC	1,3-dimesityl-4,5-dihydroimidazole-2-ylidene
PCy ₃	Tricyclohexylphosphine
Phoban	Phosphabicyclononane
Cp	Cyclopentadiene
AlCl ₃	Aluminiumtrichloride
PPh ₃	Triphenylphosphine
KOBu ^t	Tertiary-butyl potassium oxide
SASTECH	Sasol Technology
DCM	Dichloromethane
RXN	Reaction
DAB-(NH ₂) _n	Diaminobutane-polypropyleneimine
G1	Generation one
G2	Generation two
¹ H	Proton
¹³ C{ ¹ H}	Carbon decoupled to proton
FT-IR	Fourie transform infrared
ESI-MS	Electronspray ionization mass spectrometry
<i>p</i>	Para-position
ATR-IR	Attenuated total reflection infrared
NMR	Nuclear magnetic resonance spectrometry
TMSD	Trimethylsilyldiazomethane

LIST OF SCHEMES

Scheme 1.1: Metallocyclobutane Metathesis mechanism	4
Scheme 1.2: Tebbe complex reacting with a terminal olefin	5
Scheme 1.3: Illustration of different bonding between Fischer and Schrock carbenes	7
Scheme 1.4: Synthetic route to a Fischer carbene	7
Scheme 1.5: Reaction pathway that leads to synthesis of well-defined Grubbs catalysts	10
Scheme 1.6: Alternative synthetic pathway used to form ruthenium catalysts	11
Scheme 1.7: General procedure of forming new organic chemicals through ROMP and ADMET	12
Scheme 1.8: Cross metathesis of alkenes	13
Scheme 1.9: General metathesis reactions of RCM	14
Scheme 1.10: Proposed mechanism using complex 5a as a catalyst	15
Scheme 1.11: Generally accepted mechanism for the homogeneous metathesis reaction catalyzed by Ru alkylidene complexes	16
Scheme 1.12: Synthetic pathway for the production of Grubbs second generation catalysts	19
Scheme 1.13: Synthesis of the first generation Hoveyda –Grubbs catalyst 14	20
Scheme 1.14: Synthesis of the second generation of Hoveyda catalyst 15	20
Scheme 1.15: Methodology used at SASTECH to synthesize the homogeneous Phobcat catalyst	21
Scheme 1.16: Synthesis of mononuclear and dinuclear Ru(II) salicylaldimine complexes	22
Scheme 1.17: Proposed mechanisms for the mononuclear and dinuclear Ru complexes 18 and 21	24
Scheme 2.1: Model salicylaldimine ligands	45
Scheme 2.2: First generation dendritic 4-imino-pyridine functionalized ligand	45

Scheme 2.3: Synthetic route for the formation of the second generation 4-imino pyridine ligand	48
Scheme 2.4: Synthetic route for the mono-functional salicylaldimine ligands	49
Scheme 2.5: First generation dendritic salicylaldimine ligand	49
Scheme 2.6: Possible fragmentation pattern for the G2 salicylaldimine ligand, L8	52
Scheme 2.7: Formation of the second generation dendritic salicylaldimine ligand	53
Scheme 3.1: Synthesis of a 4-imino pyridyl Ru carbene complex	77
Scheme 3.2: Synthetic pathway for the formation of imino-pyridyl Ru carbene complexes	87
Scheme 3.3: Attempted synthesis of salicylaldimine Ru carbene complexes using Grubbs G1	97
Scheme 3.4: Synthesis of salicylaldimine Ru <i>p</i> -cymene complexes	99
Scheme 4.1: Metathesis of 1-octene to 7-tetradecene in the presence of a catalyst	121
Scheme 4.2: A possible mechanism for the metathesis of 1-octene using 4-imino pyridine Grubbs-type complexes	130
Scheme 4.3: Ring closing metathesis of diethyl diallylmalonate catalyzed by a ruthenium carbene complex	137
Scheme 4.4: Typical ROMP reaction of norbornene to form polynorbornene	142
Scheme 4.5: A possible mechanism for activation of <i>p</i> -cymene Ru salicylaldimine complexes in ROMP reactions	143

LIST OF FIGURES

Figure 1.1 Schrock's Mo catalyst	7
Figure 1.2 Grubbs well-defined catalysts	9
Figure 1.3 Various Ru alkylidene complexes used in homogeneous metathesis	17
Figure 1.4 The dendrimeric framework	29
Figure 2.1 Model Schiff base ligands	44
Figure 2.2 MALDI-TOF spectrum of the G1 salicylaldimine dendritic ligand, L7	51
Figure 2.3 MALDI-TOF spectrum for the G2 dendritic ligand, L8	52
Figure 2.4 FT-IR spectrum for the monofunctional <i>N, N'</i> ligand, L1	54
Figure 2.5 FT-IR spectrum for the monofunctional <i>N, O</i> ligand, L5	55
Figure 2.6 Numbering of carbon atoms in the mono-functional ligands, L1 and L2	56
Figure 2.7 Numbering of carbon atoms in the dendritic (<i>N, N'</i>) G1 ligand, L3	56
Figure 2.8 Numbering of carbon atoms in the dendritic (<i>N, N'</i>) G2 ligand, L4	57
Figure 2.9 Numbering of carbon atoms in the monofunctional (<i>N, O</i>) ligands, L5 and L6	57
Figure 2.10 Numbering of carbon atoms in the dendritic G1 (<i>N, O</i>) ligand, L7	58
Figure 2.11 Numbering of carbon atoms in the dendritic G2 ligand, L8	58
Figure 2.12 A typical ^1H NMR spectrum of a dendritic (<i>N, O</i>) ligand, L8	59
Figure 2.13 ^1H NMR spectrum of the <i>N, N'</i> dendritic ligand, L4	59
Figure 2.14 $^{13}\text{C}\{^1\text{H}\}$ NMR spectrum of G2, <i>N, N'</i> dendritic ligand, L4 showing one arm of the dendrimer	63
Figure 2.15 $^{13}\text{C}\{^1\text{H}\}$ NMR spectrum of G2, <i>N, O</i> dendritic ligand, L8 showing one arm of the dendrimer	63
Figure 3.1 General structure for the G1 dendritic 4-imino pyridyl Ru carbene complex	78
Figure 3.2 General structure for the G2 dendritic 4-imino pyridyl Ru carbene complex	78

Figure 3.3 IR spectrum of the mononuclear complex C1 , showing the mode of bonding in Grubbs G1 4-imino-pyridyl complexes	82
Figure 3.4 C-Atom labelling for mononuclear complexes, C1 and C2	83
Figure 3.5 C-Atom labelling for dendritic complexes, C3 and C4 (Note: only one arm of the dendrimer molecule is shown)	83
Figure 3.6 The ^1H NMR spectrum of the dendritic complex C3 showing typical signals of phosphine substituted 4-imino-py-Ru carbene complexes	86
Figure 3.7 General structure for the G1 dendritic Ru carbene complex, C7	88
Figure 3.8 General structure for the G2 dendritic Ru carbene complex, C8	88
Figure 3.9 IR spectrum of the mononuclear 4-imino-py Ru NHC carbene complex, C5	89
Figure 3.10 C-atom labelling of mononuclear complexes, C5 and C6	92
Figure 3.11 C-atom labelling of dendritic complexes, C7 and C8 showing only one arm of the dendrimer generation	92
Figure 3.12 ^1H NMR spectrum of the G2 dendritic Ru NHC carbene complex, C8	96
Figure 3.13 Dendritic G1 salicylaldimine Ru chloro <i>p</i> -cymene complex	99
Figure 3.14 G2 dendritic salicylaldimine Ru chloro <i>p</i> -cymene complex	100
Figure 3.15 Atom labelling for mononuclear salicylaldimine Ru- <i>p</i> -cymene complexes, C9 and C10	102
Figure 3.16 Atom labelling for dendritic salicylaldimine Ru chloro <i>p</i> -cymene complex, C11 and C12 (NB: only one of dendrimer arms shown)	102
Figure 3.17 A typical ^1H NMR spectrum of salicylaldimine Ru chloro <i>p</i> -cymene complex, C9 .	102
Figure 3.18 TG plot and its derivative for the mononuclear complex, C10	108
Figure 3.19 TG plot with its derivative for the G1 dendrimer complex, C11	109
Figure 3.20 TG analysis of G2 dendritic complex, C12	109
Figure 4.1 Neutral ruthenium carbene complexes developed by Grubbs and co-workers	119

Figure 4.2 Model complexes used in the testing of the catalytic activity for the metathesis of 1-octene	120
Figure 4.3 Dendritic complexes employed in the metathesis of 1-octene	121
Figure 4.4 ¹ H NMR spectrum showing the catalysis by C1 immediately after the addition of 1-octene	123
Figure 4.5 Selected ¹ H NMR spectra of the C1 catalysis of 1-octene	124
Figure 4.6 ¹ H NMR monitoring of 1-octene metathesis using C5 as a catalyst	125
Figure 4.7 ¹ H NMR monitoring 1-octene metathesis for longer period using C5 as a catalyst	126
Figure 4.8 A graph showing the relative formation of the product in a reaction mixture over time.	127
Figure 4.9 1-octene conversion using C1-C4 and Grubbs G1 catalyst (24h)	129
Figure 4.10 Grubbs G2 modified complexes (C5-C8) as catalysts in the metathesis of 1-octene (24h).	131
Figure 4.11 ¹ H NMR (CDCl ₃) spectra of the Grubbs G1 catalyst in solution within 16 hours.	133
Figure 4.12 ¹ H NMR (CDCl ₃) spectra of C1 in solution for a maximum period of 16h	135
Figure 4.13 ¹ H NMR (CDCl ₃) spectra of the <i>pyridine</i> modified Grubbs G1 catalyst.	136
Figure 4.14 ¹ H NMR spectrum (CDCl ₃) immediately after the addition of substrate, catalyzed by C1	138
Figure 4.15 ¹ H NMR spectrum (CDCl ₃) immediately after the addition of substrate, catalyzed by C5	138
Figure 4.16 ¹ H NMR spectra monitoring C1 activity in RCM of diethyl diallylmalonate	139
Figure 4.17 ¹ H NMR spectra monitoring C5 activity in RCM reaction of diethyl diallylmalonate	140

Figure 4.18 A graph showing the relative formation of the product in the RCM reaction mixture over time	141
Figure 4.19 ^1H NMR spectrum of the product formed from the reaction catalysed by C3	142
Figure 4.20 Complexes used in evaluating catalytic activity for ROMP, showing only one arm of the dendritic complexes	144
Figure 4.21 IR spectrum of polynorbornene, produced using Ru- <i>p</i> -cymene catalysts	145
Figure 4.22 ^1H NMR spectrum of a polynorbornene sample	145

LIST OF TABLES

Table 2.1 Selected IR, MS and Melting Point data, L1-L8	55
Table 2.2 ^1H NMR data for all ligands prepared, L1-L8	60
Table 2.3 ^{13}C NMR data for all the ligands prepared, L1-L8	64
Table 2.4 Microanalysis results for all ligand systems, L1-L8	67
Table 3.1 Selected IR, MS as well as microanalysis data for pyridyl-imino complexes, C1-C4	79
Table 3.2 ^1H NMR data for phosphine containing 4-imino pyridyl Ru carbene complexes, C1-C4	84
Table 3.3 Selected IR, MS and microanalysis data for the 4-imino-py Ru NHC carbene complexes, C5-C8	89
Table 3.4 ^1H NMR data for 4-imino-py Ru NHC carbene complexes, recorded in CDCl_3 , C5-C8	93
Table 3.5 Analytical data for salicylaldimine Ru <i>p</i> -cymene complexes, C10-C12	101
Table 3.6 ^1H NMR data for salicylaldimine Ru <i>p</i> -cymene complexes, C9-C12 recorded in CDCl_3	103
Table 3.7 $^{13}\text{C}\{^1\text{H}\}$ NMR data for salicylaldimine Ru <i>p</i> -cymene complexes, C9-C12	105

Chapter 1

OLEFIN METATHESIS REVIEW

CONTENT

1. Content of this chapter	2
1.1 General Introduction to Olefin Metathesis	2
1.2 Early metathesis reactions	4
1.3 Metal carbenes	5
1.3.1 Fischer tungsten carbenes	6
1.3.2 Schrock tungsten and molybdenum carbenes	7
1.3.3 Ruthenium carbene complexes	8
1.3.3.1 1 st Generation Grubbs catalyst [Ru(PCy ₃) ₂ Cl ₂ CHPh]	10
1.4 Applications of homogeneous Ru alkylidene complexes	11
1.4.1 Ring-Opening Metathesis Polymerization (ROMP)	12
1.4.2 Cross Metathesis (CM)	13
1.4.3 Ring-Closing Metathesis (RCM)	13
1.5 Mechanistic pathway of Ru alkylidene metathesis reactions	15
1.6 Development in catalyst design	17
1.6.1 N-heterocyclic carbenes (NHC)	18
1.6.2 Hoveyda-Grubbs catalysts	19
1.6.3 Phobcat 13-[Ru(Cl) ₂ (cyclohexyl[3.3.1]phoban) ₂ CHPh]	21
1.6.4 Bidentate Schiff base Ru alkylidene complexes	22
1.7 Proposed mechanism for olefin metathesis based on salicylaldimine Ru alkylidene complexes	23
1.8 Decomposition of Ruthenium alkylidene catalysts	24
1.9 Non metathesis reactions of ruthenium alkylidene	26
1.10 Immobilization of Ru alkylidene complexes	26
1.10.1 Dendrimers as supports	28
1.11 Aims and objectives	30
1.12 References	32

1. Content of this chapter

This chapter gives insight into the aims of the project and the main outcomes of the study. It begins by introducing the current state of the art in catalytic olefin metathesis. Part of this review involves the description of known catalysts used in this process, their synthesis and the typical nature of olefin metathesis catalysts. This is important because part of the research reported in this dissertation included the synthesis of ruthenium carbene catalysts which are known to be good catalysts and which have found wide application in different olefin metathesis reactions. Presently in industry and in academia, researchers interested in olefin metathesis have predicted improvements that are possible in order to achieve a more efficient catalytic process.

1.1 General Introduction to Olefin Metathesis

Up to the mid 1950's there were few reports on catalytic metathesis reactions of olefins [1]. It was only at a later stage that Calderon and coworkers recognized that both ring-opening polymerization (ROP) and disproportionation of acyclic olefins were the same type of reaction [2]. These researchers named the above-mentioned reactions "olefin metathesis" meaning metal catalyzed re-distribution of carbon-carbon double bonds [2b]. The process is also known as a disproportionation or transmutation of an olefin to form a new C-C double bond *via* the exchange or reorganization of the C atoms of the two C-C double bonds. The process proceeds *via* the formation of a metallacycle intermediate [3] as depicted in Scheme 1.1. This catalytic reaction has yielded a wide range of products such as oleo-chemicals, petrochemicals, polymers and fine chemicals.

Chauvin proposed a carbene mechanism [4] to explain how the metathesis reaction proceeds. Schrock and Grubbs discovered well-defined olefin metathesis catalysts [5-6] during their search for new metal alkylidene complexes. The work of the above chemists recently resulted in them jointly being awarded the Nobel Prize in chemistry in 2005.

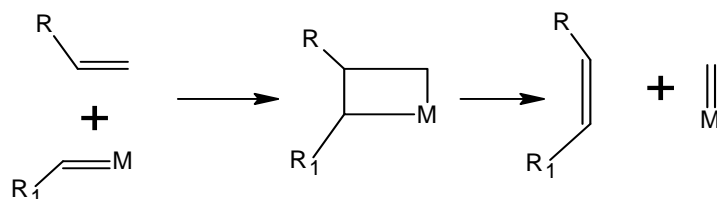
The success of olefin metathesis after the discovery of Schrock and Grubbs catalysts made it widely applicable in industrial processes, leading or enriched in synthetic organic chemistry. Many new products have been formed *via* catalytic olefin metathesis. An example of a major industrial scale use of metathesis is the production of propene *via* the reaction of ethylene and 2-butene over a heterogeneous catalyst. Another example is the Shell Higher Olefin Process (SHOP) [7] which involves homogeneous ethylene oligomerization followed by metathesis over a heterogeneous catalyst [8]. Olefin metathesis is categorized into the following catalytic reactions namely: ring-opening metathesis polymerization (ROMP), cross-metathesis (CM), ring-opening metathesis (ROM), acyclic diene metathesis (ADMET) and ring-closing metathesis (RCM).

The transformation of simple olefins to those that are more complex and valuable (pharmaceuticals or polymeric materials) is vital for many reasons. Firstly it allows facile access from easily prepared olefins to those that are difficult to prepare. Secondly, olefin metathesis reactions either do not generate a by product but give a gaseous product, which is, ethylene that can be removed by evaporation [9]. Lastly olefins are stable but reactive. Their stability is attributed to the fact that they can be stored indefinitely without decomposing. Reactivity is brought about by the presence of a π bond that is sufficiently reactive to be used in a wide range of transformations. Ruthenium was found to be one of the transition metals to exhibit selective metathesis reactivity with olefins.

1.2 Early metathesis catalyst systems

Initially olefin metathesis was accomplished by poorly defined homogeneous and heterogeneous catalysts. These catalysts were mainly group 6 transition metal chlorides combined with main group alkylating agents in homogeneous solutions whilst in the case of heterogeneous systems they were deposited on solid supports [10]. A classical example is a combination of $WCl_6/ EtAlCl_2$ or MoO_3/ SiO_2 . These complexes were commercially available and used in many catalytic applications due to their ease of preparation and the fact that they were cheap. At the same time they were limited by the need for harsh reaction conditions and were incompatible with many reactive functional groups due to the use of strong Lewis acids required by the system. Another limitation was that the active catalytic species as well as the reaction mechanism were unknown [11]. This led to the need for the development of better understood organometallic catalysts and detailed mechanistic studies on olefin metathesis. The proposed olefin metathesis mechanism by Chauvin [4] led to developments of alkylidene and metallacyclobutane complexes.

The mechanism Chauvin proposed involves interconversion of an olefin and metal alkylidene. The olefin coordinates to the metal carbene, followed by the formation of a metallacyclobutane intermediate *via* a (2+2) cycloaddition and then cyclo-reversion where the intermediate decomposes to form a new metal carbene and the desired product (Scheme 1.1).

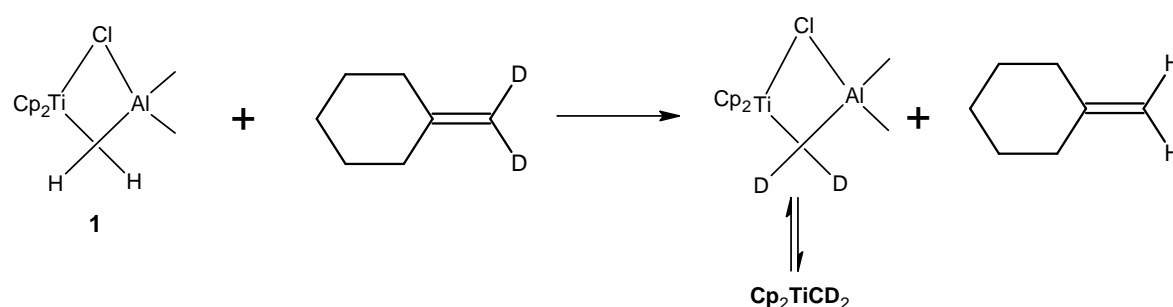


Scheme 1.1: Metallacyclobutane Metathesis mechanism.

At the time Chauvin proposed the mechanism in 1970, the first isolable metal carbene reported was made by Fischer [12] which was only reactive towards strained cycloalkenes

[10]. Thereafter around the 70's and early 80's well-defined carbene complexes were prepared. A well-defined carbene complex [13] means that the complex resembled the active site in terms of the oxidation state of the metal center and the ligand coordination sphere around the metal center. It also means that the complex must be stable enough allowing it to be characterized using spectroscopic techniques and when reacted with an olefin it must form a new alkylidene complex from the olefin it reacted with. Grubbs's explanation of a well-defined complex is one where the propagating complex can be observed and controlled [14]. A propagating species is the original species that produces a new one from itself.

The first well-defined alkylidene complex was the Tebbe complex **1** [15], which showed metathesis activity. It was generated from the reaction of Cp_2TiCl_2 with an excess of AlMe_3 . Its metathesis activity was shown when **1** was reacted with deuterated methylene cyclohexane to produce the deuterated Tebbe complex which formed an alkylidene complex (Cp_2TiCD_2) [16] and methylene cyclohexane that could be characterized (Scheme 1.2). The confirmation of the Chauvin metallacycle mechanism led to the formation of the active metathesis complex.

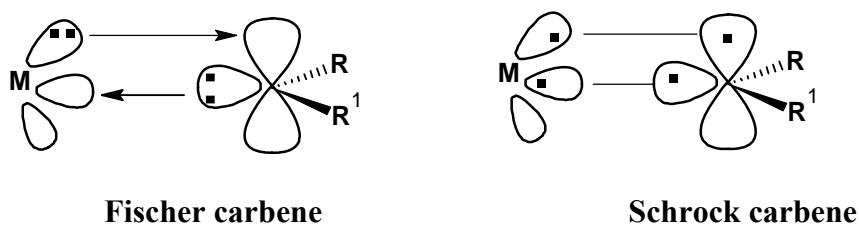


Scheme 1.2: Tebbe complex reacting with a terminal olefin

1.3 Metal carbenes

Transition metal carbenes are organometallic compounds bearing a carbon-metal double bond. They can be divided into 2 categories:-

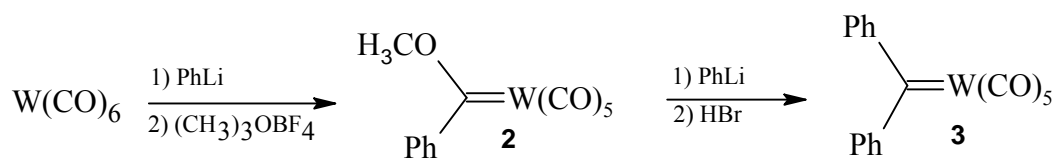
- Fischer carbenes, where a heteroatom which could be any atom other than C/H is attached to the carbene carbon. The metal carbon (M=C) linkage is formed as a result of chemical bonding between σ type donation of the filled methyldene lone pair on the C atom into an empty d-orbital on the metal. This results in δ electron back donation from a filled metal d-orbital to the empty p-orbital of the methylene.
- Shrock carbenes, contain only C atoms or H atoms at the carbene carbon [CHR alkylidene]. There is no δ acceptor in the ligand, so the 2 p-orbitals of the C atom each containing a radical, form a covalent bond with the metal. The methylene group is thus nucleophilic.



Scheme 1.3: Illustration of different bonding between Fischer and Schrock carbenes

1.3.1 Fischer Tungsten carbenes

Fischer was the first person to isolate a metal carbene complex $[(\text{CO})_5\text{W}=(\text{Ph})(\text{OCH}_3)]$, **2** [12]. The problem with it was that it only reacted with strained cycloalkenes [10]. Attempts to overcome this problem lead to an improvement of **2** by Casey [17] to form $(\text{CO})_5\text{W}=\text{CPh}_2$, **3**, which was more reactive than **2** with a number of olefins. Its catalytic capability is influenced by the lower electron donating ability of the two phenyl groups, with $[(\text{CO})_5\text{W}=\text{CPh}_2]$ yielding substoichiometric quantities of metathesis products. Fischer carbenes have found wide application in the polymerization of alkenes [10, 17] and in the rearrangement of enynes to dienes [10]. Although the initial carbene complex was isolated it was not regarded as a well-defined system due to the inability to detect of the propagating metal carbene species [10].



Scheme 1.4: Synthetic route to a Fischer carbene

1.3.2 Schrock tungsten and molybdenum carbenes

Schrock molybdenum and tungsten alkylidenes of the general formula $[(\text{NAr})(\text{OR}')_2\text{M}=\text{CHR}]$ were the first catalytic systems to find wide usage in olefin metathesis [11]. The first tungsten Schrock alkylidene isolated was an $18 e^-$ species $[\text{W}(\text{O})(=\text{CH}-t\text{-Bu})(\text{PEt}_3)_2]$ which showed low catalytic activity towards terminal olefins [18]. This was improved by introducing AlCl_3 as a co-catalyst which also influenced the ability to observe the propagating species, $[\text{W}(\text{O})(=\text{CEt})(\text{PEt}_3)_2\text{Cl}_2]$ [18, 19]. This was followed by the introduction of the alkoxide ligand which was shown to promote metathesis unlike the chloride that was found to promote side reactions which destroy alkylidenes [20]. A $14e^-$ tungsten species $[\text{W}(\text{NAr})(\text{CH}-t\text{-Bu})(\text{OR})_2]$ has been reported where imido ligands, $[\text{N}-(2,6-i\text{-Pr}_2\text{C}_6\text{H}_3)]$ (NAr) were introduced to protect the metal center and to prevent bimolecular decomposition [21].

The molybdenum complex, $\{\text{N}-(2,6-i\text{-Pr}_2\text{C}_6\text{H}_3)\text{Me}_2[\text{OC}(\text{CH}_3)(\text{CF}_3)_2]_2\text{Mo}=\text{CH}-t\text{-Bu}\}$, **4** [22, 23] is a Schrock-type catalyst that has found the most wide-spread application. The most desirable feature of this complex is its high activity towards both terminal and internal olefins as well as ROMP of low strained monomers and ring closing of sterically demanding and e^- poor substrates [22-24].

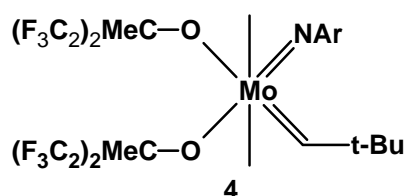


Figure 1.1: Schrock's Mo catalyst

There are however a number of limitations to the above complex and these are:-

- High oxophilicity of the metal center, making it extremely sensitive to oxygen and moisture.
- Poor functional group tolerance. This reduces the number of potential substrates that could be used.
- Extreme conditions required for catalytic processes.

The synthesis of other metal alkylidenes was motivated by the aim of overcoming the above mentioned issues.

1.3.3 Ruthenium carbene complexes

Several families of ruthenium complexes have found a wide range of applications in a variety of chemical transformations such as hydrogenation [25], hydration [26], oxidation [27], epoxidation [28], isomerisation [29], decarbonylation [30], cyclopropanation [31], olefin metathesis [32], Diels-Alder reactions [33], Kharasch additions [34], enol ester syntheses [34], atom transfer radical polymerizations [35] and other related catalytic processes. Development of Ru complexes has been achieved by coordinating different ligands e.g. hydrides, halides, water, carboxylate, phosphines, amines, oxygen, nitrogen, as well as chelating groups such as Schiff bases, arenes and carbenes etc. [36-48] to the metal center. This has enabled researchers to study the electronic and steric effects around the metal centre. From these studies, it was found that there is a need to balance the metal environment so as to control the stability, activity and chemoselectivity of the Ru complexes.

A great deal of research has been done to find a homogeneous catalyst that would not only be well-defined but also stable in terms of being tolerant to substrates or solvents. Grubbs and coworkers introduced a useful metathesis catalyst system that was well-defined and stable. Two examples are $[\text{Ru}(\text{PCy}_3)_2\text{Cl}_2(=\text{CHPh})]$ and $[\text{RuCl}_2(=\text{CHPh})(\text{NHC})(\text{PCy}_3)]$, Figure 1.2. The use of Ru as the metal center was a result of the findings that this metal preferentially

reacted with carbon-carbon double bonds rather than with other species, making the catalyst stable towards functional groups such as alcohols, amides, aldehydes and carboxylic acids. It was as a result of these observations that Ru alkylidene complexes were found to have an advantage over Schrock's active catalysts, which were rather oxophilic.

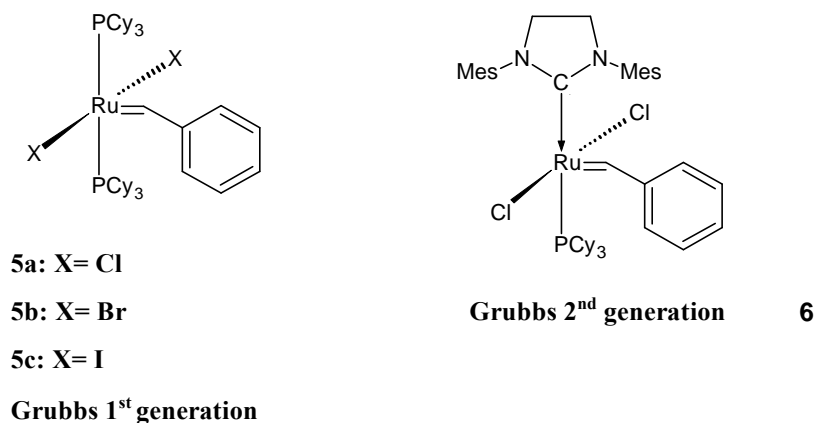


Figure 1.2: Grubbs well-defined catalysts

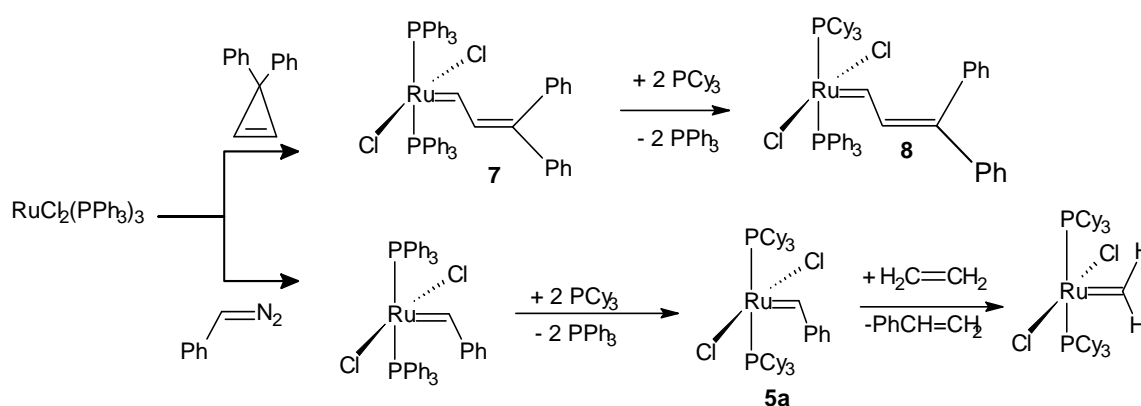
As a result of studying the above mentioned Ru complexes it was observed that these complexes displayed enhanced activity and selectivity in many organic transformations [49]. Some of the ligands made the catalyst tolerant towards organic functionalities, air and moisture, in other words it was possible for these to be used in many more applications [50].

1.3.3.1 1st Generation Grubbs catalyst [Ru(PCy₃)₂Cl₂CHPh]

The first well-defined active metathesis Ru alkylidene complex, **8** was developed by the Grubbs group [37b] when they applied the method used for synthesizing tungsten alkylidenes to the synthesis of ruthenium alkylidenes. The tungsten reaction involved the use of 3,3-disubstituted cyclopropenes as carbene precursors with W(V) whilst in the case of the ruthenium carbene complex, RuCl₂(PPh₃)₃ was reacted with diphenylcyclopropene resulting in the formation of complex **7** depicted in Scheme 1.5. This complex could only metathesize highly strained cyclic olefins. They then modified the ligands by replacing chlorides with other electron withdrawing ligands based on trends followed by early transition metal

catalysts with the hope of increasing activity with the presence of ligands with more electron withdrawing character [23]. They also introduced the di bromide **5b** and the di iodide **5c** (Figure 1.2) [37] using Finkelstein-type chemistry. The Finkelstein reaction is used in organic chemistry to exchange Cl or Br to I. In organometallic chemistry it is also used to carry out halide exchange on various organometallic complexes using halide salts in THF or acetone [51]. Grubbs and coworkers reacted the Grubbs catalyst with LiBr in a mixture of THF and dichloromethane. They then tested these complexes and found them less active and less stable than chloride containing catalyst.

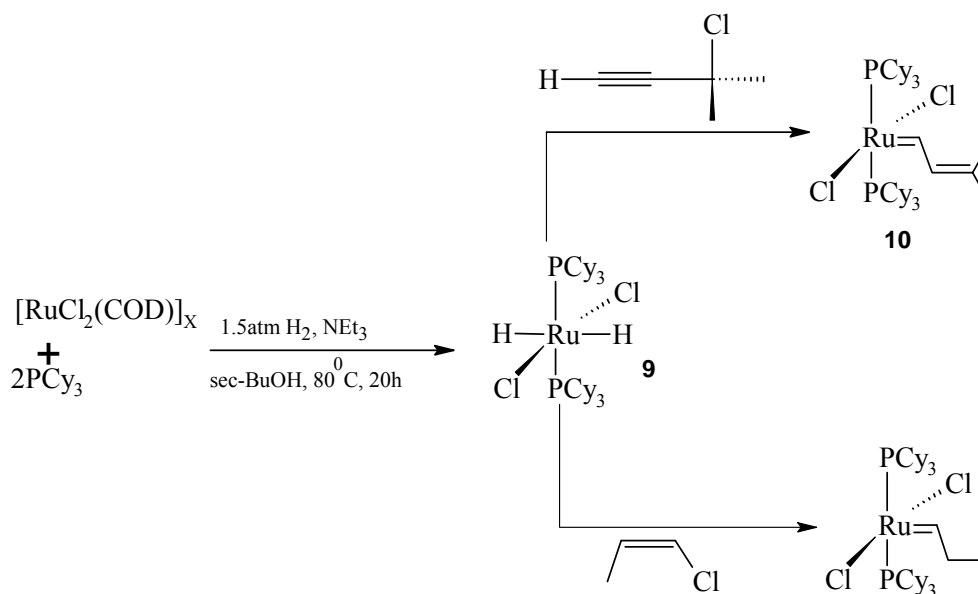
It was eventually decided to replace PPh₃ with a more basic phosphine *i.e.* PCy₃. This resulted in the formation of complex **8** which was found to be the first ruthenium alkylidene to be active towards acyclic olefins. A conclusion was made that an increase in the basicity of the phosphine results in higher metathesis activity.



Scheme 1.5: Reaction pathway that lead to synthesis of well-defined Grubbs catalysts

The limited availability of diphenylcyclopropene and the need for bulk samples led to an alternative reaction of RuCl₂(PPh₃)₃ with alkyl- and aryl-diazoalkanes compounds that lead to the synthesis of Grubbs catalyst **5a**. This route was not ideal as it had several problems associated with it. Firstly there is the potential of diazoalkanes being explosive. Secondly it requires large amounts of solvent and finally it also requires phosphine exchange. Therefore

attempts were made to develop a better synthetic method [11]. In Scheme 1.6 an alternative pathway to the Grubbs generation I catalyst is outlined. The hydrido chloride complex **9** reacts rapidly with vinyl or olefinic halides to give the desired alkylidene complex **10**. This route gives good yields and is used commercially.



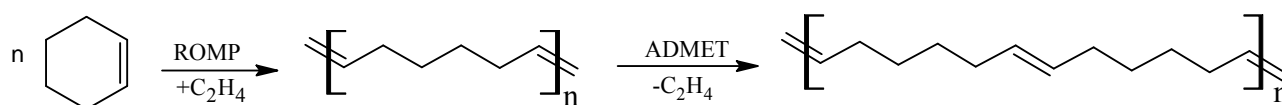
Scheme 1.6: The alternative synthetic pathway used to form ruthenium catalysts

1.4 Applications of homogeneous Ru alkylidene complexes

Grubbs alkylidene complexes of the type $\text{L}_2\text{X}_2\text{Ru}=\text{CHR}$ raised the profile of olefin metathesis in the eyes of organic chemists due to its ability to produce a variety of organic compounds essential in the production of fine chemicals and other pure inexpensive chemicals. Due to the activity and functional group tolerance of these complexes, different substrates have been used under different conditions to produce a wide range of products from different classes of metathesis reactions. There is a wide range of chemical reactions which can be classified under olefin metathesis; cross-metathesis (CM), ring-opening metathesis polymerization (ROMP), ring-closing metathesis (RCM) and acyclic diene metathesis (ADMET). The use of Ru alkylidenes is advantageous in that the catalytic reactions can be operated under mild conditions and only volatile side products are generated.

1.4.1 Ring-Opening Metathesis Polymerization (ROMP)

There are several transition metals that have been used as ROMP catalysts including Ti, W, Mo and Ru systems. The advances in forming a well-defined catalyst and the functional group tolerance of Ru catalysts have extended ROMP to a more diverse set of monomers. It is the most commonly classified metathesis reaction [52a] and it has been extensively applied to produce new chemicals. It is schematically shown in (Scheme 1.7). ROMP produces unsaturated polymers through the reaction of cyclic olefins with linear monomers and these polymers can also be obtained *via* intermolecular acyclic diene metathesis ADMET [52b]. It is known that the driving force of these reactions is the release of strain in ring structures that also ensures that back tracking is avoided [53]. Back-tracking is the re-conversion of the product to the starting material.



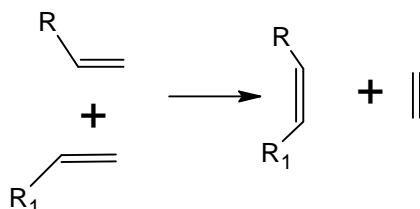
Scheme 1.7: General procedure of forming new organic chemicals through ROMP and ADMET.

ROMP is an example of living polymerization because of the absence of chain termination reactions. It produces monodispersed polymers and allows the length of the polymer chain to be controlled by chain termination or by the adjustments of the monomer/catalyst ratio. In this way block co-polymers may be synthesized [54] due to the fact that the propagating species remains attached to the end of the polymer chain even after the monomer has been completely consumed. It is always advisable to control secondary metathesis reactions from occurring which could result in intermolecular chain transfer or intramolecular chain transfer within the growing chain. Intermolecular chain transfer is the metathesis between two growing polymer

chains resulting in transfer of the metathesis active site from one chain to the other. This causes deactivation of some chains that leads to an increase in the molecular weight distribution. In intramolecular chain transfer also known as backbiting, cyclic and macrocyclic molecules are formed.

1.4.2 Cross-Metathesis (CM)

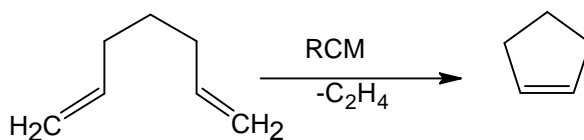
CM occurs when two alkenes react in the presence of a suitable catalyst to form new alkenes (Scheme 1.8). When the reacting alkenes are the same, the reaction is known as self metathesis. It has been reviewed in detail by Cannon and Blechert [55]. Another type of cross metathesis is called ethenolysis where, ethylene is used as one of the starting materials to react with other olefins and always affords alpha-olefins as the product. The ethenolysis reaction was first used in petroleum reformation for the synthesis of higher olefins (Shell higher olefin process – SHOP), with nickel catalysts under high pressure and at high temperatures. Nowadays, even polyenes with MW > 250,000 are produced industrially in this way [9].



Scheme 1.8: Cross metathesis of alkenes

1.4.3 Ring-Closing Metathesis (RCM)

The most widely used olefin metathesis reaction is RCM (Scheme 1.9) where dienes react intramolecularly releasing the volatile by-product ethylene which is removed so that the reaction can proceed to completion. It is often applied in the synthesis of compounds for fine chemicals and in pharmaceutical applications [11].

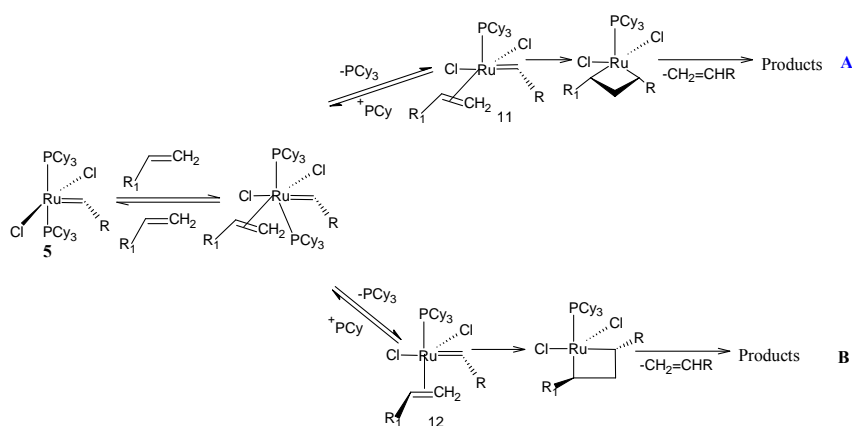


Scheme 1.9: General reaction illustrating RCM

1.5 Mechanistic pathway of Ru alkylidene metathesis reactions

The mechanistic study of Grubbs's catalysts began at the same time they were discovered. These complexes were studied from the perspective of the accepted mechanism proposed by Chauvin [4] in which he proposed that the metathesis reaction involves a carbene and proceeds *via* the formation of a metallacyclobutane.

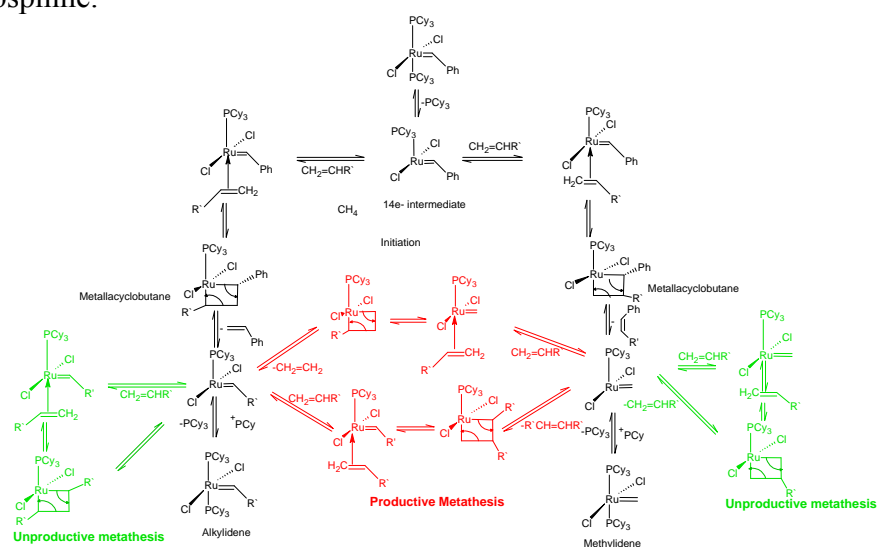
Through kinetic studies of the catalytic reaction, it was found that the reaction of the Ru alkylidene species can occur either *via* a dissociative or associative mechanism. In 1997 Grubbs and co-workers [56] proposed the mechanism depicted in Scheme 1.10. The first step involves olefin coordination to the metal center, assuming a position *cis* to the alkylidene. In pathway **A**, the phosphine dissociates and the alkylidene rotates in order to generate the 16e⁻ species **11** which is the intermediate that undergoes metallacyclobutane formation that is *cis* to the phosphine. This is then followed by bond rearrangement to release the metathesis products. In another possible pathway **B**, the phosphine dissociates and then the olefin rearranges to be *trans* to the remaining phosphine. The intermediate species **12** then undergoes metallacyclobutane formation *trans* to the phosphine resulting in the collapse of the intermediate to form the product. Because phosphine dissociation was not an obvious part of the mechanism and pathway **B** was not considered a favourable option due to reversibility considerations, it was decided to study this process in more detail.



Scheme 1.10: First mechanism proposed using complex **5a** as a catalyst.

Grubbs *et al.* [44e] extensively studied several Ru alkylidene catalysts using ^{31}P magnetization transfer NMR and $1\text{D } ^1\text{H}$ NMR techniques. What they found was that the rate of metathesis is inversely proportional to the amount of free phosphine present meaning that at a high rate of metathesis, less free phosphine was present. Also their study showed that the rate of phosphine dissociation is independent of phosphine concentration meaning that the metathesis reaction takes place *via* the dissociative mechanism.

The now accepted mechanism for Ru alkylidene complexes in homogeneous metathesis reactions is illustrated in Scheme 1.11. The first step is the dissociation of one of the phosphine ligands to form a 14e^- species after which the olefin coordinates *trans* to the remaining phosphine.



Scheme 1.11: Generally accepted mechanism for the homogeneous metathesis reaction catalyzed by Ru alkylidene complexes

This is then followed by the formation of a Ru metallacyclobutane that undergoes bond rearrangement, to form the product olefin and a $14e^-$ Ru species ready for coordination of more olefin which could either result in productive metathesis or unproductive metathesis where in the latter case the olefin product is the same as the substrate. A third possibility is re-coordination of free phosphine to form a propagating methylidene and alkylidene from the precursor.

Scheme 1.11: Generally accepted mechanism for the homogeneous metathesis reaction catalyzed by Ru alkylidene complexes.

1.6 Development in catalyst design.

The mechanistic studies gave insight into other factors that contribute to the activity of Ru alkylidene complexes. Because the structure of the active intermediate species (mono-phosphine Ru species) was well established through these studies, it became the starting point for the development of improved catalysts. Various Ru alkylidene complexes are represented in Figure 1.3 showing different ligands incorporated into the Grubbs design motif.

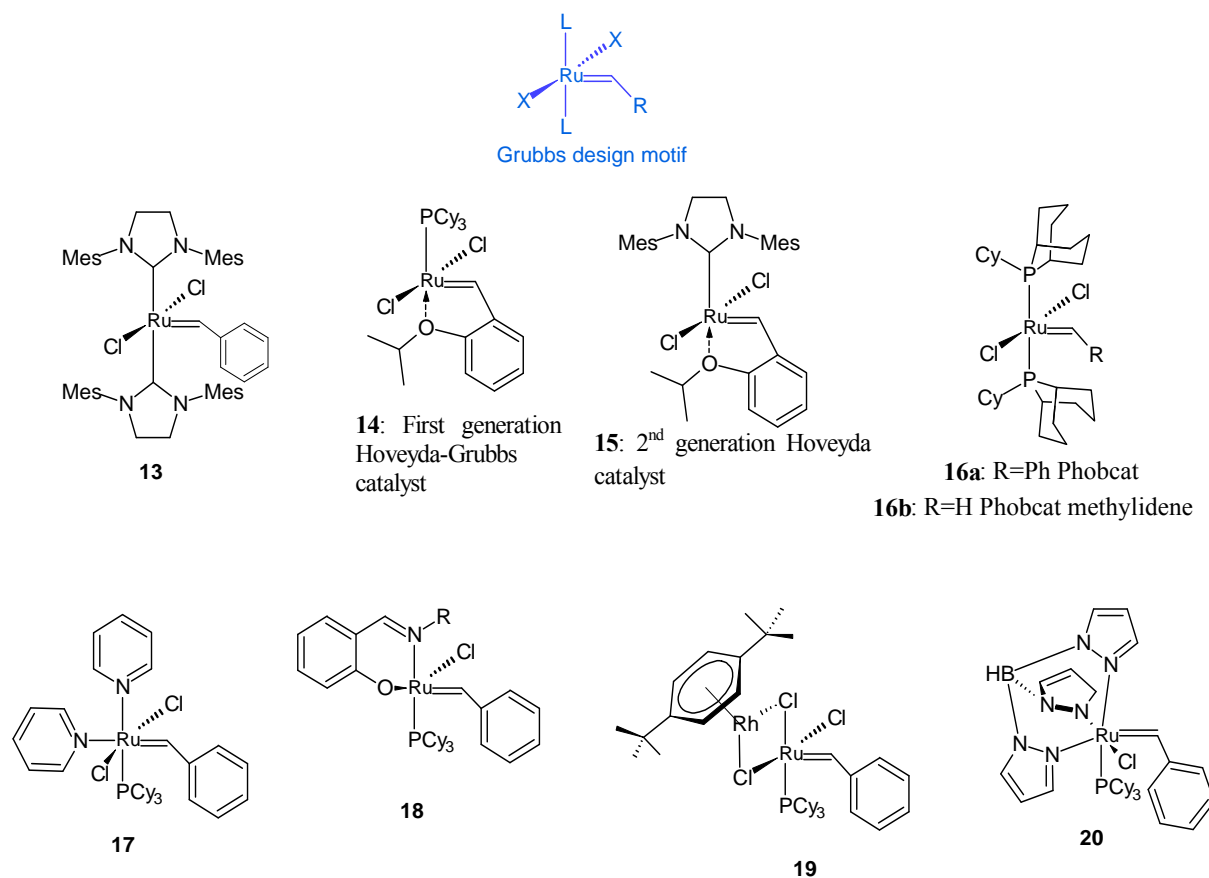


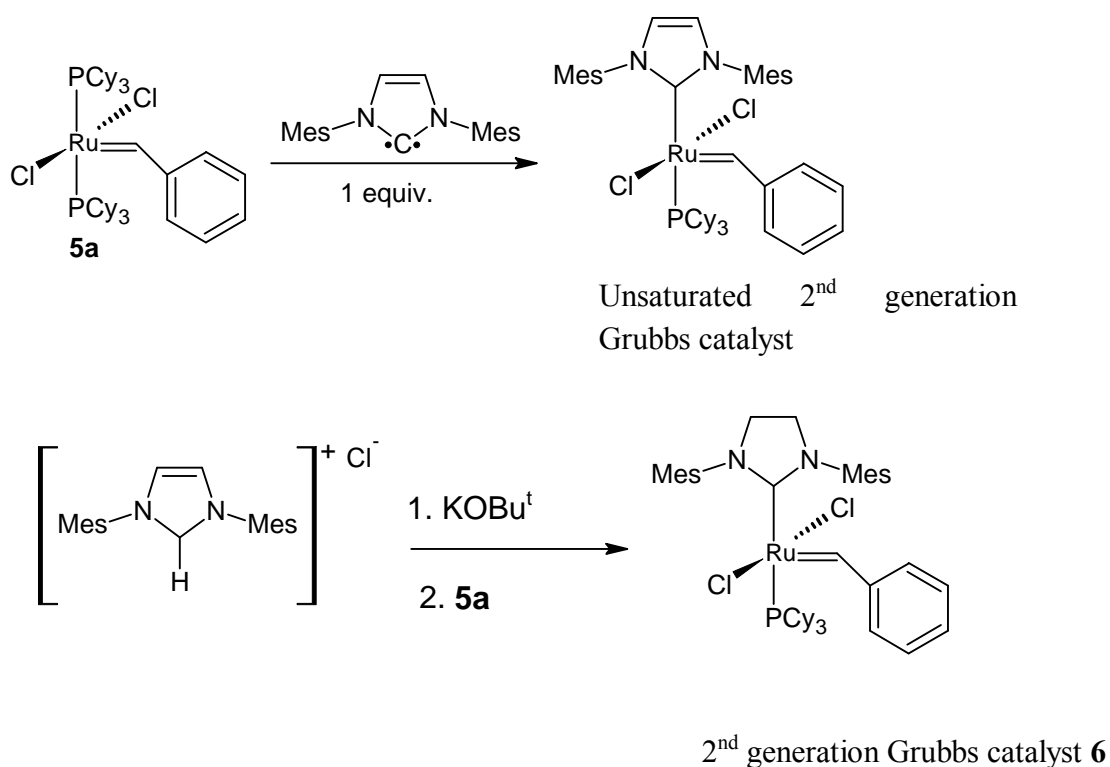
Figure 1.3: Various Ru alkylidene complexes used in homogeneous metathesis

The properties of the complexes above, illustrated several mechanistic points one of which is that one of the ancillary ligands must be labile enough to allow for the catalyst activation. The activity of complex **5a** (Scheme 1.5) was found to be highly dependant on the identity of L and X. Catalytic activity increased with large and more electron donating phosphines whilst it decreased with large and more electron donating halides [11]. With all this in mind the researchers became interested in the potential of N-heterocyclic carbenes.

1.6.1 N-heterocyclic carbenes (NHC)

Hermann and co-workers [58] were the first group to report complex **13** (Fig. 1.3) which they formed by reacting Grubbs catalyst **5a** with two equivalents of the NHC (1,3-dimethyl-4,5-dihydroimidazole-2-ylidene). This species did not show much improvement in terms of catalyst activity when compared to the parent complex **5a**. The Grubbs group attempted to

make the monophosphine complex based on the knowledge that the NHC ligand is a strong σ donor and less labile [59] so it would enhance phosphine dissociation at the same time increase the rate of the metathesis reaction. What they anticipated was true as they successfully synthesized complex **6** shown in Scheme 1.12. The catalysts showed improved stability and reaction rates but it was found that the rate of phosphine dissociation was not increased [60-61]. The second generation Grubbs catalyst **6** with a saturated backbone was more active [62] in ROMP for low strain and sterically hindered substrates. This catalyst is also active in RCM of sterically demanding dienes but has been reported to show significant side reactions, *e.g.* isomerization.

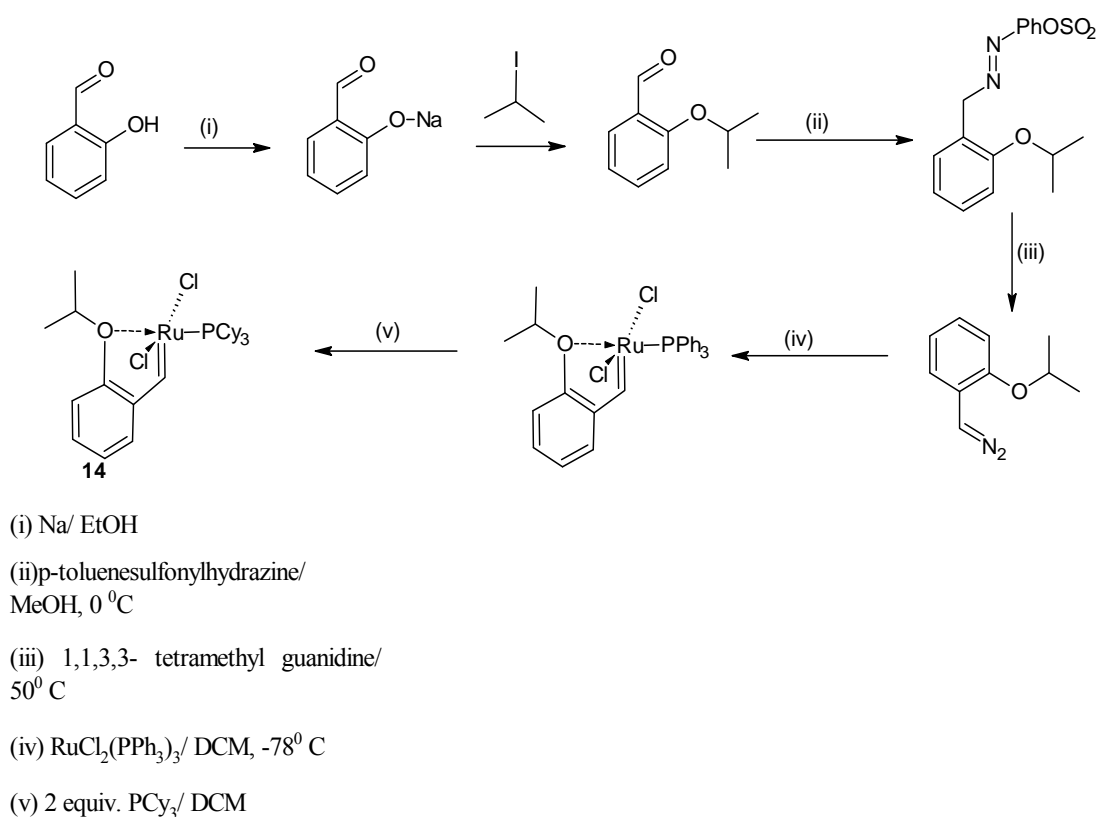


Scheme 1.12: Synthetic pathway for the production of Grubbs second generation catalysts.

1.6.2 Hoveyda-Grubbs catalysts

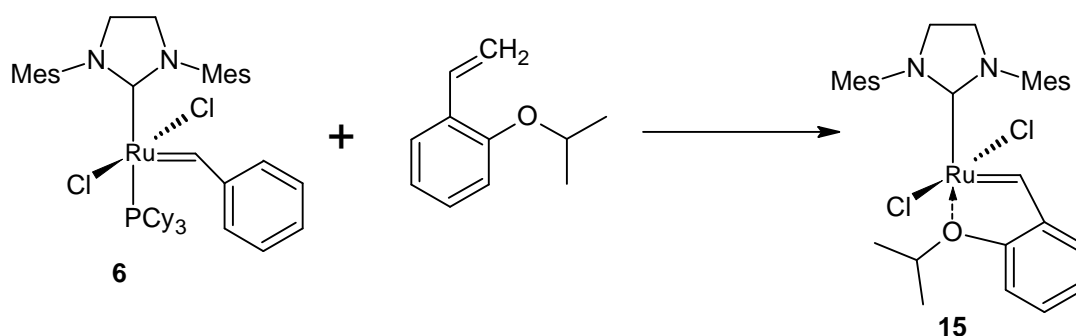
Hoveyda synthesized complex **14** by reacting isopropoxy vinyl ether with Grubbs **5a** [63]. He was prompted to do this after realizing that the action of the Grubbs **5a** catalyst in ROMP

reactions was inhibited by the presence of isopropoxy vinyl ether. The method they used was found to be less efficient and expensive so an alternative pathway was initiated (Scheme 1.13). The expensive nature of the synthesis of **14** could not be reduced as the alternative pathway was a multistep reaction. The most important feature of **14** is the fact that it was the first catalyst reported to be recovered from the reaction mixture by column chromatography and it is also known for its catalytic robustness [64].



Scheme 1.13: Synthesis of the first generation Hoveyda –Grubbs catalyst **14**

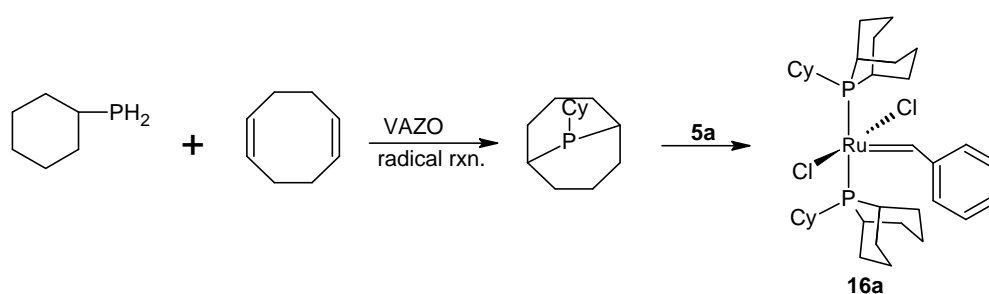
The second generation Hoveyda catalyst **15** was also synthesized by directly reacting Grubbs second generation **6** with isopropoxy vinylstyrene [65-66] shown in Scheme 1.14. Synthesis of these complexes follows Blechert [67] patent method. Recovery of this catalyst has also been claimed.



Scheme 1.14: Synthesis of the second generation of Hoveyda catalyst **15**

1.6.3 Phobcat 13-[Ru(Cl)₂(cyclohexyl)[3.3.1]phoban)₂CHPh]

This complex was developed at SASOL technology R&D in South Africa [68]. They modified the Grubbs catalyst **5a** by introducing the highly basic phobane ligand, also used in hydroformylation technology [69]. Cyclohexylphoban was used to maximize the bulkiness around the metal centre. It was successfully synthesized as illustrated in Scheme 1.15. In ROMP, CM and RCM, complex **16a** is useful and has longer lifetime and stability than the parent complex **5a**. Isomerization rarely occurs when used in CM reactions. The exchange of halides was also attempted and from the results it was concluded that the use of Br instead of Cl gives low initial activity but a much more stable catalyst.



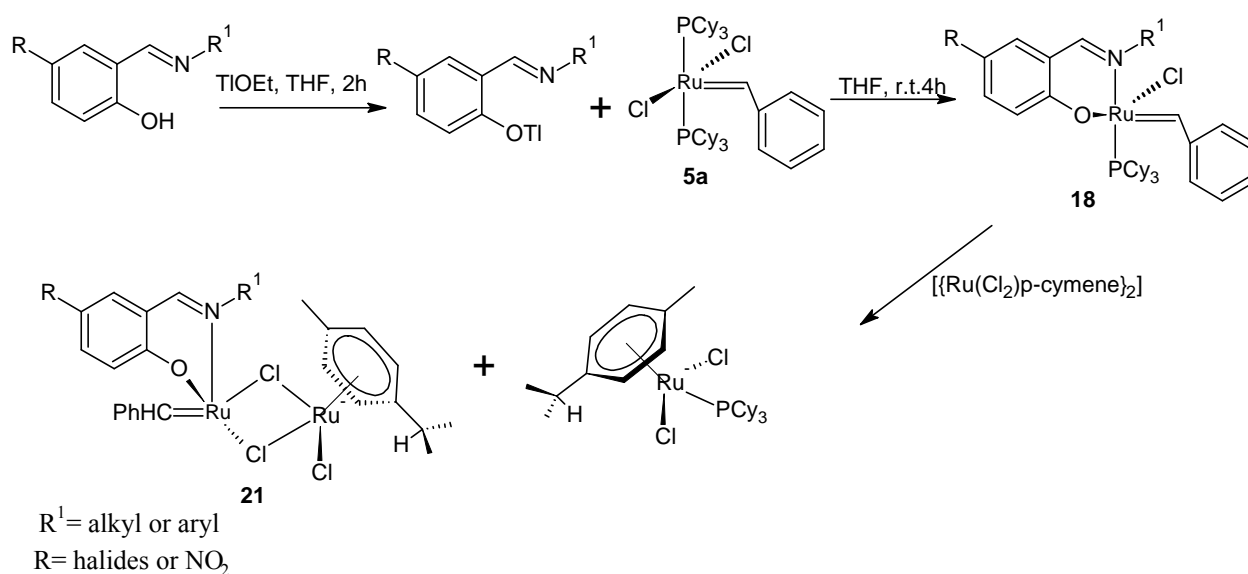
Scheme 1.15: Methodology used at SASTECH to synthesize the homogeneous Phobcat catalyst

Complexes **17-20** in Figure 1.3 have also been developed to attempt to improve catalyst efficiency. The pyridine coordinated complex **17** and the heterobimetallic complexes **19** have been found to have very high activity for a short period of time before they start to decompose

[70]. This is attributed to the presence of a highly labile ligand that is not capable of effectively stabilizing the reaction intermediate as the reaction proceeds. The tris(pyrazolyl) borate catalyst, **20**, has similar problems in that an acid needs to be added for initiation of catalysis and this does not improve the activity dramatically [44d].

1.6.4 Bidentate Schiff base Ru alkylidene complexes

The first group to successfully synthesize complex **21** and related complexes was the Grubbs group. In 1998 Grubbs and co-workers [71] reported the synthesis and full characterization of these complexes. From the catalysis study they found that the bidentate salicylaldimine complex **18** is more stable than the complex **5a** at elevated temperatures but its activity is much lower. In 2002 Verpoort reported similar results using the Grubbs method. He then further developed the dinuclear Ru(II) salicylaldimine complex, **21** shown in Scheme 1.16. In addition, Schiff base Ru NHC alkylidene complexes, Schiff base Ru indenylidene, vinylidene and cyclodiene complexes as well as supported complexes were also developed.

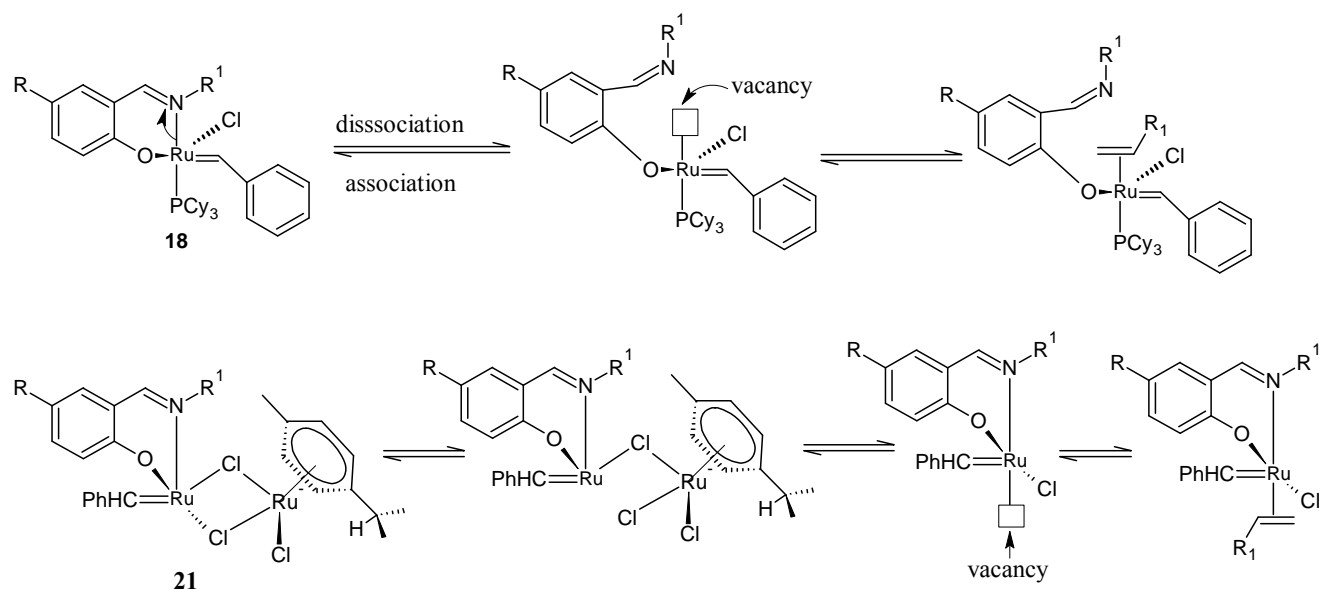


Scheme 1.16: Synthesis of mononuclear and dinuclear Ru(II) salicylaldimine complexes

The catalytic findings revealed that complexes **18** and **21** had high activity and good stability in RCM of linear dienes and ROMP of highly strained cycloalkenes. It was then proposed that a dissociative mechanism [72] similar to the one previously proposed for analogous complexes [44e, h] was operative and which explained the results obtained in metathesis reactions.

1.7 Proposed mechanism for olefin metathesis based on salicylaldimine Ru alkylidene complexes.

The mechanistic pathway (Scheme 1.17) of the mononuclear complex **18** involves dissociation of one arm of the bidentate ligand instead of the usual PCy₃ ligand dissociation encountered in conventional phosphine based complexes. Drozdak *et al.* [72] explained why the N bonded arm was the one that dissociates. Firstly they added CuCl which is a phosphine scavenger, with the expectation that metathesis reaction rate would increase but this was not observed. Secondly they took into account the *trans* effect [73] which is prominent when N and P atoms are combined as donor ligands because of differences in their e⁻ donating properties as well as the difference in behaviour in terms of the hard and soft acid-base theory. The argument was that Ru is a fairly soft metal that will prefer to bond with a softer P atom than N atom which is a harder donor than P [74]. Even though the O atom is a harder donor than the N atom, its dissociation was not considered because there is no *trans* position of O and P atom as well as the fact that M-O bonds are generally stronger than M-N bonds. Further evidence was obtained from the study of the ROMP of norbornene monitored by ³¹P NMR, where there was no evidence to show the release of the PCy₃ ligand.



Scheme 1.17: Proposed mechanisms for the mononuclear and dinuclear Ru complexes **18** and **21**

In the dinuclear Ru complex, the mechanism is a two step dissociation mechanism involving a sequential heterolytic cleavage of 2 chloro bridges with the liberation of RuCl₂(*p*-cymene).

1.8 Decomposition of Ruthenium alkylidene catalysts

Despite the high activity of Grubbs generation one and two as well as their functional group tolerance, these catalysts have other short-comings especially when they are applied to large scale commercial catalysis. The major challenge is the short lifetime of the catalyst. The other disadvantages are side reactions like double bond isomerization that reduces the selectivity to form the desired products. It is thus important to understand the decomposition reactions these catalysts undergo. This may lead to the design of better catalysts and catalyst systems.

The Grubbs type catalysts have been thermally and kinetically studied to understand their stability. Several decomposition processes that it undergoes have been reported. These include: substrate induced decomposition, bimolecular decomposition reactions, thermal

decomposition of methylenes [75] as well as decomposition reactions between Grubbs type catalysts with water, alcohol and oxygen.

In substrate induced decomposition reactions, the Grubbs methylene catalysts were subjected to ethenolysis conditions *via* a β -hydride transfer from a metallocyclobutane intermediate with the formation of propene amongst other short chain hydrocarbons.

Bimolecular decomposition reactions of propylidene revealed that the major decomposition products are free PCy_3 , trans-3-hexene, which is formed from dimerization of the alkylidene fragment [75] as well as unidentified ruthenium products which are believed to include several hydrides. This was also seen when the benzylidene compound was tested as the catalyst [76]. Thermal decomposition reactions are first order with respect to phosphine concentration and are not inhibited by excess phosphine. All the evidence showed that a unimolecular reaction takes place and involves intramolecular activation of the phosphine ligand. Grubbs *et al.* [77] studied the decomposition of the second generation ruthenium methylene catalyst in benzene which resulted in formation of methyltricyclohexylphosphonium chloride and an isomerization active dinuclear ruthenium carbyne complex which was isolated.

Decomposition of Grubbs generation one and two catalysts when reacted with water, alcohol and air were studied by Mol and co-workers [78]. They found that the Grubbs G1 catalyst (**5a**) is degraded to form Ru hydride species when reacted with primary alcohols or water whilst it forms carbonyl species in the presence of oxygen. The studies also showed that the second generation Grubbs catalyst reacts with water, primary alcohols or oxygen to form carbonyl ruthenium complexes [79]. This was confirmed by Ki-Won Jun *et al.* [80] who reported that the Grubbs second generation catalyst reacts with water to form benzaldehyde

and a ruthenium aqua complex. These studies give insight into the reaction conditions under which the Grubbs type catalysts should be handled, that is, in dry, inert atmosphere in order to avoid decomposition of the catalysts.

1.9 Non metathesis reactions of ruthenium alkylidene

There are some side reactions that occur during metathesis reactions. These non metathesis reactions include isomerization, degenerate alkylidene proton exchange, halide exchange and the Kharasch reaction. Isomerization is regarded as the major side reaction and hampers the selectivity of the catalyst towards the desired products. Sworen [81] and Lehman [64] have reported extensively on isomerization reactions when using Grubbs complexes **5** and **6**.

Degenerate alkylidene proton exchange of the carbene proton was observed when soluble Ru alkylidenes were dissolved in protic solvents such as D₂O and CD₃OD. Grubbs *et al.* [82] reported that the rate of exchange is inversely proportional to the concentration of Cl⁻ added in aqueous solution. Halide exchange is possible in protic media as Cl⁻ dissociates from the benzylidene catalyst. This affects the activity and selectivity of the complex.

The Kharasch reaction is the addition of a haloalkane, *e.g.*, CHCl₃, across olefin substrates to form polyhalogenated alkanes. Ru alkylidene complexes have been observed to catalyze this reaction under milder conditions rather than the conventional Kharasch catalyst RuCl₂PPh₃ [83].

1.10 Immobilization of Ru alkylidene complexes

The focus on immobilization of metathesis catalysts is vital to increase selectivity of the homogeneous catalyst as well as to achieve ease of separation of the catalyst from the

substrate with the aim of catalyst recycling. This allows for the combination of the advantages of both homogeneous and heterogeneous catalysis.

Supported Ru metathesis catalysts have been reported [84] where the phosphine ligand is bound to the support but this suffered from metal leaching that occurred when ligand dissociation takes place.

The second generation Hoveyda “boomerang” system was successfully synthesized with good activity and the catalyst was recycled [85-88]. In a boomerang system the catalyst is effectively dispersed into a reaction mixture upon being freed after the initial catalytic cycle but is then recaptured by a resin when the reaction is complete [89]. Second generation Hoveyda catalyst bound to dendrimer and polymer supports have also been reported [90]. These systems however showed that Ru was released from the support during the metathesis reaction and the activity diminished after recycling the catalyst.

Grubbs complex, **5a**, was immobilized on a functionalized polystyrene resin doped with silver nitrate and the supported catalyst was easily separated from the reaction mixture forming products free of Ru and the catalyst was recycled [91]. A second generation Grubbs catalyst supported on silica was also reported [92] where one of the mesityl group was replaced with a R-Si(OEt)₃ tail which ultimately reacts with silanol groups on the silica surface to give a supported complex. The catalytic results from RCM showed that the catalyst can be recycled 5 times without losing activity.

Verpoort and coworkers anchored a salicylaldimine Ru complex on MCM-41 by modifying the salicylaldimine Ru carbene complex with a triethoxysilyl group attached to the terminus of N atom of the imine functionality. This was then reacted with the hydroxyl groups on the

silica [72] which allows for the ligand to be bound to the silica support. These results were preliminary and it is envisaged that other ways of studying activity, selectivity and recycling of the catalyst would be possible.

1.10.1 Dendrimers as supports

The formation of dendritic macromolecules with a highly branched three dimensional framework was first reported in the mid 1980's [93]. Ever since then these macromolecules have gained increasing attention with many research groups focusing on their synthesis and application in several catalytic reactions [94]. The generic procedures to synthesize dendrimers follow two possible paths, that is, the divergent and the convergent pathways (Figure 1.4). In the divergent approach, the starting reagent is the core molecule reacting with active monomers resulting in a core with peripheral clusters around it. The convergent approach starts with the reaction of monomers to form a periphery which is then reacted with the core at the end. These pathways result in dendrimeric structures that are highly branched, well-defined 3D molecules. It is as a result of the characteristic branched motifs as well as their unique physical and chemical properties that dendrimers have been applied in many processes such as catalysts, as novel amphiphiles, complexing agents and magnetic resonance imaging contrast agents [95]. Dendrimers can also be used in the synthesis of nanoparticles [96] and the dendritic encapsulation of active molecules that can be used as biosensors [97].

It was in the early 1990's when Balzani *et.al.* [98] and Newkome [100] reported the use of metal centers for structural branching and framework connectivity for metallodendrimer construction *via* metal coordination with polypyridines. Metals were added to or incorporated into the dendritic framework where they serve as branching centers or as the core and or structural auxiliaries at the termini of the dendrimer.

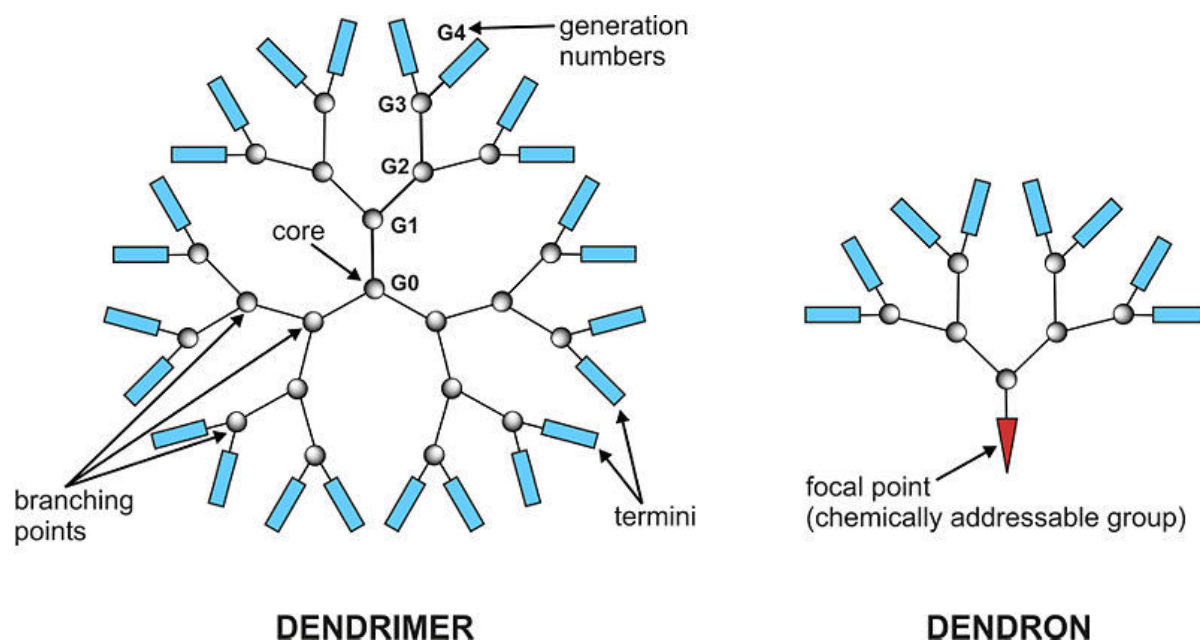


Figure 1.4: The dendrimeric framework.

There are a number of reasons for the synthesis of dendritic catalysts. Firstly there is a possibility of creating large dendrimers with many active sites because of the unique structure of dendrimers. Therefore the combination of high surface area and high solubility makes dendrimers useful as nanoscale catalysts. The presence of many chain ends is responsible for high solubility, miscibility and high activity [101]. This lead to the production of dendrimeric catalysts that combine the advantages of both homogeneous and heterogeneous catalysts. Homogeneous catalysts are effective due to good accessibility of active sites but they are often difficult to separate from the reaction mixture. Heterogeneous catalysts are easy to separate from the reaction stream by filtration [96b] but the rate of the reaction is limited by mass transport problems. Another point of importance in the synthesis of dendritic catalysts is the possibility of encapsulating a single catalytic site whose activity and selectivity become enhanced by the dendritic superstructure [102]. The encapsulated guest molecules e.g. metals are found in the interior of the macromolecule. These positive attributes of dendrimeric catalysts open a wide range of applications in industrial processes as well as environmentally friendly processes.

There are many reports on the synthesis and application of catalytic dendrimers. The first case was described by the group of van Koten [96b]. They functionalized soluble polycarbosilane dendrimers with diamino arylnickel(II) complexes. Such dendrimers can be used in addition reactions of polyhaloalkanes. Cooper and co-workers [103] reported a synthesis of fluorinated dendrimers which were soluble in supercritical CO₂ and can be used to extract strongly hydrophilic compounds from water into liquid CO₂. This may help to develop technologies in which hazardous organic solvents are replaced by liquid CO₂. There are several reports in which metallodendrimers have been used in many catalytic processes such as polymerization, oligomerization, C-C coupling reactions, Diels-Alder reactions etc.

Ongoing research to provide convincing practical demonstrations of the obvious advantages of catalysts containing multiple active sites (dendrimeric catalysts) in terms of its synthesis and application in many industrial processes is still a growing field. One of the advantages of these systems is recycling of catalysts and thus the possibility to practice green chemistry.

1.11 Aims and objectives

The project has the aim of synthesizing modified Grubbs complexes that would be further used as catalysts in catalytic reactions *viz.* olefin metathesis. The modification of Grubbs catalysts is motivated by the fact that these catalysts are largely homogeneous in nature, meaning that they cannot be recycled and that they have short life times in the reaction mixture leading to permanent decomposition of the complexes. The intended modification is to heterogenize metathesis catalysts by complexing them to dendrimer ligands. The type of ligands that would be explored are generally of the Schiff base type and resemble the well known salicylaldimine (N,O) chelators as well as the pyridine-imine (N,N) ligands. As explained in 1.6.4 mononuclear salicylaldimine complexes have been previously reported in which the N,O chelate had been bound to either Grubbs generation 1 or generation 2 catalysts.

The intent of this work was to expand these systems to dendritic ligands. This will lead to formation of a bulk substance that could be potentially separated by ultra-filtration. It also combines some advantages of both homogeneous and heterogeneous catalysis. The use of a dendrimer provides a new type of Grubbs catalyst that could show different selectivity and can potentially have different activity when compared to conventional catalysts as well as having the ability to be recycled. The work that will be covered involves the synthesis of dendritic ligands. These ligands will be complexed to Ru by reacting Grubbs generation one and two complexes with appropriate dendrimeric (N, O) and (N, N') Schiff base ligands. Chapter 2 covers a detailed description of the synthesis and full characterization of the dendritic ligands. Chapter 3 will cover a detailed description of the synthesis of new dendritic Ru complexes. The application of some of these complexes in olefin metathesis catalysis will also be evaluated comparing the influence of the type of donor ligands in terms of activity as well as selectivity. This is covered in Chapter 4 of the thesis.

1.12 References:

1. (a) Eleuterio, H. S., *J. Mol. Catal.*, **1991**, *65*, 55. (b) Eleuterio, H., *CHEMTECH.*, **1991**, *93*. (c) Banks, R. L., *CHEMTECH.*, **1986**, 112. (d) Anderson, A. W., *Chem. Abstr.*, **1956**, *50*, 3008i.
2. (a) Calderon, N., *Acc. Chem. Res.*, **1972**, *5*, 127. (b) Calderon, N.; Chen. H. Y.; Scott, K. W., *Tetrahedron Lett.*, **1967**, *34*, 3327.
3. (a) Leconte, M.; Basset, J. M.; Quignard, F.; Larroche, C. Mechanistic Aspects of the Olefin Metathesis Reaction in Reactions of Coordinated Ligands; Braterman, P. S. Ed.; Plenum: New York, **1986**, *1*, 371. (b) Grubbs, R. H. Alkene and Alkyne Metathesis Reactions, in: *Comprehensive Organometallic Chemistry*; Wilkinson, G.; Stone F. G. A., Abel, E. W.; Eds. Pergamon: Oxford, **1982**, *8*, 54, 499. (c) Katz, T. J.; McGinnis, J. *J. Am. Chem. Soc.*, **1977**, *99*, 1903. (d) Grubbs, R. H.; Carr, D. D.; Hoppin, C.; Burk, P. L., *J. Am. Chem. Soc.*, **1976**, *98*, 3478.
4. Herrison, J. L.; Chauvin, Y., *Macromolecules*, **1971**, *141*, 161.
5. Murdzek, J. S.; Schrock, R. R., *Organometallics*, **1987**, *6*, 1373.
6. Nguyen, S.T.; Johnson, L. K.; Grubbs, R. H.; Ziller, J. W., *J. Am. Chem. Soc.*, **1992**, *114*, 3974.
7. van Leeuwen, P. W. N. M., *Homogeneous Catalysis, Understanding the Art*, Kluwer Academic Publishers: Dordrecht, **2004**, 176.
8. Mol, J. C., *J. Mol. Catal. A, Chemical*, **2004**, *213*, 39.
9. Chauvin, Y., *Angew. Chem. Int. Ed.*, **2006**, *45*, 3740.
10. Katz, T. J.; Grubbs, R. H., *Handbook of Metathesis* Ed.; Wiley VCH: Weinheim, **2003**, *1*, 47.
11. Trnka, M.; Grubbs, R. H., *Acc. Chem. Res.*, **2001**, *34*, 18.
12. Fischer, E. O.; Maasbol, A. A., *Angew. Chem. Int. Ed. Engl.*, **1964**, *3*, 580.
13. Schrock, R. R., *J. Mol. Catal. A*, **2004**, *213*, 21.

14. Grubbs, R. H., *Tetrahedron*, **2004**, *60*, 7117.
15. Grubbs, R. H., *Handbook of Metathesis* Ed.; Wiley VCH: Weinheim, **2003**, *1*, 4.
16. Tebbe, F. N.; Parshall, G. W.; Reddy, G. S., *J. Am. Chem. Soc.*, **1978**, *100*, 3611.
17. (a) Casey, C. P.; Burkhardt, T. J., *J. Am. Chem. Soc.*, **1973**, *95*, 5833. b) Casey, C. P.; Burkhardt, T. J.; Bunnell, C. A.; Calabrese, J. C., *J. Am. Chem. Soc.*, **1977**, *99*, 2127.
18. Wengrovius, J. H.; Schrock, R. R.; Churchill, M. R.; Missert, J. R.; Youngs, W. J., *J. Am. Chem. Soc.*, **1980**, *102*, 4515.
19. Schrock, R. R.; Rocklage, S. M.; Wengrovius, J. H.; Rupprecht, G. A.; Fellman, J., *J. Mol. Catal.*, **1980**, *8*, 103.
20. Pedersen, S. F.; Schrock, R. R.; Churchill, M. R.; Wasserman, H. J., *J. Am. Chem. Soc.*, **1982**, *104*, 6808.
21. Schaverien, C. J.; Dewan, J. C.; Schrock, R. R., *J. Am. Chem. Soc.*, **1986**, *108*, 832.
22. (a) Bazan, G. C.; Oskam, J. H.; Cho, H. N.; Park, L. Y.; Schrock, R. R., *J. Am. Chem. Soc.*, **1991**, *113*, 6899. (b) Bazan, G. C.; Khosravi, E.; Schrock, R. R.; Feast, W. J.; Gibson, V. C.; O'Regan, M. B.; Thomas, J. K.; Davis, W.M., *J. Am. Chem. Soc.*, **1990**, *112*, 8378. (c) Murdzek, J. S.; Bazan, G. C.; Robbins, J.; DiMare, M.; O' Regan, M. J.; Schrock R. R., *J. Am. Chem. Soc.*, **1990**, *112*, 3875.
23. (a) Schrock, R. R., *Tetrahedron*, **1999**, *55*, 8141. (b) Schrock, R. R., *Acc. Chem. Res.*, **1990**, *23*, 158.
24. (a) Kirkland, T. A.; Grubbs, R. H., *J. Org. Chem.*, **1997**, *62*, 7310. (b) Grubbs R. H.; Miller, S. J.; Fu, G.C., *Acc. Chem. Res.*, **1995**, *28*, 446.
25. (a) Clapham, S. E.; Hadzovic, A.; Morris, R. H., *Coord. Chem. Rev.*, **2004**, *248*, 2201. (b) Csabai, Joo, P. F., *Organometallics*, **2004**, *23*, 5640. (c) Genet, J. P., *Acc. Chem. Res.*, **2003**, *36*, 908. (d) Barbaro, P.; Bianchini, C.; Meli, A.; Moreno, M.; Vizza, F., *Organometallics*, **2002**, *21*, 1430. (e) Zhou, Y. G.; Thang, W.; Wang, W.; Li, B.; Zhang,

- W. X., *J. Am. Chem. Soc.*, **2002**, *124*, 4952. (f) Louie, J.; Bielawski, C.W.; Grubbs, R. H., *J. Am. Chem. Soc.*, **2001**, *123*, 11312.
26. (a) Tokunaga, M.; Suzuki, T.; Koga, N.; Fukushima, T.; Horiuchi, A.; Wakatsuki, Y., *J. Am. Chem. Soc.*, **2001**, *123*, 11917. (b) Bianchini, C.; Peruzzini, M.; Zanobini, F.; Lopez, C.; De los Rios, I.; Ramerosa, A., *Chem. Commun.*, **1999**, 443. (c) Bianchini, C.; Casares, J.A.; Peruzzini, M.; Romerosa, A.; Zanobini, F., *J. Am. Chem. Soc.*, **1996**, *118*, 4585.
27. (a) Ramesh, R., *Inorg. Chem. Commun.*, **2004**, *7*, 274. (b) Miyata, A.; Furukawa, M.; Irie, R.; Katsuki, T., *Tetrahedron Lett.*, **2002**, *43*, 3481. (c) Miyata, A. Murakami, Irie, M. R. Katsuki, T., *Tetrahedron Lett.*, **2001**, *42*, 7097. (d) Rajendran, S.; Trivedi, D. C., *Synthesis*, **1995**, 153. (e) Kuwabara, T.; Saito, T.; Kumobayashi, H.; Akutagawa, S., *J. Am. Chem. Soc.*, **1990**, *112*, 7812.
28. (a) Shrikanth, A.; Nagendrappa, G.; Chandrasekaran, S., *Tetrahedron*, **2003**, *59*, 7761. (b) Groves, T. J.; Quinn, R., *J. Am. Chem. Soc.*, **1985**, *107*, 5790.
29. (a) Antonya, R.; Tembea, G. L.; Ravindranathana, M.; Ramb, R. N., *Polymer*, **1998**, *39*, 4327. (b) Matteoli, U.; Bianchi, M.; Frediani, P.; Menchi, G.; Boteghi, C.; Marchetti, M., *J. Organomet. Chem.*, **1984**, *263*, 243.
30. (a) Jenner, G.; Nahmed, E. M.; Leismann, H., *J. Organomet. Chem.*, **1990**, *38*, 7315. (b) de Vries, J. G.; Roelfes, G.; Green, R., *Tetrahedron Lett.*, **1998**, *39*, 8329. (c) Jung, C. W.; Garou, P. E., *Organometallics 1*, **1982**, *9*, 658.
31. (a) Lebel, H.; Marcoux, J. F.; Molinaro, C.; Charette, A. B., *Chem. Rev.*, **2003**, *103*, 977. (b) Werle, T.; Maas, G., *Adv. Synth. Catal.*, **2001**, *343*, 37. (c) Noels, A. F.; Demonceau, A., *J. Phys. Org. Chem.*, **1998**, *11*, 602. (d) Maas, G.; Werle, T.; Alt, M.; Mayer, D., *Tetrahedron*, **1993**, *49*, 881. (e) Demonceau, A.; Saive, E.; de Froidmont, Y.; Noels, A. F.; Hubert, A. J.; Chizhevsky, I. T.; Lobanova, I. A.; Bregadze, V. I.,

- Tetrahedron Lett.*, **1992**, *33*, 2009. (f) Demonceau, A.; Noels, A. F.; Saive, E.; Hubert, A. J., *J. Mol. Catal.*, **1992**, *76*, 123.
32. (a) Fürstner, A., *Alkene Metathesis in Organic Synthesis*, Springer: Berlin, **1998** (b) Fürstner, A., *Angew. Chem.*, **2000**, *112*, 3140. (c) Fürstner, A., *Angew. Chem. Int. Ed.*, **2000**, *39*, 3012. (c) Pariya, C.; Jayaprakash, K. N.; Sarkar, A., *Coord. Chem. Rev.*, **1998**, *168*, 1. (d) Dragutan, V.; Dragutan, I.; Balaban, A. T., *Platinum Met. Rev.*, **2001**, *45*, 155.
33. Odenkirk, W.; Reingold, A. L.; Bosnich, B., *J. Am. Chem. Soc.*, **1992**, *114*, 6392.
34. De Clercq, B.; Verpoort, F., *Adv. Synth. Catal.*, **2002**, *344*, 639.
35. (a) Kamigaito, M.; Ando, T.; Sawamoto, M., *Chem. Rev.*, **2001**, *101*, 3689. (b) Sawamoto, M.; Kamigaito, M., *Chemtech.*, **1999**, *29*, 30. (c) Simal, F.; Delaude, L.; Jan, D.; Demonceau, A.; Noels, A. F., *Polym. Prepr., (Am. Chem. Soc. Div. Polym. Chem.)* **1999**, *40*, 336.
36. (a) Grundwald, C.; Gevert, O.; Wolf, J.; Gonzales-Herrero, P.; Werner, H., *Organometallics*, **1996**, *15*, 1960. (b) Drouin, S. D.; Yap, G. P. A.; Fogg, D. E., *Inorg. Chem.*, **2000**, *39*, 5412.
37. (a) Nguyen, S. T.; Johnson, L. K.; Grubbs, R. H.; Ziller, J. W., *J. Am. Chem. Soc.*, **1992**, *114*, 3974. (b) Johnson, L. K.; Grubbs, R. H.; Ziller, J. W., *J. Am. Chem. Soc.*, **1993**, *115*, 8130.
38. (a) Michelotti, F. W.; Keaveney, W. P., *J. Polym. Sci. A3*, **1965**, 895. (b) Rinehart, R. E.; Smith, P. H., *Polym. Lett.*, **1965**, *3*, 1049.
39. (a) Novak, B. M.; Grubbs, R. H., *J. Am. Chem. Soc.*, **1988**, *110*, 7542. (b) Ancieux, A. J.; Hubert, A. J.; Noels, A. F.; Petiniot, N.; Teyssie, P., *J. Org. Chem.*, **1980**, *45*, 695.
40. (a) Lee, H. M.; Bianchini, C.; Jia, G.; Barbaro, P., *Organometallics*, **1999**, *18*, 1961. (b) Demonceau, A.; Diaz, E. A.; Lemoine, C. A.; Stumpf, A. V.; Petraszuk, C.; Gulinski, J.; Marcinec, B., *Tetrahedron Lett.*, **1995**, *36*, 3519.

41. (a) Tfouni, E.; Ferreira, K. Q.; Doro, F. G.; DaSilva, R. S.; DaRocha, Z. N., *Coord. Chem. Rev.*, **2005**, *249*, 405. (b) Distefano, A. J.; Nishart, J. F.; Isied, S. S., *Coord. Chem. Rev.*, **2005**, *249*, 507. (c) Toledo, J. C.; Neto, B. S. L.; Franco, D. W., *Coord. Chem. Rev.*, **2005**, *249*, 419.
42. (a) Harrity, J. P. A.; La, D. S.; Visser, M. S.; Hoveyda, A. H., *J. Am. Chem. Soc.*, **1998**, *120*, 2343. (b) Kingsbury, J. S.; Harrity, J. P.; Bonitatebus, P. J.; Hoveyda, A. H., *J. Am. Chem. Soc.*, **1999**, *121*, 791. (c) Gessler, S.; Randl, S.; Blechert, S., *Tetrahedron Lett.*, **2000**, *41*, 9973. (d) Wakamatsu, H.; Blechet, S., *Angew. Chem.*, **2002**, *114*, 832. (e) Wakamatsu, H.; Blechet, S., *Angew. Chem. Int. Ed.*, **2002**, *41*, 794. (f) Grela, K.; Harutyunyan, S.; Michrowska, A., *Angew. Chem.*, **2002**, *114*, 4210.
43. Michrowska, A., *Angew. Chem. Int. Ed.*, **2002**, *41*, 4038. (h) Zaja, M.; Connon, S. J.; Dunne, A. M.; Rivard, M.; Buschmann, N.; Jiricek, J.; Blechert, S., *Tetrahedron*, **2003**, *59*, 6545.
44. (a) Mühlebach, A.; van der Schaaf, P. A.; Hafner, A.; Kolly, R.; Rime, F.; Kimer, H. J., *In Ring-opening Metathesis Polymerisation and Related Chemistry*; E. Khosravi, T. Szymanska-Buzar Ed.; Kluwer Academic Publishers: Dordrecht, Netherlands, 2002, p. 23. (b) van der Schaaf, P. A.; Kolly, R.; Kirner, H. J.; Rime, F.; Mühlebach, A.; Hafner, A., *J. Organomet. Chem.*, **2000**, *606*, 65. (c) Hafner, A.; Mühlebach, A.; van der Schaaf, P. A., *Angew. Chem.*, **1997**, *109*, 2213. (d) Hafner, A.; Mühlebach, A.; van der Schaaf, P. A., *Angew. Chem. Int. Ed.*, **1997**, *36*, 2121. (e) Karlen, T.; Ludi, A.; Mühlebach, A.; Bernhard, P.; Pharisa, C., *J. Polym. Sci., Pt. A: Polym. Chem.*, **1995**, *33*, 1665. (e) Ung, T.; Hejl, A.; Grubbs, R. H.; Schrodi, Y., *Organometallics*, **2004**, *23*, 5399.
45. (a) Slugovc, C.; Schmid, R.; Kirchner, K., *Coord. Chem. Rev.*, **1999**, *186*, 109. (b) Buriez, B.; Cook, D. J.; Harlow, K. J.; Hill, A. F.; Welton, T.; White, A. J. P.; Williams, D. J.; Wilton-Ely, J. D. E. T., *J. Organomet. Chem.*, **1999**, *578*, 264. (c) Togni, A.; Venanzi, L. M., *Angew. Chem. Int. Ed.*, **1994**, *33*, 497. (d) Sanford, M. S.; Henling, L.

- M.; Grubbs, R. H., *Organometallics*, **1998**, *17*, 5384. (e) Sanford, M. S., Love, J. A., Grubbs, R. H., *J. Am. Chem. Soc.*, **2001**, *123*, 6543. (f) Nishiyama, H.; Itoh, Y.; Sugawara, Y.; Matsumoto, H.; Aoki, K.; Itoh, K., *Bull. Chem. Soc. Jpn.*, **1995**, *68*, 1247. (g) Wong, C.-Y.; Chan, M. C. W.; Zhu, N.; Che, C.-M., *Organometallics*, **2004**, *23*, 2363. (h) Weskamp, T.; Kohl, F.J.; Hieringer, W.; Gleich, D.; Herrmann, W. A., *Angew. Chem., Int. Ed. Engl.*, **1999**, *83*, 2416.
46. (a) Iwasa, S.; Tsushima, S.; Nishiyama, K.; Tsuchiya, Y.; Takesawa, F.; Nishiyama, H., *Tetrahedron: Asymm.*, **2003**, *14*, 855. (b) Chelucci, G.; Saba, A.; Vignola, D.; Solinas, C., *Tetrahedron*, **2001**, *57*, 1099. (c) Bianchini, C.; Lee, H. M., *Organometallics*, **2000**, *19*, 1833. (d) Nishiyama, H.; Itoh, Y.; Sugawara, Y.; Matsumoto, H.; Aoki, K.; Itoh, K., *Bull. Chem. Soc. Jpn.*, **1995**, *68*, 1247.
47. (a) Yao, X.; Qiu, M.; Li, W.; Chen, H.; Zheng, Z., *Tetrahedron Asymm.*, **2001**, *12*, 197. (b) Zheng, Z.; Yao, X.; Li, C.; Chen, H.; Hu, X., *Tetrahedron Lett.*, **2001**, *42*, 2847. (c) Munslow, I. J.; Gillespie, K. M.; Deeth, R. J.; Scott, P., *Chem. Commun.*, **2001** 1638.
48. Stumpf, A.W.; Saive, E.; Demonceau, A.; Noels, A. F., *Chem. Commun.*, **1995** 1127.
49. (a) Schwab, P.; France, M. B.; Ziller, J. W.; Grubbs, R. H., *Angew. Chem. Int. Ed.*, **1995**, *34*, 2039. (b) Dragutan, V.; Dragutan, I.; Verpoort, F., *Platinum Met. Rev.*, **2005**, *49*, 33. (c) Jafarpour, L.; Schanz, H.-J.; Stevens, E. D.; Nolan, S. P., *Organometallics*, **1999**, *18*, 5416. (d) Katayama, H.; Ozawa, F., *Coord. Chem. Rev.*, **2004**, *248*, 1703.
50. Doyle, M. P.; McKervey, M. P.; Ye, T., *Modern Catalytic Methods for Organic Synthesis with Diazo Compounds*, Wiley: New York, 1998.
51. (a) Finkelstein, H., *Ber.*, **1910**, *43*, 1528. (b) Richardson, T. I., Rychnovsky, S. D., *J. Am. Chem. Soc.*, **1977**, *119*, 12360.
52. (a) Zoebel, B.; Lim, A. E. K.; Dunn, K.; Dakternieks, D., *Organometallics*, **1999**, *18*, 4990. (b) Pikina, E. I.; Talalaeva, T. N.; Kocheschov, K. A., *J. Gen. Chem. USSR.*, **1938**, *8*, 1844. (c) Kocheschov, K. A.; Nesmeyanov, A. N., *Chem. Ber.*, **1931**, *64*, 628.

53. (a) Grubbs R. H., Ed.; *Handbook of Metathesis*, Wiley–VCH: Weinheim, **2003**; vol. III.
(b) Hopkins, T.E.; Wagener, K. B., *Macromolecules*, **2004**, *37*, 1180.
54. Trost, B. M., *The atom economy-a search for synthetic efficiency science*, **1991**, *254*, 1471.
55. Cannon, S. J.; Blechert, S., *Angew. Chem. Int. Ed.*, **2003**, *42*, 1900.
56. Maughon, B. R.; Weck, M.; Mohr, B.; Grubbs, R. H., *Macromolecules*, **1997**, *30*, 257.
57. Chatterjee, A. K.; Choi, T.-L.; Sanders, D. P.; Grubbs, R. H., *J. Am. Chem. Soc.*, **2003**, *125*, 11360.
58. Herrmann, W. A.; Köcher, C., *Angew. Chem., Int. Ed. Engl.*, **1997**, *36*, 2163.
59. Dias, E. L.; Nguyen, S. T.; Grubbs, R. H., *J. Am. Chem. Soc.*, **1997**, *119*, 3887.
60. (a) Bourissou, D.; Guerret, O.; Gabbaï, F. P.; Bertrand, G. *Chem. Rev.*, **2000**, *100*, 39.
(b) Arduengo, A. J., *Acc. Chem. Res.*, **1999**, *32*, 913.
61. (a) Weskamp, T.; Schattenmann, W. C.; Spiegler, M.; Herrmann, W. A., *Angew. Chem., Int. Ed.*, **1998**, *37*, 2490. (b) Weskamp, T.; Schattenmann, W. C.; Spiegler, M.; Herrmann, W. A., *Angew. Chem., Int. Ed.*, **1999**, *38*, 262.
62. Nguyen, S. T., Trnka T. M., *Handbook of Metathesis*, Ed. Grubbs, R. H., Wiley VCH: Weinheim, 2003; Vol 1, 68.
63. Scholl, M.; Ding, S.; Lee, C. W.; Grubbs, R. H., *Org. Lett.*, **1999**, *1*, 953.
64. Lehman, S. E.; Scwendeman, J. E.; O'Donnell, P. M.; Wagener, K. B., *Inorg. Chem. Acta*, **2003**, *345*, 190.
65. Kingsbury, J. S.; Harrity J. P. A.; Bonitatebus, Jr, P. J.; Hoveyda, A. H., *J. Am. Chem. Soc.*, **1999**, *121*, 791.
66. Hoveyda, A. H.; Gillingham, D. G.; Van Veldhuizen, J. J.; Kataoaka, O.; Garber, S. B.; Kingsbury, J. S.; Harrity, J. P. A., *Org. Biomol. Chem.*, **2004**, *2*, 8.
67. US patent number US2003/0220512 A1, 27 Nov 2003.

68. Forman, G. S.; McConnell A. E.; Hanton, M. J; Slawin, A. M. Z.; Tooze, R. P.; van Rensberg, W.; Meyer, W. H.; Dwyer, C.; Kirk, M. M.; Serfontein, D. W., *Organometallics*, **2004**, *23*, 4824.
69. Forman, G. S.; McConnell, A. E.; Tooze, R. P.; Dwyer, C.; Serfontein, D. W. Sasol Technology UK, *World Patent*, 2003, ZA03/00087.
70. Crause, C.; Bennie, L.; Damoense, L.; Dwyer, C. L.; Grove, C.; Grimmer, N.; Janse van Rensburg, W.; Kirk, M. M.; Mokheseng, K.; Otto, S.; Steynberg, P. J., *Dalton Trans.*, **2003**, 2036.
71. a) Dias, E. L.; Grubbs, R. H. ,*Organometallics*, **1998**, *17*, 2758. (b) Dias, E. L. Ruthenium-Based Olefin Metathesis Catalysts: Synthesis, Mechanism, and Activity. Ph.D. Thesis, California Institute of Technology, 1998; Chapter 3.
72. Drozdak, R.; Allaert, B.; Ledoux, N.; Dragutan, I.; Dragutan, V.; Verpoort, F., *Coord. Chem. Rev.*, **2005**, *249*, 3055.
73. Chang, S.; Jones, L.; Wang, C.; Henling, L. M.; Grubbs, R. H. *Organometallics*, **1998**, *17*, 3460.
74. Burdett, J. K., *Molecular Shapes. Theoretical Models in Inorganic Stereochemistry*, Wiley: New York, 1980.
75. Pearson, R.G. *Hard and Soft Acids and Bases*, Dowden, Hutchinson and Ross Inc.: Pennsylvania, 1973.
76. Sanford M. S.; Love J. A., *Handbook of Metathesis* vol 1, Ed. Grubbs, R.H., Wiley VCH: Weinheim, **2003**, vol 1, 118.
77. Hong, S. H.; Day, M. W.; Grubbs, R. H., *J. Am. Chem. Soc.*, **2004**, *126*, 7414.
78. Dinger, M. B.; Mol, J. C., *Organometallics*, **2003**, *22*, 1089.
79. Dinger, M. B.; Mol, J. C., *Eur. J. Inorg. Chem.*, **2003**, 2827.
80. Mieock, K.; Eum, M.; Jin, M. J.; Jun, K.; Lee, C. W.; Kucn, K. A.; Kim, C. H.; Chin, C. S., *J. Organomet. Chem.*, **2004**, *689*, 3535.

-
81. Sworen, A.; Pawloa, J. H.; Case, W.; Lever, J.; Wagener, K., *J. Mol. Catal. A: Chem.*, **2003**, *194*, 69.
82. Grubbs, R. H.; Lynn, D. M., *J. Am. Chem. Soc.*, **2001**, *123*, 3187.
83. Snapper, M. L.; Tallaricao, J. A.; Malnick, L. M., *J. Org. Chem.*, **1999**, *64*, 344.
84. Melis, K.; De Vos, D.; Jacobs, P.; Verpoort, F., *J. Mol. Catal. A: Chem.*, **2001**, *169*, 47.
85. Nguyen, S. T.; Grubbs, R. H., *J. Organomet. Chem.*, **1995**, *497*, 195.
86. Dowden, J.; Savovic, J., *J Chem. Commun.*, **2001**, 37.
87. Yao, Q., *Angew. Chem. Int. Ed.*, **2000**, *39*, 3896.
88. Connon, S. J.; Blechert, S., *Bioorg. Med. Chem. Lett.*, **2002**, *12*, 1873.
89. Kingsbury, J. S.; Garber S. B.; Giftos, J. M.; Gray, B. L.; Okamoto, M. M; Farrer, R. A.; Foukras J. T.; Hoveyda, A. H., *Angew. Chem. Int. Ed.*, **2001**, *40*, 4251.
90. Ahmed M.; Barrett, A. G. M.; Braddock, D. C.; Cramp S. M.; Prociou, P., *Tetrahedron Lett.*, **1999**, *40*, 8657.
91. Grela, C.; Tryznowski M.; Bieniek, M., *Tetrahedron Lett.*, **2002**, *43*, 9055.
92. Niecypor, P.; Buchowicz, W.; Meester, W. J. N.; Rutjes F. J. P. T.; Mol, J. C., *Tetrahedron Lett.*, **2001**, *42*, 7103.
93. Cetinkaya B.; Gurbuz, N.; Seckin, T.; Ozdemir, I., *J Mol. Catal. A: Chem.*, **2002**, *184*, 31.
94. Bosman, A. W.; Jansen, H. M.; Meijer, E. W. ,*Chem. Rev.*, **1999**, *99*, 1665.
95. Hecht, S.; Frechet, J. M., *J. Angew. Chem. Int. Ed.*, **2001**, *40*, 74.
96. (a) Astruc, D.; Chardac, F., *Chem. Rev.*, **2001**, *101*, 2991. (b) Knapen, J. W. J.; van der Made, A. W.; de Wilde, J. C.; van Leewen, P. W. N. M.; Wijkens, P.; Grove, D. M.; van Koten, G., *Nature*, **1994**, *372*, 659. (c) Roy, R.; Zanini, D.; Meunier, S. J.; Romanowska,, A., *Chem. Commun.*, **1993**, 1869.
97. Crook, R. M.; Zhao, M.; Li, S.; Chechik, V.; Lee, K. Y., *Acc. Chem. Res.*, **2001**, *34*, 181.

-
98. (a) Jain, K. K., *Science*, **2001**, 294, 621. (b) Muller, W.; Ringsdorf, H.; Rump, E.; Wildburg, G.; Zhang, X.; Angermaier, L.; Knoll, W.; Liley, M.; Spinke, J., *Science*, **1993**, 262, 1706.
99. Murdzek, J. S.; Bazan, G. C.; Robbins, J.; DiMare, M.; O' Regan M. J.; Schrock, R. R., *J. Am. Chem. Soc.*, **1990**, 112, 3875.
100. Newkome, G. R.; He, E.; Moorefield, C. N., *Chem. Rev.*, **1999**, 99, 1689.
101. Fréchet, J. M. J., *Science*, **1994**, 263, 1710.
102. Brunner, H., *J. Organomet. Chem.*, **1995**, 500, 39.
103. Cooper, A. L.; Londono, J. D.; Wignall, G.; McClain, J. B.; Samulski, E. T.; Lin, J. S.; Dobrynin, A.; Burke, A. L. C.; Fréchet, J. M. J.; DeSimone, J. M., *Nature*, **1997**, 389, 368.

CHAPTER 2

SYNTHESIS AND CHARACTERIZATION OF MONOFUNCTIONAL AND DENDRITIC (N'N) AND (N'O) SCHIFF BASE LIGANDS

CONTENT

2.1 Introduction	43
2.2 Results and Discussion	44
2.2.1 Synthesis of 4 pyridyl-imine ligands	44
2.2.2 Synthesis of Salicylaldimine ligands (N,O) ligands	48
2.3 Characterization data of ligands	50
2.3.1 FT-IR characterization	53
2.3.2 ¹ H NMR characterization	56
2.3.3 ¹³ C{ ¹ H} NMR characterization	62
2.3.4 Elemental Analysis characterization	66
2.4 Conclusion	67
2.5 Experimental Section	67
2.5.1 Materials and Instrumentation	67
2.5.2 Synthesis of ligands	68
2.6 References	71

2.1 Introduction

This chapter covers the synthesis and characterization of new Schiff base ligands. Schiff bases are classified into several sub-groups such as salicylaldimines or diimines. Figure 2.1 shows typical examples of Schiff base ligands. Salicylaldimines have two donor sites comprising oxygen and nitrogen for the coordination of the ligand with transition metals. When the N, O donor sites are linked *via* a hydrocarbon bridge giving a tetradentate ligand i.e. [N, O, N', O'], the ligand is known as a salen-type ligand [1]. On the other hand diimine ligands have two N, N' donor sites. Diimines can be further sub-divided into chelating and non chelating ligands. This depends on the positioning of the donor sites. In Figure 2.1 it is type-I diimines are non-chelating because it has been found that only one donor site binds to the metal during complexation reactions, whereas type-II is a chelating ligand. The type of Schiff bases that will be of particular interest in this thesis will be salicylaldimines [N, O] and type-I diimines [N, N']. These ligands have found wide-ranging application due to their ease of preparation and their ability to coordinate metals through the imine nitrogen together with other groups that are usually bonded to the aryl substituents of the imine group. These ligands are commonly used in complexation reactions with metals. They are known to stabilize various metal oxidation states as well as controlling the performance of metals in a large variety of catalytic transformations. In the salicylaldimines, the phenolate O atom is regarded as a hard donor that stabilizes metals in higher oxidation states whereas the N atom, known as a soft donor. These ligands can be tuned appropriately to study steric and electronic effects around the metal center [2]. This chapter also describes the synthesis and characterization of dendrimeric ligands which are prepared *via* typical Schiff base condensation processes.

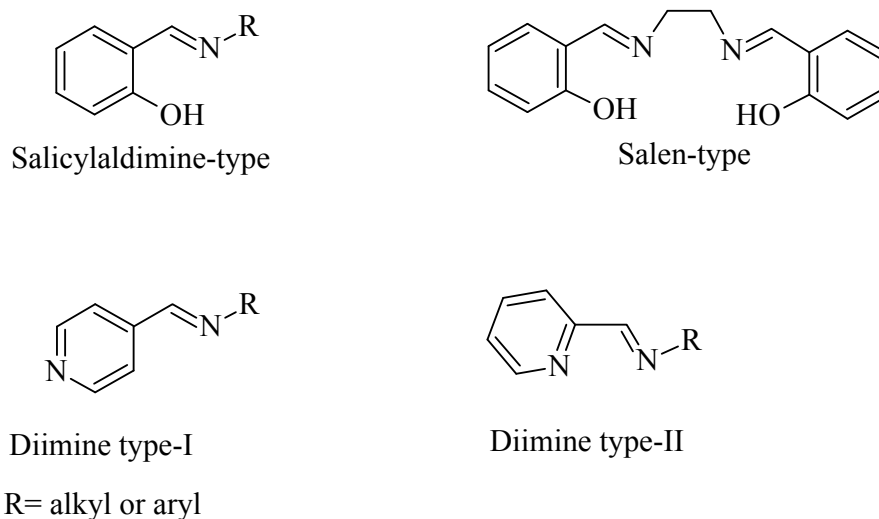
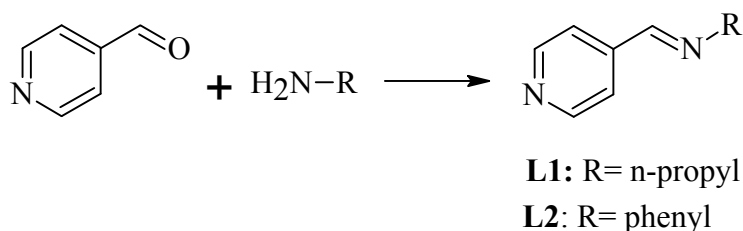


Figure 2.1: Model Schiff base ligands

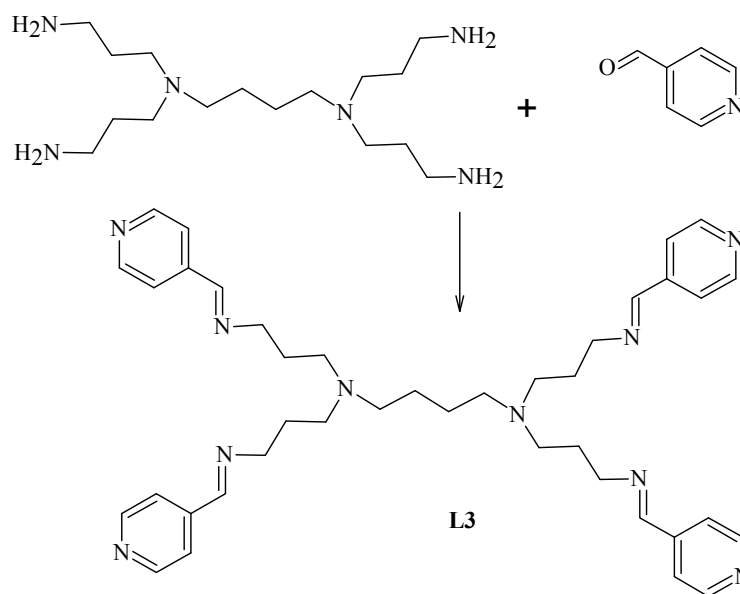
2.2 Results and Discussion

2.2.1 Synthesis of 4 pyridyl-imine ligands

The 4-imino pyridyl imine compounds are classified as diimines but are of the non-chelating type. Synthesis of these ligands proceeded *via* a Schiff base condensation reaction. The monofunctional ligands (**L1** and **L2**) shown in Scheme 2.1 were synthesized by reacting an appropriate primary amine with 4-pyridine carboxylaldehyde and are used as model ligands for the purpose of comparing the behaviour of their complexes with that of multifunctional (dendritic) compounds (**L3** and **L4**). Synthesis of dendritic imino-pyridine ligands was achieved through the reaction of the diaminobutane cored polypropyleneimine dendrimers, [DAB-(NH₂)_n] where (n=4 or 8) with 4-pyridine carboxylaldehyde. The reactions are outlined below in Schemes 2.1-2.3.



Scheme 2.1: Model salicylaldimine ligands.



Scheme 2.2: First generation dendritic 4-imino-pyridine functionalized ligand.

Similar ligands that resemble that of the model ligand (**L1**) has been previously reported [3], whilst ligand **L2** is a well known compound [4]. **L1** was isolated as a pale yellow oil while **L2** was obtained as a pale yellow crystalline solid. All the ligands (**L1-4**) were characterized by a range of analytical techniques (¹H and ¹³C{¹H} NMR) and FT-IR spectroscopy as well as ESI-MS. The characterization data of the resulting products demonstrated that they were successfully prepared. In the case of **L1** the ¹H NMR spectrum showed the typical HC=N resonance occurring at 8.21 ppm which is shielded relative to that of the protons attached to the C-atoms in the pyridine ring adjacent to the N-atom. The proton of the imine external to the ring has also shifted relative to the aldehyde proton resonance peak of the starting material which occurs at 10.04 ppm. FT-IR spectroscopy further confirms successful condensation by

the presence of the imine band at $\sim 1645\text{ cm}^{-1}$ which agrees well with that reported for similar compounds [3]. This spectrum is depicted in Figure 2.4. The ESI-MS shows a molecular ion peak at m/z 149 and is assigned as $[M+H]^+$.

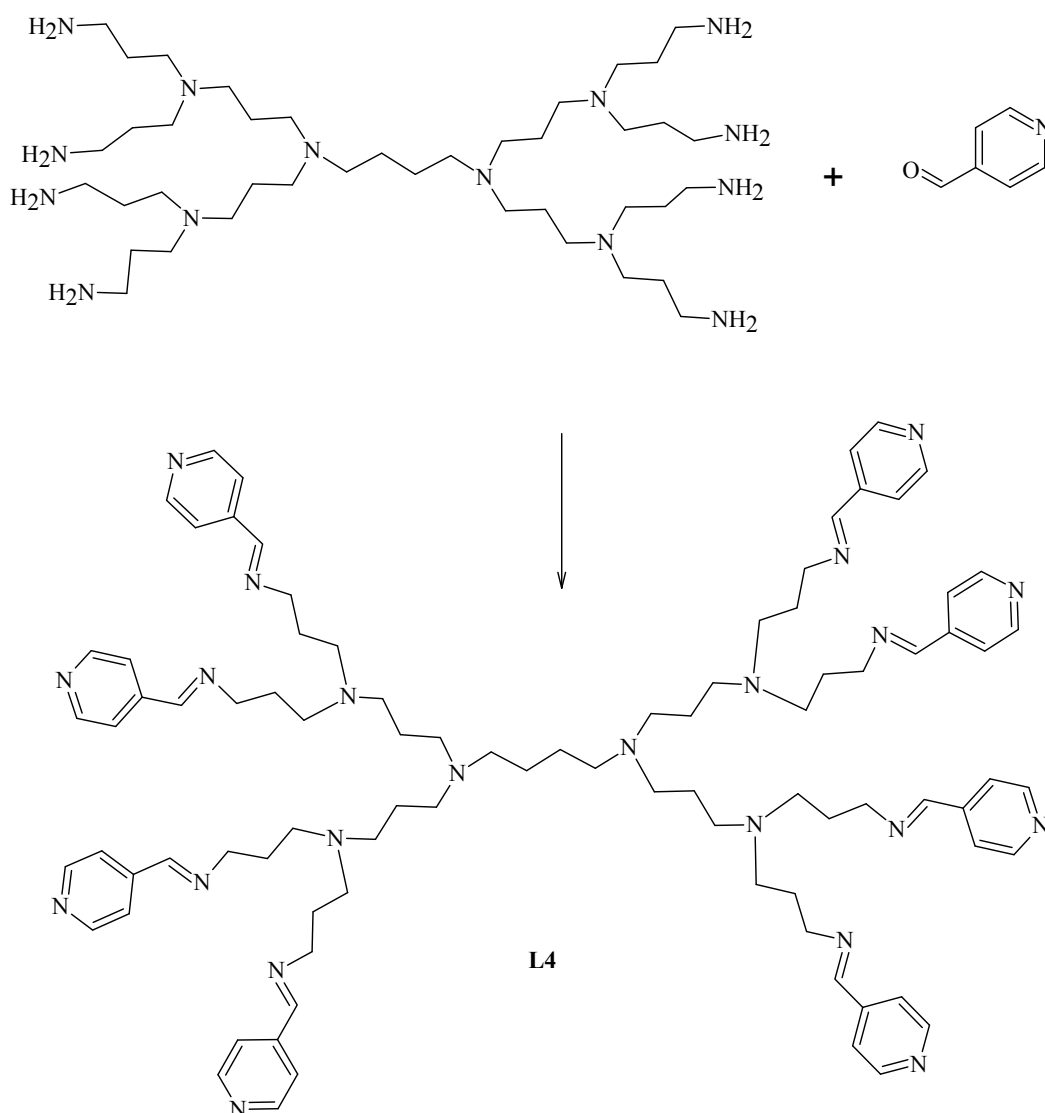
^1H NMR spectrum results for **L2** once again showed that condensation occurred as seen by the presence of the imine signal observed at 8.45 ppm. The FT-IR spectrum shows the imine peak at 1621 cm^{-1} . This agrees well with that reported by Wong *et al.* [4a]. ESI-MS shows a molecular ion peak at m/z 183 which is due to $[M+H]^+$. This is also in agreement with that reported by Steed *et al.* [4b].

The dendritic ligands with 4-imino pyridine units, have not previously been reported in the literature. The crude product was isolated as an orange oily residue. In order to purify these ligands, they were washed with diethyl ether to remove any impurities and were recovered as light orange waxy materials. In both cases the yields range between 70-80%. These ligands were found to be soluble in chlorinated solvents e.g. dichloromethane and chloroform whilst being insoluble in other common organic solvents. These N, N' ligands are stable in both solution as well as in the solid state provided they are kept under an inert atmosphere. Exposure to air for long periods lead to these ligands changing colour and yielding dark orange-brown sticky residues. Their characterization data are comparable to that of the monofunctional ligand (**L1**). This is seen from the ^1H NMR spectra which show the imine peaks around 8.18 ppm while the alkyl dendritic framework, typical of polypropyleneimine (PPI) dendrimers, are well resolved and all its protons accounted for. A typical ^1H NMR spectrum for this type of compound is shown in Figure 2.13. The FT-IR spectra of these ligands also show an imine stretch around 1645 cm^{-1} .

The ESI-MS of **L3** shows the molecular ion peak at m/z 673 whilst for **L4** the molecular ion peak is at m/z 1486. Besides the molecular ion peak, there were other fragment ions observed.

The important factor is that the dendrimers show similar fragmentation patterns regardless of the dendrimer generation. A doubly charged fragment at m/z 108 assigned to a peripheral imino-pyridine unit which had been cleaved from the original dendrimer is observed in the mass spectra of both **L3** and **L4**. A peak at m/z 584 for **L3** and m/z 1397 for **L4** show that the dendritic ligands undergo hydrolysis of one of the imine bonds on the periphery of the dendrimer. It also confirmed the symmetrical nature of a dendrimer where both had peaks at m/z 337 in **L3** and m/z 744 in **L4** which are due to cleavage of the DAB core resulting in the symmetrical fragments being formed.

Similar dendritic pyridyl Schiff base ligands but which are chelating in nature have been reported previously [5]. In the latter case the reported ligand is a generation one type dendrimer. The aldehyde used in this case is 2-pyridine carboxaldehyde instead of 4-pyridine carboxaldehyde. The characterization data of the chelating diimine are similar to that found for ligand **L3**, the only difference being, the signals of the pyridine ring.

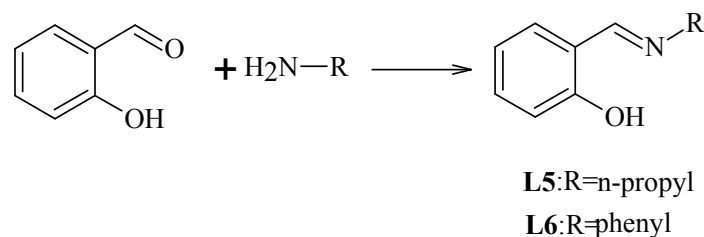


Scheme 2.3: Synthetic route for the formation of the second generation 4-imino pyridine ligand.

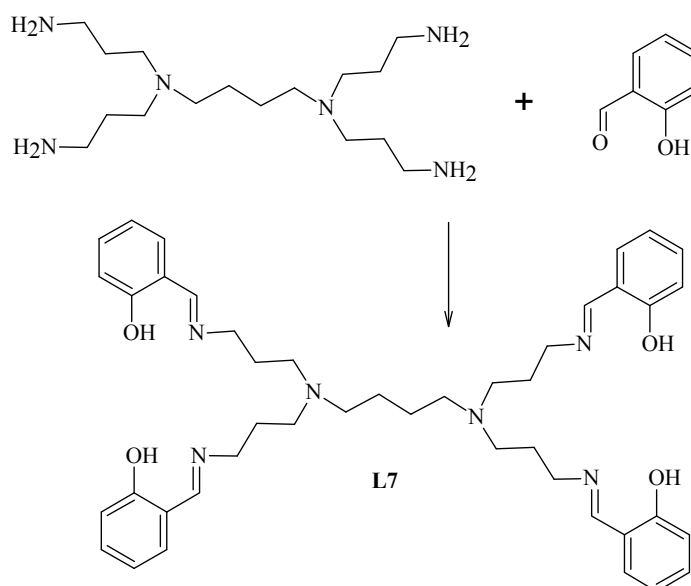
2.2.2 Synthesis of Salicylaldimine ligands (N,O) ligands

In addition to the synthesis of the above ligands, dendritic salicylaldimine ligands were also synthesized. A previously reported method by Smith [6] was used. It involved the reaction of diaminobutane tetraamine generation 1 dendrimer (DAB-(NH₂)₄) with salicylaldehyde using toluene as the solvent. This reaction gives off water so anhydrous magnesium sulphate was

used as a dehydrating agent. The reaction is shown below in Schemes 2.5-2.6. In addition to these dendritic ligands the monofunctional analogues (**L5** and **L6**) were also prepared.



Scheme 2.4: Synthetic route for the mono-functional salicylaldimine ligands.



Scheme 2.5: First generation dendritic salicylaldimine ligand

The purification of **L7** and **L8** was achieved by dissolving the ligands in dichloromethane followed by slow diffusion of pentane into the solution at low temperature. In the case of **L7** the product is isolated as a yellow solid while in the case of (**L8**) a bright yellow oil is formed. The second generation was also synthesized using DAB-(NH₂)₈ as shown in Scheme 2.6. The yields for all the ligands were good, ranging between 80%-90%. Spectroscopic data obtained correlated well with those reported by Malgas *et al.* [7]. Evidence that condensation

occurred for both ligands is seen in the IR spectra which show the presence of a peak in the $\nu(\text{C}=\text{N})$ region, at 1631 cm^{-1} . In the ^1H NMR spectrum, the absence of the NH_2 signal as well as appearance of ($\underline{\text{H}}\text{C}=\text{N}$) imine proton at ~ 8.30 ppm are clearly observed as depicted in Figure 2.12.

The mass spectra (MALDI-TOF) for **L7** and **L8** are shown in Figure 2.2 and 2.3 respectively. The mass spectrum showed peaks of adducts due to $[\text{M}+\text{Na}]^+$, $[\text{M}+\text{K}]^+$ and $[\text{M}+\text{H}]^+$ at m/z 755.69, 771.60 and 733.70 respectively for **L7**. The peak at m/z 523.04 is due to a fragment formed as a result of hydrolysis of two imine bonds on the periphery of the ligand. The (MALDI-TOF) mass spectrometry results for **L8** gave a spectrum with an intense peak at m/z 1606.47 which correlates well with the expected molecular ion and another peak appearing at m/z 1628.58 showing a Na ion adduct of the ligand as well as a peak at m/z 830.25 due to a cyclic quaternary ammonium ion species which is due to an intramolecular nucleophilic substitution reaction (see Scheme 2.6). This type of species was also observed by Van Wyk [8] for similar ligands.

The monofunctional ligands (**L5** and **L6**) have been previously prepared and reported in the literature [9-10]. They were produced in good yields. The imine resonances in the ^1H NMR spectra occur around ~ 8.30 ppm for the propyl imine product whereas they appear at ~ 8.50 ppm in the ligand with an aryl group attached to the imine N atom.

2.3 Characterization data of ligands

The ligands were characterized by ^1H NMR, ^{13}C NMR spectroscopy and infrared spectroscopy. Ligands **L1-L4** were further characterized by ESI mass spectrometry whilst ligands **L7** and **L8** were studied using MALDI-TOF mass spectrometry.

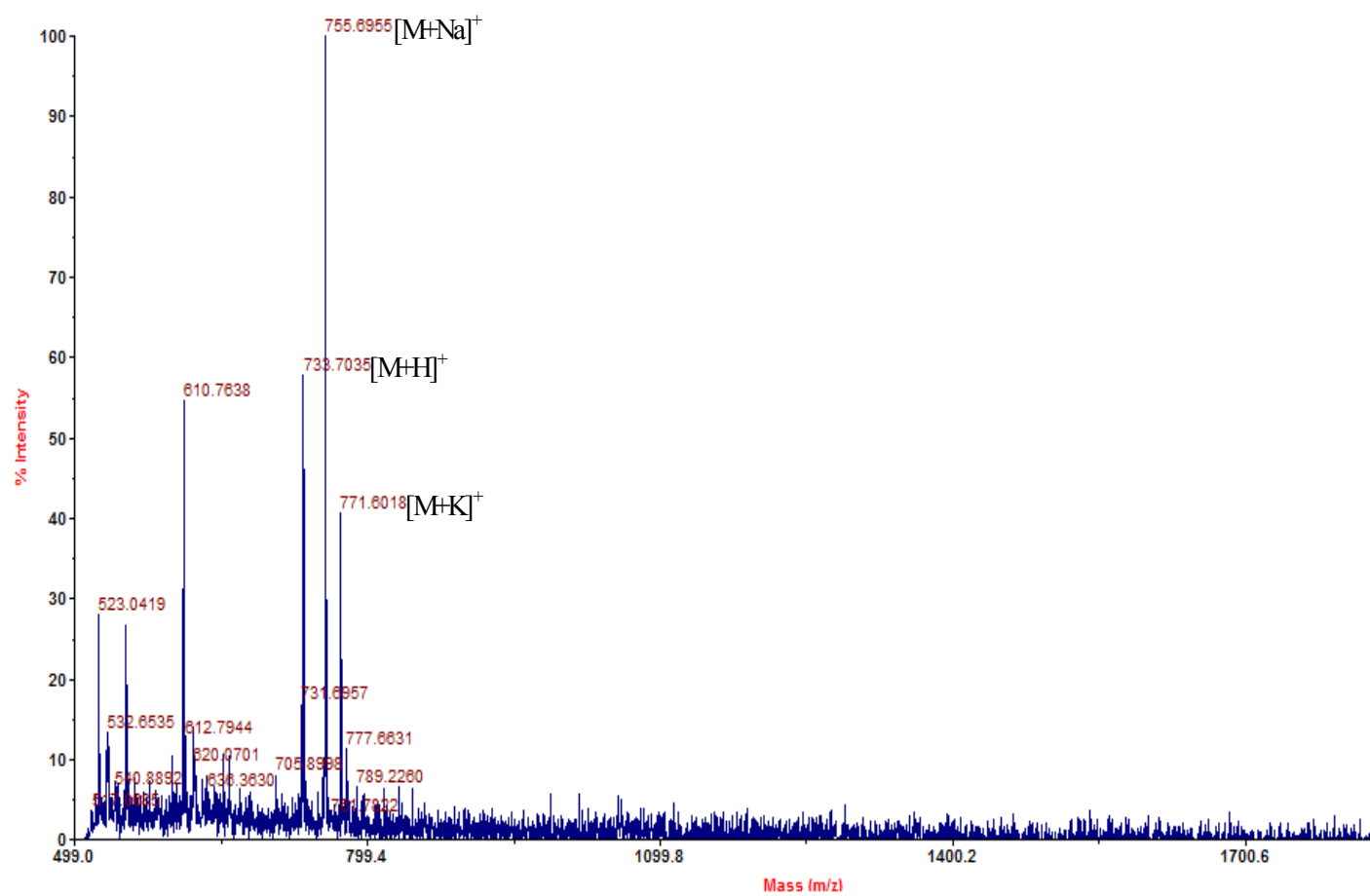


Figure 2.2 MALDI-TOF spectrum of the G1 salicylaldimine dendritic ligand, L7.

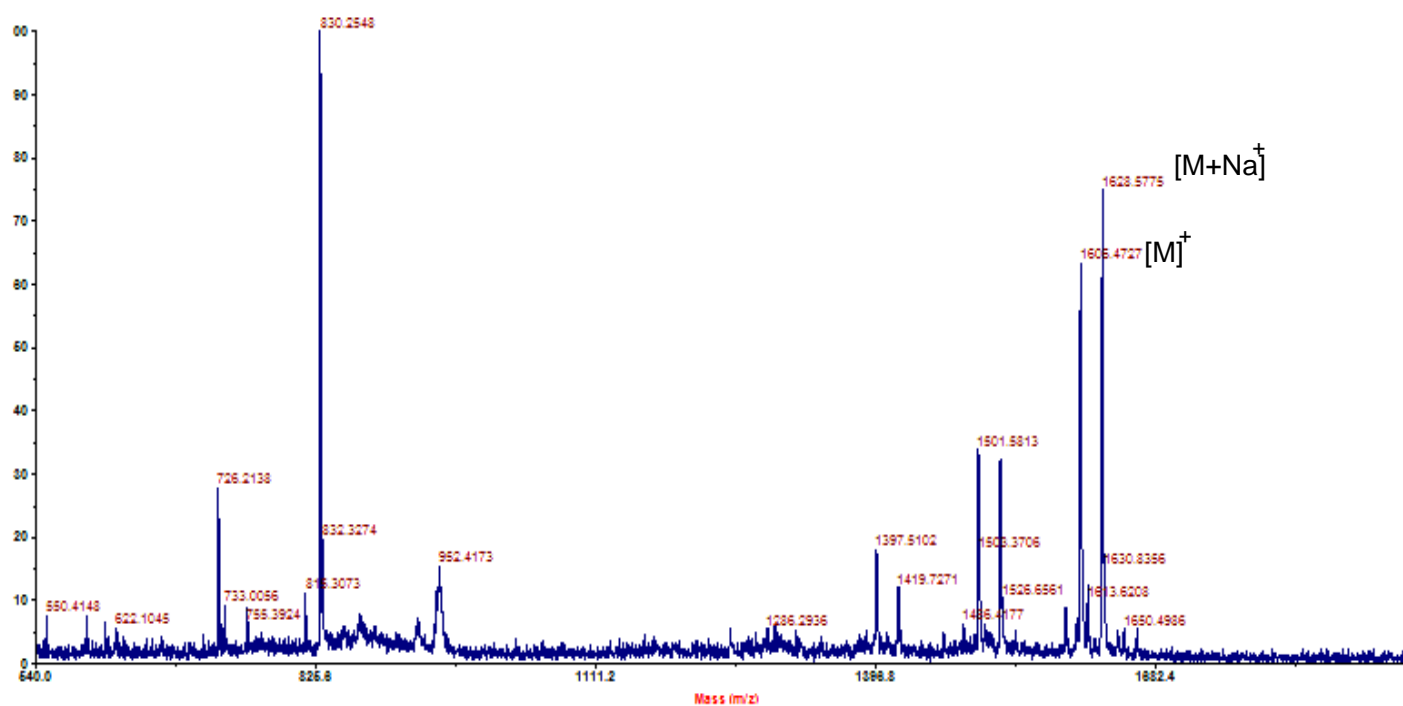
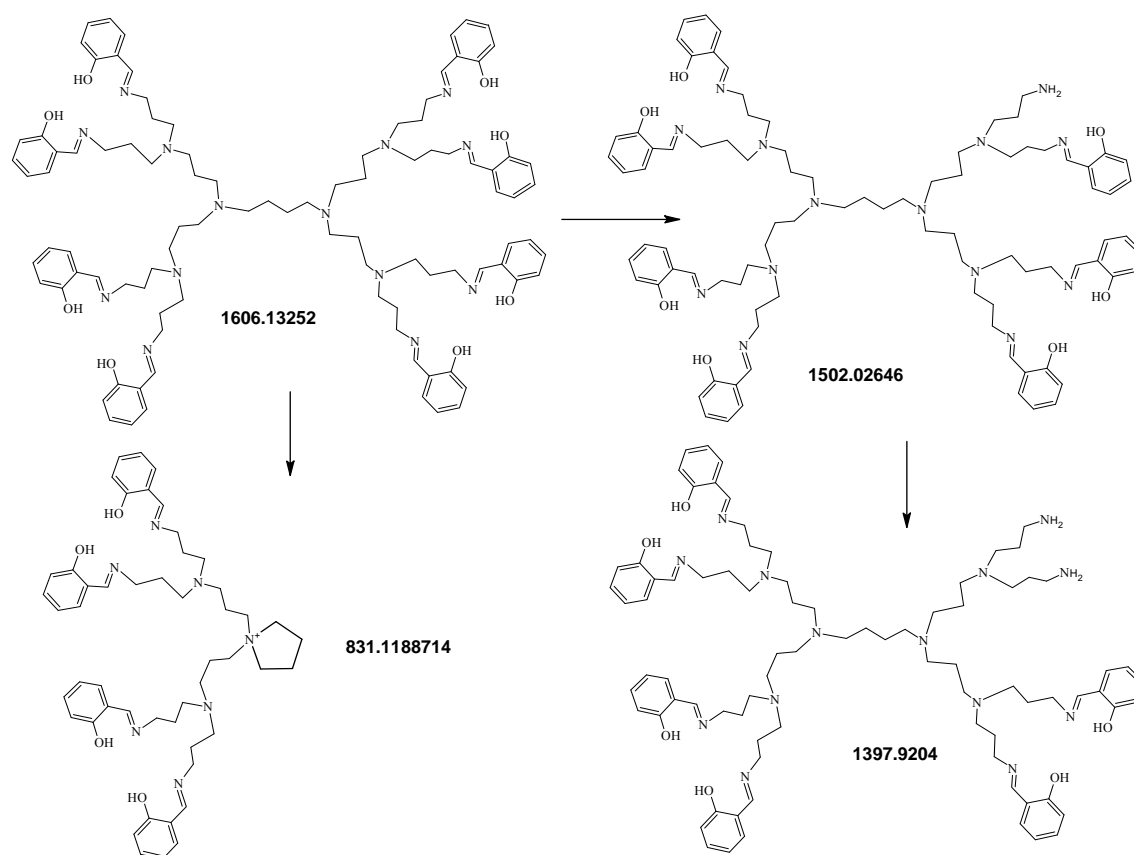
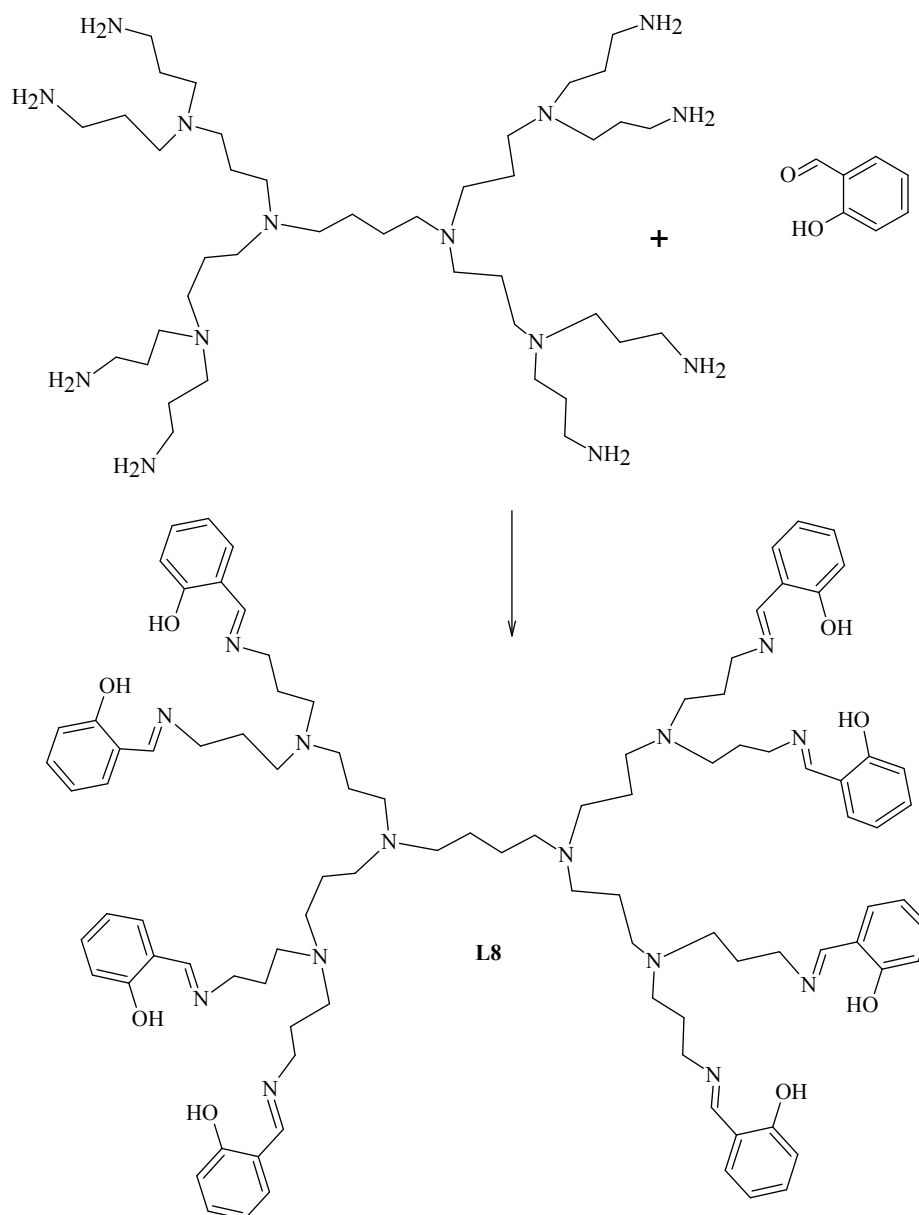


Figure 2.3 MALDI-TOF spectrum for the G2 dendritic ligand, **L8**.



Scheme 2.6 Possible fragmentation pattern for the G2 salicylaldimine ligand, **L8**.



Scheme 2.7: Formation of second generation dendritic salicylaldimine ligand.

2.3.1 FT-IR characterization

The salicylaldimine type ligands showed the imine band, ν (C=N) in the region of $1624 - 1632 \text{ cm}^{-1}$. The position of this signal was further proof that condensation occurred. Other peaks that show the ligand was isolated as expected are the ν (C-O) and ν (O-H) bands which appeared at $1150-1185 \text{ cm}^{-1}$ and $3300-3312 \text{ cm}^{-1}$ respectively.

In the spectra of the pyridyl-imine ligands, the non-ring ν (C=N) band occurred in the region $1645\text{-}1647\text{cm}^{-1}$ for all of the ligands. The pyridine ring ν (C=N) bands were observed around 1597cm^{-1} for all the ligands. The difference in the positioning of the imine band in both types of ligands, that is salicylaldimine and imino pyridine, explicitly shows the different nature these ligands.

Figures 2.4 and 2.5 are the FT-IR spectra showing different signals for the various functional groups in each type of ligand that is, 4-imino-pyridine and salicylaldimine respectively.

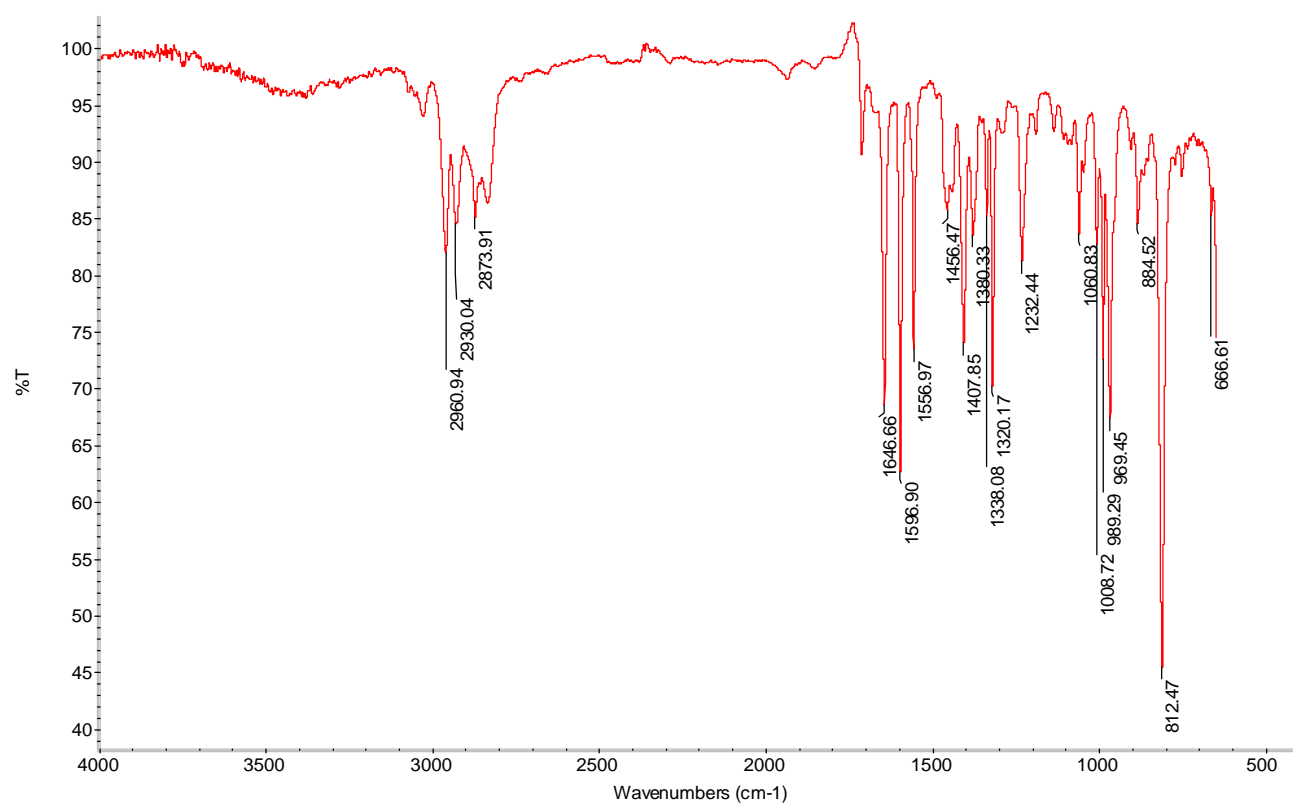


Figure 2.4 FT-IR spectrum for the monofunctional N, N' ligand, **L1**.

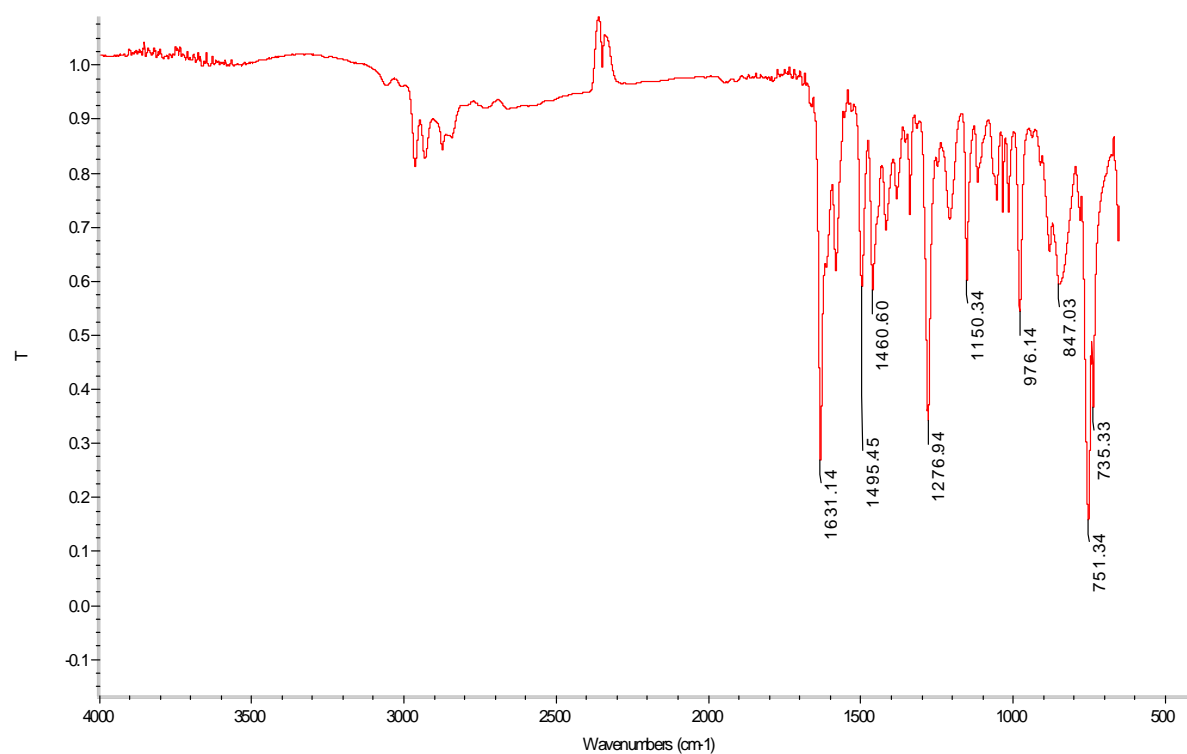


Figure 2.5 FT-IR spectrum for monofunctional N, O ligand, **L5**.

Table 2.1 Selected FT-IR, Mass spectral and Melting Point data, **L1-L8**

Ligands	FT-IR ^a			MS (m/z)	M.P. (°C)
	$\nu(\text{C}=\text{N})$	$\nu(\text{O}-\text{H})$	$\nu(\text{C}-\text{O})$		
L1	1646	-	-	149 ^b	Oil
L2	1621	-	-	183 ^b	55-58
L3	1647	-	-	673 ^b	Oil
L4	1647	-	-	1486 ^b	Oil
L5	1631	3312	1150	-	Oil
L6	1621	3300	1184	-	38-45
L7	1631	3309	1149	733 ^c	60-68
L8	1631	3310	1148	1606 ^c	Oil

^a Recorded as neat materials (ATR).

^b Recorded as ESI-MS spectra.

^c Recorded as MALDI-TOF spectra.

2.3.2 ^1H NMR characterization

Table 2.2 gives the proton NMR data for ligands **L1-L8**. Figures 2.4-2.9 shows the numbering in the general structures of the ligands that can be associated with the corresponding data in Table 2.2.

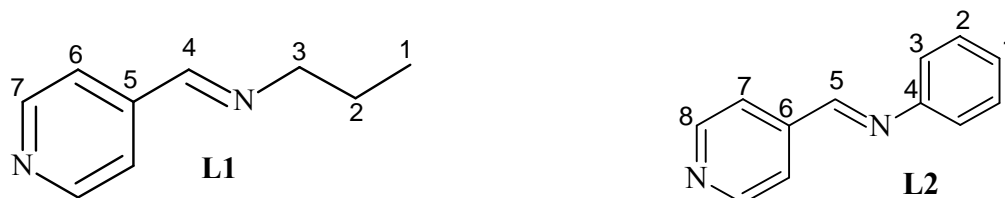


Figure 2.6: Numbering of the carbon atoms in mono-functional ligands, **L1** and **L2**.

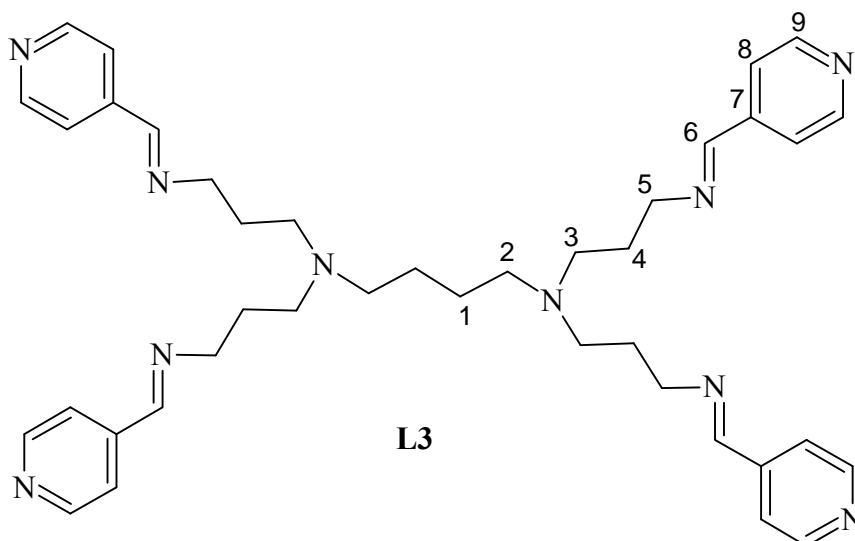


Figure 2.7: Numbering of the carbon atoms in dendritic (N, N') G1 ligand, **L3**.

Figures 2.12 and 2.13 shows the difference in the spectra of the salicylaldimine G2 dendritic ligand and the imino-pyridine G2 dendritic ligand respectively. These illustrate the different signals which are typically expected for each type of ligand. In the salicylaldimine ligand, the expected signal of the hydroxyl group is observed at 13.56 ppm. The relative chemical shift of the aromatic protons are also different for the different types of ligands and the imine signal is

far more shielded in **L8** when compared to **L4**. In addition to this, in **L4** the free imine occurs in-between the proton signals of the pyridine ring. The presence of the pyridine N also influences the chemical shift of the aromatic protons in the spectrum due to increased ring electron density. The aliphatic regions (1 ppm-3.6 ppm) are similar in the two ligands and essentially show the protons of the DAB framework. A significant signal in both spectra is the peak for the protons of the carbon attached to imino nitrogen. This occurs around 3.60 ppm. This is also indicative of the successful condensation of the amine. In the imino dendrimer starting material the N-CH₂ signal appears at 3.90 ppm.

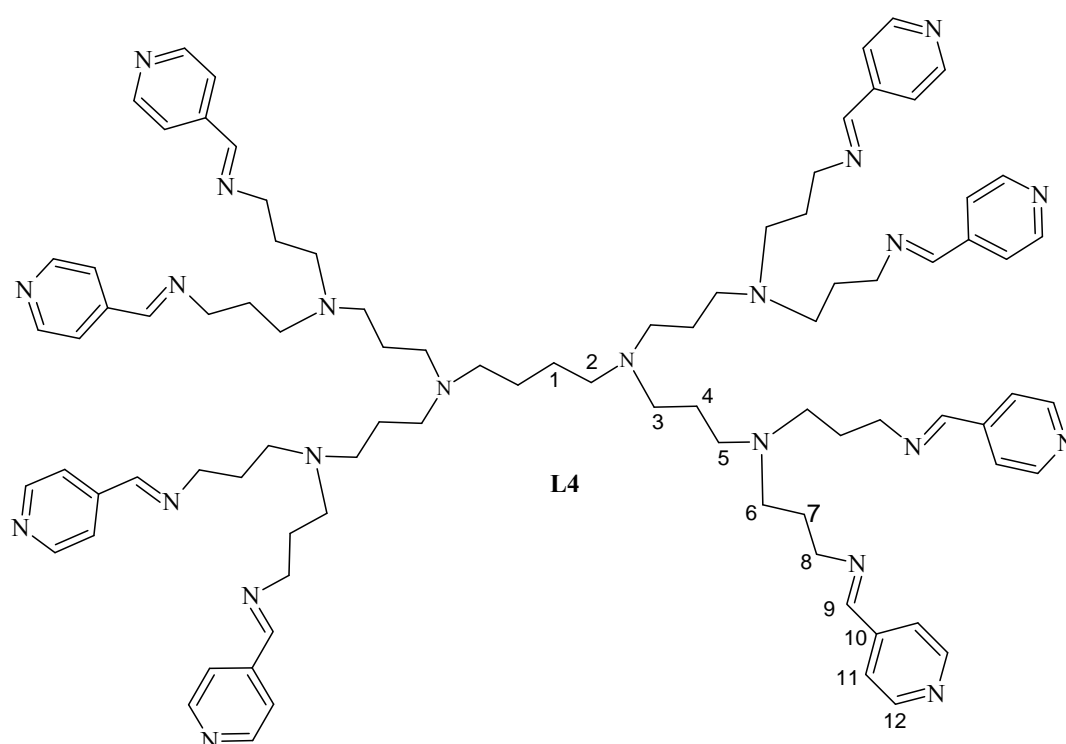


Figure 2.8: Numbering of the carbon atoms in dendritic (N, N') G2 ligand, **L4**



Figure 2.9: Numbering of the carbon atoms in monofunctional (N, O) ligands, **L5** and **L6**

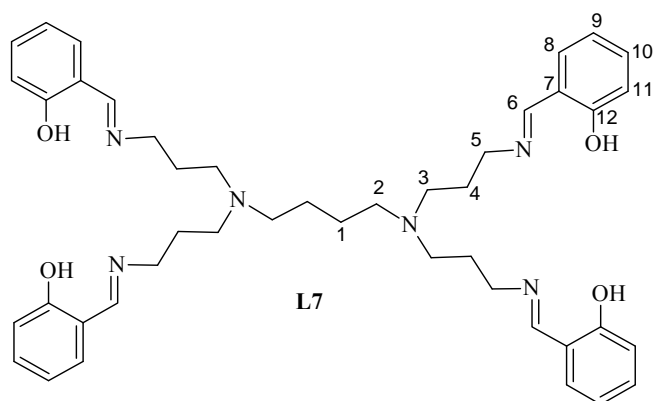


Figure 2.10: Numbering of the carbon atoms in dendritic G1 (N, O) ligand, **L7**

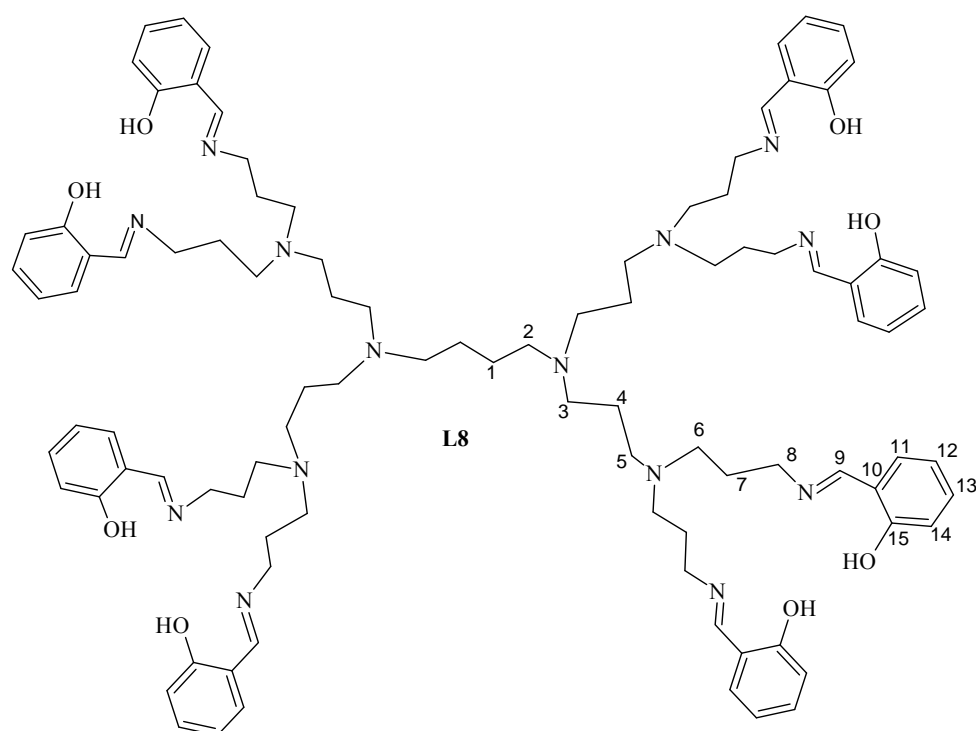


Figure 2.11: Numbering of the carbon atoms in dendritic G2 ligand, **L8**

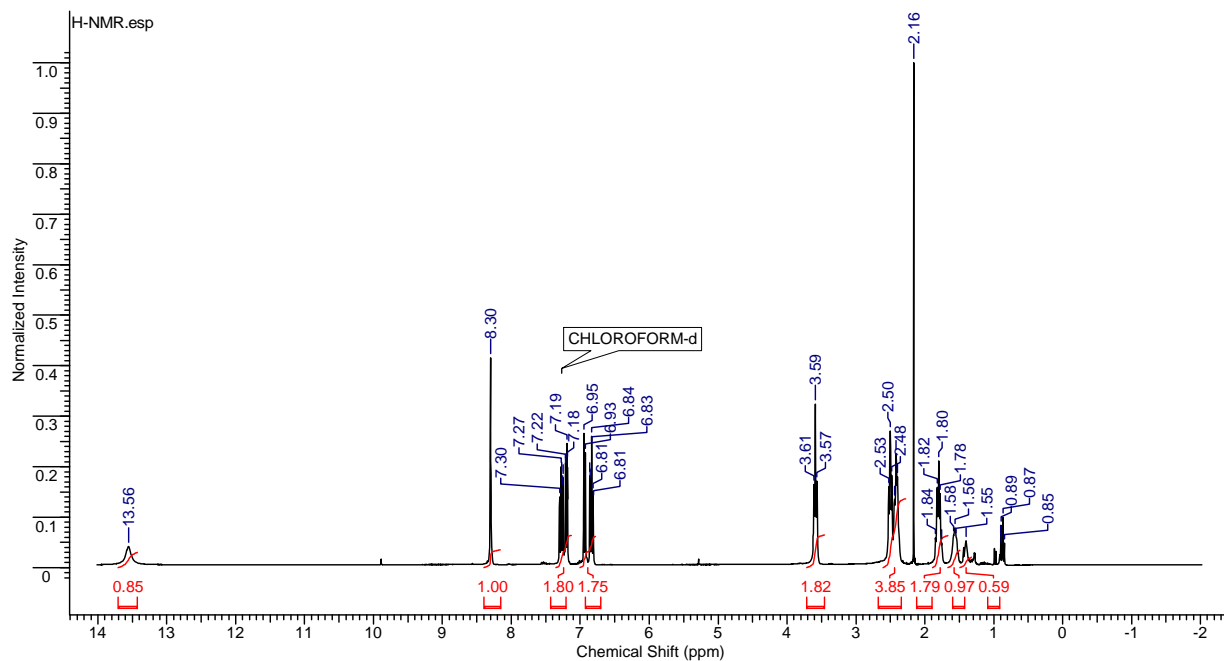


Figure 2.12: A typical ^1H NMR spectrum of a dendritic (N, O) ligand, **L8**.

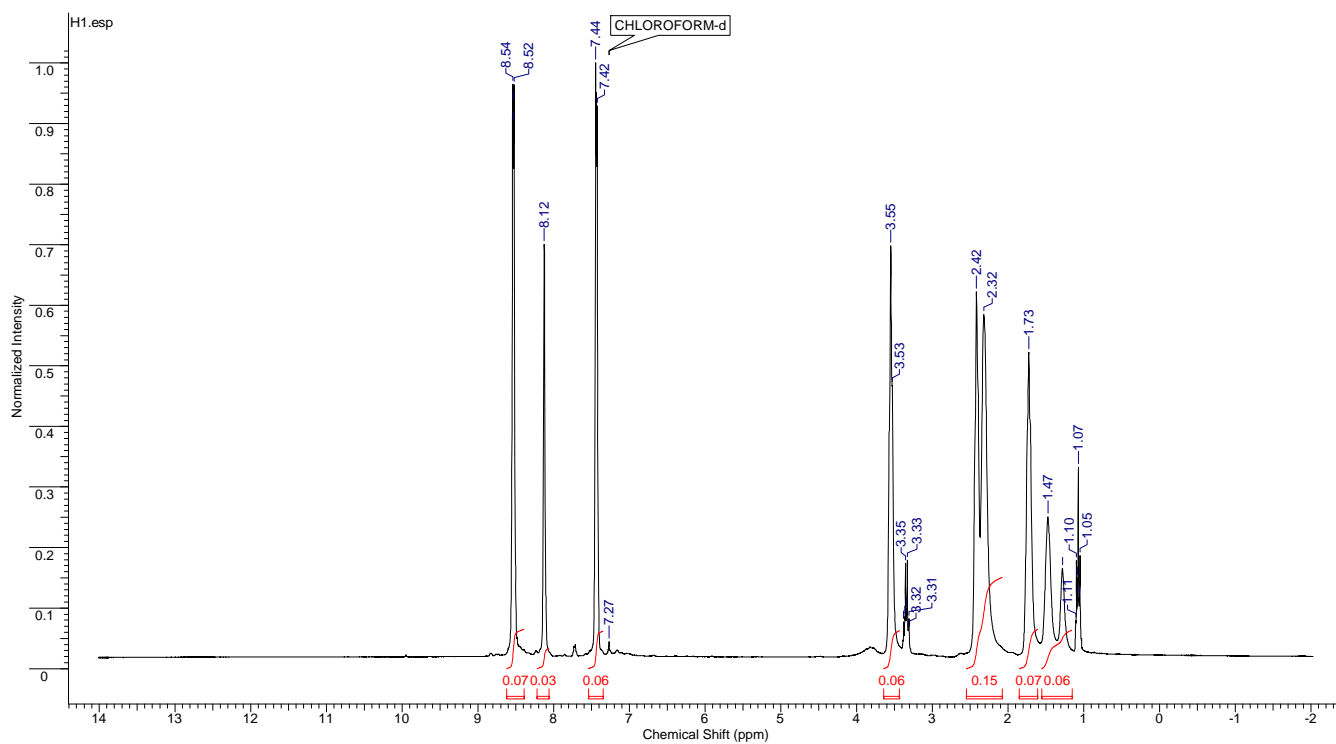


Figure 2.13: ^1H NMR spectrum of the N, N' dendritic ligand, **L4**.

Table 2.2: ^1H NMR data for all ligands prepared, **L1-L8**

Ligands	Chemical shift (δ - ppm) ^a	Assignment
L1	0.92 t	H1
	1.71 m	H2
	3.58 t	H3
	8.21 s	H4
	7.56 d	H6
	8.64 d	H7
L2	8.45 s	H5
	7.42 d	H3
	7.31 t	H2
	7.25 t	H1
	7.76 d	H5
	8.76 d	H6
L3	1.37 s.	H1
	2.37 s,	H2
	2.47 t	H3
	1.78 m	H4
	3.60 t	H5
	8.18 s	H6
	7.48 d	H8
	8.57 d	H9
L4	1.37 s	H1
	1.47 s	H7
	1.73 m	H4
	2.32 t	H2/3
	2.42 t	H5/6
	3.55 t	H8
	8.12 s	H9
	7.44 d	H11
	8.54 d	H12

^a Recorded in CDCl_3 .

Table 2.2 Cont.

L5	1.02 t	H1
	1.78 m	H2
	3.60 t	H3
	8.37 s	H4
	7.34 d	H6
	7.01 t	H7
	6.90 d	H8
	6.88 dt	H9
	13.42 s	O-H
L6	8.51 s	H1
	7.38 d	H2/6
	7.32 d	H3/5
	7.18 t	H4
	7.33 d	H9
	7.22 dd	H10
	6.83 dt	H11
	6.97 d	H12
	13.15 s	O-H
L7	1.40 s	H1
	2.39 t	H2
	2.50 t	H3
	1.81 m	H4
	3.61 t	H5
	8.32 s	H6
	7.22 d	H8
	6.95 d	H9
	6.85 dt	H10
	7.29 d	H11
	13.51 s	O-H

Table 2.2 Cont.

L8	1.28 s	H1
	2.51 t	H2
	1.56 t	H3
	1.80 m	H4
	2.48 t	H5
	2.50 t	H6
	2.53 t	H7
	3.59 t	H8
	8.30 s	H9
	7.30 d	H11
	6.95 d	H12
	6.83dt	H13
	7.19 d	H14
	13.56 s	O-H

2.3.3 $^{13}\text{C}\{^1\text{H}\}$ NMR characterization

Table 2.4 gives the $^{13}\text{C}\{^1\text{H}\}$ NMR data for ligands **L1-L8**. Signals for all the carbons were observed for each ligand synthesized thus giving further evidence that the desired ligands were obtained. Figures 2.14 and 2.15 show typical spectra for each type of ligand. In both cases the imine C atom is the most deshielded at 158.30 ppm (**L4**) and 164.33 (**L8**). For the N, N' ligands the C atoms in the pyridine ring are symmetrical whereas in N, O ligands all the aromatic C's give separate chemical shifts. This is expected due to the O-H substituent on the ring. The alkyl C's occur in similar chemical shift regions in both cases with some of the signals overlapping one another. The dendrimer generation has little effect on the positions of the chemical shifts. This is seen from the fact that similar results are obtained for the different generation of dendrimeric ligands. This is expected because the presence of extra alkyl chains in the higher generation dendrimers is envisaged not to have a great effect.

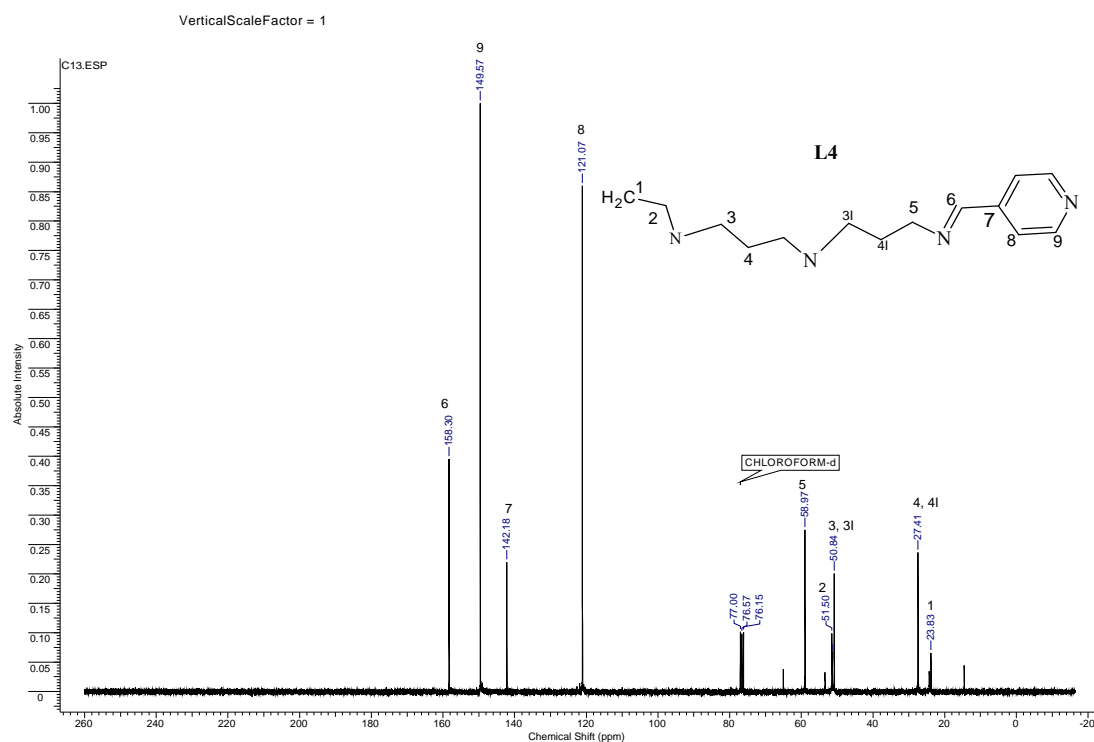


Figure 2.14 $^{13}\text{C}\{^1\text{H}\}$ NMR spectrum of G2 N, N' dendritic ligand, **L4**, showing one arm of the dendrimer.

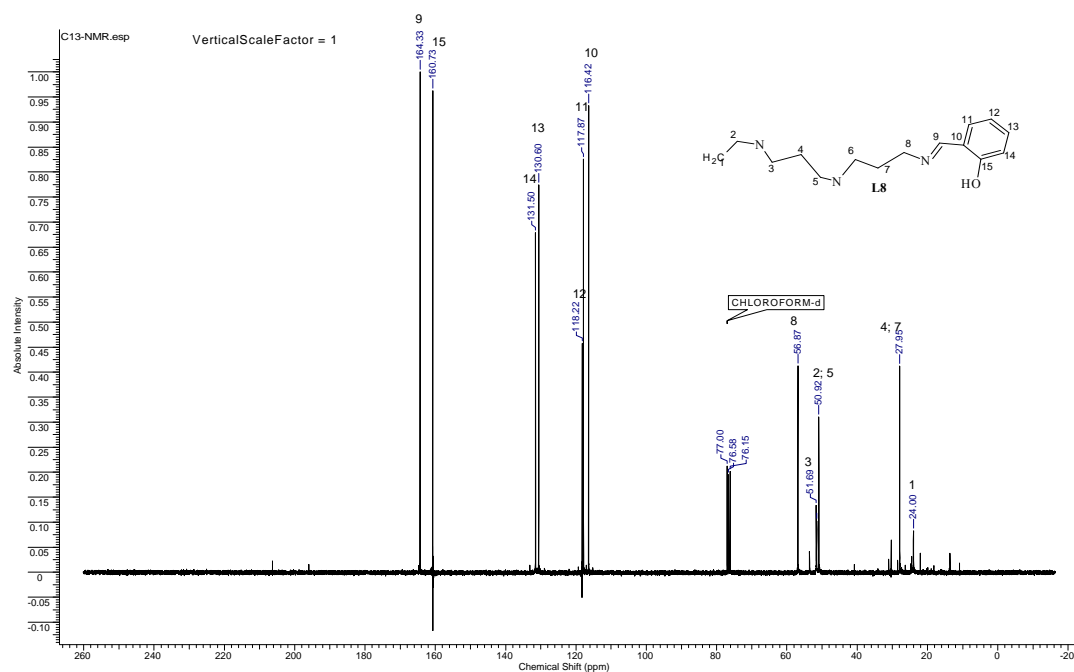


Figure 2.15 $^{13}\text{C}\{^1\text{H}\}$ NMR spectrum of G2 N, O dendritic ligand, **L8** showing one arm of the dendrimer.

Table 2.3: $^{13}\text{C}\{^1\text{H}\}$ NMR data for all the ligands prepared, **L1-L8**

Ligands	^{13}C Chemical shift (ä- ppm)	Assignment
L1	11.68	C1
	23.69	C2
	63.60	C3
	158.68	C4
	142.96	C5
	121.76	C6
	150.18	C7
L2	120.88	C1
	122.23	C2
	126.98	C3
	142.75	C4
	157.91	C5
	150.92	C6
	129.26	C7
	150.56	C8
L3	24.89	C1
	51.32	C2
	53.57	C3
	27.89	C4
	59.51	C5
	158.88	C6
	142.75	C7
	121.63	C8
	150.11	C9
L4	23.83	C1
	27.41	C4/7
	50.87	C2/3

^a Recorded in CDCl_3 .

Table 2.3 Cont.

	51.50	C3/6
	58.97	C8
	158.30	C9
	142.18	C10
	121.07	C11
	149.57	C12
L5	11.21	C1
	23.57	C2
	60.73	C3
	164.03	C4
	116.53	C5
	117.87	C6
	118.30	C7
	130.59	C8
	131.52	C9
	160.03	C10
L6	162.66	C1
	117.24	C8
	161.11	C13
	131.15	C12
	126.87	C11
	133.12	C10
	148.50	C9
	129.38	C6
	121.14	C5
	119.04	C4
L7	25.12	C1
	51.37	C2
	53.93	C3

Table 2.3 Cont.

	28.44	C4
	57.36	C5
	164.82	C6
	116.95	C7
	118.37	C8
	118.74	C9
	131.08	C10
	132.01	C11
	161.26	C12
L8	24.00	C1
	50.92	C2/3
	27.96	C4
	30.36	C7
	51.69	C5
	56.87	C8
	164.33	C9
	116.42	C10
	117.87	C11
	118.22	C12
	130.60	C13
	131.50	C14
	160.73	C15

2.3.4 Elemental analysis

The identities of the ligands were further confirmed by microanalysis where the obtained data were found to correlate well with those expected. Table 2.4 gives the results for all the ligand systems except **L1** which proved difficult to purify fully due to its sensitive nature.

Table 2.4 Microanalysis results for all ligand systems, L1-L8

Ligands	Calculated (%)			Found (%)		
	C	H	N	C	H	N
L2	79.10	5.53	15.37	79.34	5.58	15.60
L3^a	63.42	7.22	18.59	63.00	7.75	18.69
L4^a	62.78	7.30	17.70	62.58	7.82	18.35
L5	73.59	8.03	8.58	73.11	8.37	7.67
L6	79.16	5.62	7.10	78.58	5.69	6.71
L7	72.10	7.70	11.47	72.77	7.53	12.21
L8	71.79	8.03	12.21	70.90	8.14	12.29

^asome solvent inclusion

2.4 Conclusion

Both monofunctional and dendrimeric (G1 and G2) salicylaldimine and 4-imino pyridyl ligands were prepared in moderate to good yields. Full characterization was carried out using a range of analytical techniques. These types of ligands proved to be stable under ambient conditions especially when stored under nitrogen at room temperature. These ligands will therefore be utilized in coordination reactions with ruthenium Ru(II) salts with the aim of forming metal carbene complexes that are active in olefin metathesis reactions.

2.5 Experimental Section

2.5.1 Materials and Instrumentation

All chemical procedures and manipulations were carried out under argon or nitrogen using standard Schlenk techniques. The commercially available chemicals used without further purification were the following: Salicylaldehyde, DAB-(NH₂)₄, DAB-(NH₂)₈, aniline, propylamine, 4-pyridine carboxylaldehyde, all obtained from Sigma-Aldrich Ltd. The

solvents, toluene, diethyl ether, ethanol and dichloromethane were obtained from Kimix Chemicals and were dried using the appropriate drying agent for each solvent.

^1H NMR and ^{13}C NMR spectra were recorded on Varian 400MHz and 300MHz spectrometers. Infrared spectra were recorded on a Nicolet Avator 330 FTIR spectrophotometer using an ATR accessory. ESI Mass spectra were recorded using dichloromethane as solvent employing a cone voltage of 15V using a Waters API Quattro Micro spectrometer. Microanalysis was done at the University of Cape Town.

2.5.2 Synthesis of ligands

The ligand preparation involves a Schiff base reaction between an aldehyde and a primary amine to form an imine ligand [1].

Synthesis of L1

Propylamine (0.6 mL, 5 mmol) was dissolved in dry Et_2O (20 ml) and slowly added to pyridine-4-carboxaldehyde (0.7 ml, 5 mmol) dissolved in dry Et_2O (10 ml). The mixture was stirred for 2h under reflux. After this time the solvent was removed. A yellow oil was obtained which was purified by vacuum distillation (Koegel Rühr) at 75°C for several hours. The yield, 0.521 g (70%).

Synthesis of L2

In a 100 ml round bottom flask containing a stirrer bar and an equimolar amount of 4-pyridine carboxylaldehyde (0.7 mL, 7 mmol) was reacted with aniline (0.65 g, 7 mmol) in EtOH (20 ml). This resulted in a colourless reaction mixture which was stirred for 4h at room temperature. On completion of the reaction, it was placed in the freezer overnight. A pale

yellow crystalline solid formed which was vacuum filtered. The solid was redissolved in petroleum ether (40-60 °C) upon which the impurities precipitated out. The solution was decanted into a clean flask and the solvent removed giving a crystalline white yellow solid. Yield, 0.914 g (72%).

Synthesis of L3

G1-DAB-(NH₂)₄ dendrimer (0.301 g, 0.8 mmol) was dissolved in dry toluene (10 ml) in a round bottom flask, under nitrogen. Pyridine-4-carboxylaldehyde (0.34 ml, 3.2 mmol) was added to this solution. The mixture was allowed to stir for 48h at room temperature. The solvent was evaporated on a rotary evaporator and an orange oil was obtained. The ligand was extracted 5 times with Et₂O yielding a waxy orange material after removal of the solvent. Yield, 0.369 g (69%).

Synthesis of L4

The same procedure was followed as that for synthesis of **L3** including the work up. The reaction is done in 1:8 mol ratio of G2-DAB-(NH₂)₈ (0.595 g, 0.8 mmol) to 4-pyridine carboxylaldehyde (0.68 ml, 6.4 mmol) in toluene (20ml) and the yield is relatively high, 0.956 g (80%).

Synthesis of L5

An equimolar amount of salicylaldehyde (5 mmol, 0.61 g) was reacted with amine propyl (5 mmol, 0.29 g) in dry THF (20 ml). The reaction mixture was allowed to reflux at 60 °C for 2h. The solvent was removed by rotary evaporator, resulting in a yellow oil. Yield, 0.644 g (79%).

Synthesis of L6

This ligand was synthesized in the same way as **L5** using aniline as the starting material in EtOH. The reaction mixture was then stored in the freezer overnight upon which light yellow crystals formed. These crystals were then filtered by vacuum filtration and washed 3 times with cold EtOH and dried under vacuum. The resulting yellow crystals were produced in yield, 0.689 g (70%).

Synthesis of L7

DAB-G1 dendrimer (0.510 g, 1.6 mmol) was added to dry toluene (10 ml) in a round bottom flask, under nitrogen. Salicylaldehyde (0.77 ml, 6.3 mmol) was added to this solution. The mixture was allowed to stir for 48h at room temperature. The solvent was evaporated on a rotary evaporator and a yellow oil was obtained. Dichloromethane (10 ml) was added to the oil, after which pentane (20 ml) was added. This solution was stored in the freezer for 72 hours at -40 °C. The yellow precipitate obtained, was filtered off *via* vacuum filtration to obtain the product in a good yield of 0.875 g (75%).

Synthesis of L8

The generation 2 ligand was synthesized similarly to ligand **7** using a 1:8 DAB-G2 dendrimer (2.054 g, 1.6 mmol): salicylaldehyde (1.61 ml, 12.8 mmol) mol ratio in toluene (20 ml) under the same reaction conditions. The solvent was evaporated on a rotary evaporator and a yellow oil was obtained. Dichloromethane (20 ml) was added to the product and this was extracted 3 times with water to remove excess DAB. The dichloromethane layer was dried over magnesium sulphate after which the latter was filtered off. The filtrate was evaporated *via* rotary evaporation producing a bright yellow oil. Yield, 2.042 g (80%).

2.6 References:

1. (a) Cozzi, P. G., *Chem. Soc. Rev.*, **2004**, *33*, 410. (b) Drury III, A. P. *PNAS.*, **2004**, *101*, 5723.
2. (a) Drozdak, R.; Allaert, B.; Ledoux, N.; Dragutan, I.; Dragutan, V.; Verpoort, F., *Coord. Chem. Rev.*, **2005**, *249*, 3055. (b) Iwasa, S.; Tsushima, S.; Nishiyama, K.; Tsuchiya, Y.; Takesawa, F.; Nishiyama, H., *Tetrahedron: Asymm.*, **2003**, *14*, 855. (c) Chelucci, G.; Saba, A.; Vignola, D.; Solinas, C., *Tetrahedron*, **2001**, *57*, 1099. (d) Bianchini, C.; Lee, H.M., *Organometallics*, **2000**, *19*, 1833. (e) Nishiyama, H.; Itoh, Y.; Sugawara, Y.; Matsumoto, H.; Aoki, K.; Itoh, K., *Bull. Chem. Soc. Jpn.*, **1995**, *68*, 1247.
3. Bernardo, P.; Zanonato, P. L.; Vigato, P. A. *Inorg. Chim. Acta*, **2007**, *360*, 1083.
4. (a) Wong, W.-Y.; Wong, W.-T., *J. Organomet. Chem.*, **1999**, *584*, 485. (b) Dickson, S. J.; Paterson, M. J.; Williams, C. E.; Anderson, K. M. and Steed, J. W., *Chem. Eur. J.*, **2008**, *14*, 7296.
5. Smith, G.; Chen, R.; Mapolie, S. F., *J. Organomet. Chem.*, **2003**, *673*, 111.
6. Smith, G.S. Ph.D. Thesis: An investigation into the synthesis, characterization and some applications of novel metal-containing polymers and dendrimers of transition metals, University of the Western Cape, Cape Town, South Africa, 2003.
7. Malgas, R.; Mapolie, S. F.; Ojwach, S. O.; Smith, G.S.; Darkwa, J., *Catal. Commun.*, **2008**, *9*, 1612.
8. Van Wyk, J. L. Ph.D. Thesis: Mononuclear and multinuclear salicylaldimine metal complexes as catalyst precursors in the oxidation of phenol and cyclohexene, University of the Western Cape, Cape Town, South Africa, 2008.
9. Torzilli, M. A.; Colquham, S.; Douart, D.; Beer, R. H., *Polyhedron*, **2002**, *21*, 697.
10. Van Wyk, J. L.; Mapolie, S. F.; Lennartson, A.; Hakansson, M.; Jagner, S., *Inorg. Chim. Acta*, **2008**, *361*, 2094.

CHAPTER 3

SYNTHESIS AND CHARACTERIZATION OF MONONUCLEAR AND DENDRITIC RUTHENIUM COMPLEXES BASED ON 4-IMINO PYRIDINE AND SALICYLALDIMINE/ *P*-CYMENE LIGANDS.

CONTENT

3.1 Introduction	73
3.2 Results and Discussion	76
3.2.1 Synthesis of model and dendritic 4-imino pyridine Ru carbene complexes using Grubbs G1	76
3.2.1.1 Characterization by means of infrared spectroscopy	79
3.2.1.2 Characterization by means of ESI-MS and elemental analysis	80
3.2.1.3 Characterization by means of ¹ H NMR spectroscopy	80
3.2.2 Synthesis of model and dendritic 4-imino pyridine Ru NHC carbene complexes using Grubbs G2	86
3.2.2.1 Characterization by means of infrared spectroscopy	87
3.2.2.2 Characterization by means of ESI-MS and elemental analysis	90
3.2.2.3 Characterization by means of ¹ H NMR spectroscopy	90
3.2.3 Attempted synthesis of model and dendritic salicylaldimine Ru carbene Complexes	96
3.2.4 Synthesis of model and dendritic salicylaldimine Ru <i>p</i> -cymene complexes	98
3.2.4.1 Characterization by means of infrared spectroscopy	99
3.2.4.2 Characterization by means of ESI-MS and elemental analysis	100
3.2.4.3 Characterization by means of ¹ H NMR spectroscopy	101
3.2.4.4 Characterization by means of ¹³ C{ ¹ H} NMR spectroscopy	105
3.2.4.5 Thermogravimetric analysis	108
3.3 Conclusion	110
3.4 Experimental	111
3.4.1 General	111
3.4.2 Synthesis of complexes	111
3.5 References	116

3.1 Introduction

The coordination chemistry of ruthenium complexes containing Schiff base ligands has been explored extensively. The typical coordination of Schiff base ligands to ruthenium could either be bidentate or tetradentate in nature. The earliest paper on ruthenium complexes with Schiff bases was reported by Wilkinson *et al.* [1] involving salicylaldimines. It reported on the use of chloro-carbonyls or chloro-phosphine Ru(II) precursors reacting with sodium salts of salicylaldimines. The exploration of these ligands with Ru(II) as a precursor has grown due to the catalytic activity of the complexes and this has led to numerous Ru complexes being investigated. This has been extended by introducing other donor atoms such as sulphur and phosphorus [2]. The studies of Ru complexes as catalysts in olefin transformations lead to the discovery of well-defined Grubbs catalysts amongst others. These catalysts have been modified in order to improve catalyst selectivity, activity and catalyst life time. This was discussed in depth in Chapter 1. As part of this catalyst development, salicylaldimines have been complexed with Grubbs-type catalysts. This was first reported by Grubbs *et al.* [3]. Other researchers such as Verpoort *et al.* [4] extended this work by introducing different substituents on the salicylaldimines. In addition to salicylaldimines several ligands were tested in order to improve the stability of the Grubbs type catalysts. The ligands that have been used, include pyridines and functionalized pyridines. Grubbs *et al.* [5] had previously reported the synthesis and activity of *pyridine* modified Grubbs G1 and Grubbs G2 complexes. Salicylaldimine modified Grubbs complexes were designed in order to generate more stable catalysts especially for applications at elevated temperatures whilst, the pyridine modified Grubbs complexes were designed to achieve high activities as pyridine is rather more labile than phosphines. This is considered important in catalysis since according to mechanistic and theoretical considerations it is possible to increase the reaction rate by combining a strongly binding NHC ligand and a labile ligand [6]. Other researchers have opted to combine stable and labile NHC moieties with chelating pyridinyl-alcoholato ligands

[7] or 2-pyridylethanyl ligands [8] in order to maintain both stability and activity of the Ru carbene precursor. These complexes were only mononuclear in nature. We thus wanted to further explore these salicylaldimine and pyridinyl ruthenium carbene complexes by anchoring them onto dendrimers, producing multinuclear catalysts.

Much work has been done in trying to address the issue of achieving a catalyst that would combine the advantages of both homogeneous and heterogeneous catalysts. This has been attempted by anchoring homogeneous Grubbs type catalysts on polymers, silica supports or onto dendrimers. Grubbs *et al.* [9] first reported the synthesis of an active solid phase polystyrene supported Grubbs type catalyst but this was found to be less active and had a slower initiating rate than its homogeneous counterpart. A further study by Procopiou *et al.* [10] led to the development of a Grubbs type catalyst that was supported by a “boomerang” polymer resin. In a “boomerang” catalyst the active catalyst becomes homogeneous in the reaction mixture to allow for catalysis to occur but at the same time it can be re-trapped by the polymer resin on completion of the catalysis. It was reported that the catalyst was active and also recyclable. In addition to polymer bound Grubbs-type catalysts, Lamaty *et al.* [11] reported a soluble polymer onto which was anchored Grubbs generation 1 and 2 complexes as well as Hoveyda-Grubbs generation 1 and 2 catalysts. They found that the Hoveyda-Grubbs catalysts could be recovered and recycled although the catalyst with a NHC ligand (G2) had the highest activity.

Following these reports, in 2002, dendritic ruthenium based metathesis catalysts were reported [12]. All the reported papers used carbosilane dendrimers but with a different Ru carbene precursor. Hoveyda *et al.* [12a] used Hoveyda-Grubbs G1 as the anchored catalyst and found the anchored catalyst to be highly active and recyclable. Verdonck’s group [12b]

used the conventional Grubbs G1 catalyst and it was found to be very active for ROMP of norbornene (NBE). Van Koten's group [12c] reported the use of a 2-hydroxylalkylpyridyl functionalized dendrimer complexed to $[\text{Ru}(=\text{CHPh})\text{Cl}_2(\text{PR}_3)_2]$ (R=isopropyl or cyclohexyl) to give five coordinated dendritic Ru complexes in which the alkoxy ligand is in an equatorial position and the pyridyl ligand in the axial position. Only Astruc's group studied polypropylenediphosphine dendrimers with Hoveyda-Grubbs G1 catalyst. The formed compounds consisted of dendritic ruthenium carbene complexes anchored through chelating diphosphine ligands. These complexes were also found to be very active [13].

Our work was initially aimed at extending the work already done by Grubbs *et al.* [3] as well as that by Verpoort and co-workers [4] by anchoring Grubbs catalysts on a salicylaldimine-functionalized dendrimer. These researchers synthesized mononuclear salicylaldimines Grubbs generation 1 and 2 catalysts.

Our attempts at synthesizing salicylaldimine dendritic ruthenium complexes did not succeed due to problems resulting from the formation of unwanted ruthenium species. This work is further explained later in this chapter. The second approach reported in this chapter is the synthesis of polypropyleneimine dendrimers functionalised with 4-imino pyridyl moieties (**L3** and **L4**) which were reacted with Grubbs G1 and G2 to form metallodendrimers. In addition the model complexes of 4-imino pyridyl ruthenium carbene complexes with either an alkyl or aryl substituent at the imine N atom (**L1** and **L2**) were also prepared. The last approach employed to synthesize dendritic ruthenium complexes involved the use of a ruthenium precursor different to the Grubbs catalysts, *viz.* the ruthenium dichloride *p*-cymene dimer, $[\text{Ru}(\mu\text{-Cl})_2\text{p-cymene}]_2$. The latter was anchored on dendritic salicylaldimine ligands.

3.2 Results and Discussion:

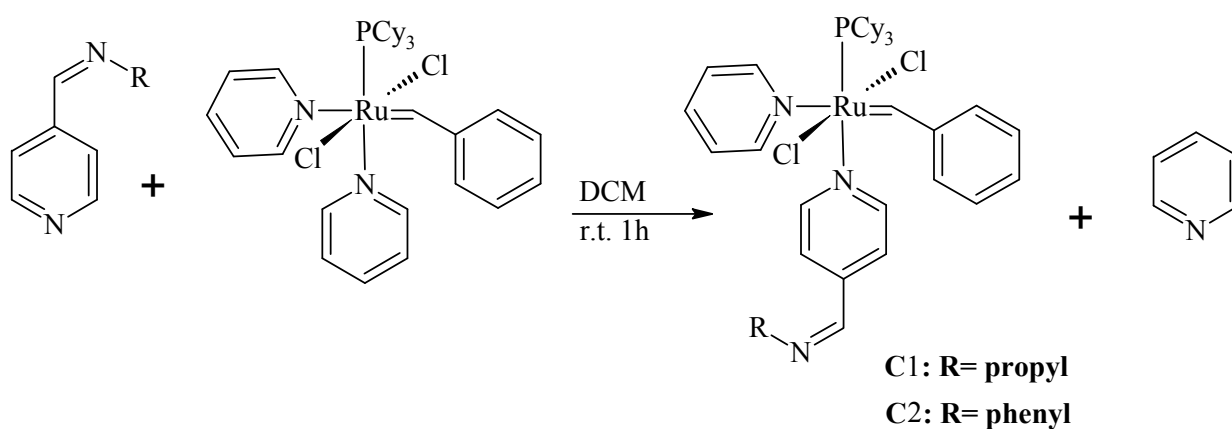
3.2.1 Synthesis of model and dendritic 4-imino pyridine Ru carbene complexes using Grubbs G1 as a precursor.

The synthesis of 4-imino pyridine Ru carbene complexes were attempted using a series of different reactions. This first involved the use of the conventional Grubbs G1 catalyst. Based on the product obtained in this reaction, there was some evidence of complexation taking place, however a fair amount of the expected by-product, tricyclohexyl phosphine (PCy₃) was also obtained. Several work-up protocols were attempted to purify the product. This included the use of non-polar solvents such as hexane, pentane or petroleum ether in washing the crude product; slow diffusion of one of the non-polar solvents into dichloromethane solutions of the crude material as well as cooling of these mixtures at temperatures ranging between 0°C to -78°C. Cooling was employed after it was observed that the mononuclear products tend to decompose in solution at room temperature and that they were fairly soluble in most organic solvents. The above mentioned work-up procedures resulted in very low yields of the desired product and also led to some hydrolysis of the imine and in some cases also the metal carbene occurring.

Another approach used involves the precursor, Grubbs G1 first being modified with pyridine and then reacted with the 4-imino pyridine ligands. This approach was taken in order to eliminate the step of trying to get rid of free PCy₃, which proved to be challenging. Getting rid of pyridine on the other hand could be effected by simple drying of the product formed under vacuum. The *pyridine* modified Grubbs G1 complex was prepared by reacting Grubbs G1 with excess pyridine, this displaces one of the PCy₃ ligands.

The challenge faced by monofunctional ligands to getting rid of the PCy₃ was not an issue for dendritic complexes. Regardless of the precursor used the dendritic Ru carbene complexes were formed as orange-brown solids after work up. These dendritic complexes were found to be insoluble in all solvents including acetone, dimethyl sulfoxide, diethyl ether, toluene, dichloromethane, chloroform and benzene. They could thus be purified by washing extensively with organic solvents to get rid of any by-products. The insoluble nature of these complexes however limited the full characterization of the dendritic complexes. Thus we were unable to carry out any NMR or mass spectral studies.

The reaction of **L1-L4** with the *pyridine* modified Grubbs generation 1 complex in dichloromethane affords complexes (**C1-C4**) within an hour. This is shown in Scheme 3.1. The mononuclear complexes (**C1** and **C2**) were formed as sticky residues and were purified by redissolving them in pentane and cooling the mixture in an ice bath upon which they precipitate out as dark orange-brown solids in moderate yields, 55%-65%. The dendritic complexes (**C3** and **C4**) shown in Figures 3.1 and 3.2 respectively, were simply purified by dissolving these in a minimum volume of dichloromethane and precipitating them with the addition of excess pentane. The yields were moderate ranging between 60%-68%.



Scheme 3.1: Synthesis of a 4-imino pyridyl Ru carbene complex.

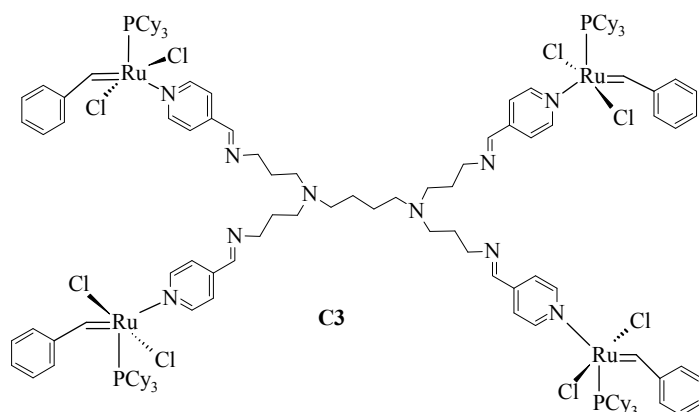


Figure 3.1: General structure for the G1 dendritic 4-imino pyridyl Ru carbene complex.

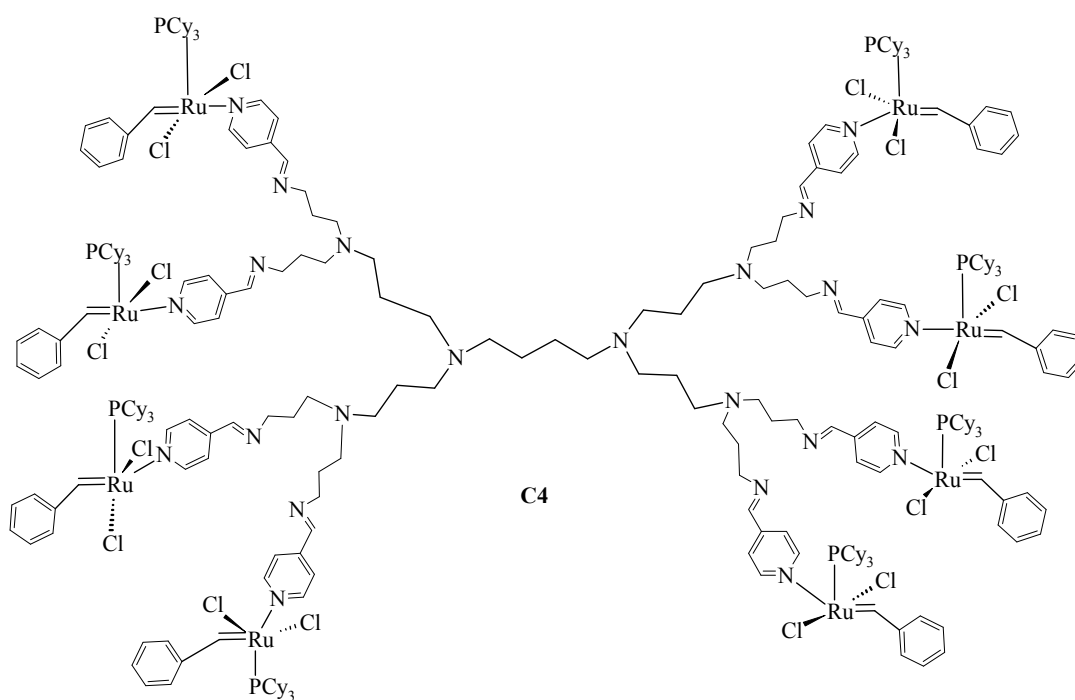


Figure 3.2: General structure for the G2 dendritic 4-imino pyridyl Ru carbene complex.

Attempts to prepare **C1** and **C2** directly from unmodified Grubbs precursor were unsuccessful since it was difficult to completely remove liberated tricyclohexylphosphine from the product.

The expected structures of **C1-C4** were confirmed by various spectroscopic techniques. Due to the nature of the ligands, it was initially uncertain whether the coordinating donor atom

would be the pyridine ring nitrogen or the nitrogen of the free imine functionality. The mode of coordination could however be determined using IR and NMR spectroscopy.

3.2.1.1 Characterization by means of infrared spectroscopy

IR spectroscopy was employed to establish the mode of bonding. Through the shifting of only the $\nu(\text{C}=\text{N})$ band of the pyridine ring it was confirmed that the coordination was taking place through the N donor atom in the ring. The results from ATR-IR spectroscopy showed the shifting of $\nu(\text{C}=\text{N})$ from $\sim 1597\text{cm}^{-1}$ to higher wavenumbers of around $\sim 1610\text{cm}^{-1}$. This is clearly illustrated in Figure 3.3 which shows that the mode of bonding between **L1** and Ru in **C1** is *via* the ring imine. The free imine $\nu(\text{C}=\text{N})$ band at 1647 cm^{-1} remained unchanged as in **L1**, whereas the ring $\nu(\text{C}=\text{N})$ shifted to 1606 cm^{-1} . The IR results for all the complexes are tabulated in Table 3.1. The mononuclear complexes were found to decompose at temperatures between 105°C - 140°C to form black solids. The dendritic complexes were stable even at temperatures above 285°C .

Table 3.1 Selected IR, MS as well as microanalysis data for 4-imino pyridine complexes, **C1**-**C4**

Complexes	IR		ESI-MS (m/z)	Elemental analysis % Found (calculated)		
	$\nu(\text{C}=\text{N})$	$\nu(\text{C}=\text{N})_{\text{py}}$		C	H	N
C1	1645	1606	690	54.83(54.20) ^a	6.95(6.89) ^a	4.59(3.61) ^a
C2	1621	1609	724	61.21(61.32)	6.65(6.81)	5.04(3.87)
C3 ^b	1647	1610		58.94(59.14)	7.12(7.37)	4.61(4.93)
C4 ^b	1647	1600		63.41(63.79)	7.92(8.63)	4.15(4.40)

^a Calculated for $\text{C}_{34}\text{H}_{51}\text{Cl}_2\text{PN}_2\text{Ru}\cdot\text{1CH}_2\text{Cl}_2$

^b No ESI-MS due to low solubility

3.2.1.2 Characterization by means of ESI-MS spectrometry and elemental analysis

The mononuclear complexes (**C1** and **C2**) were further characterized by electron spray ionization mass spectrometry which confirmed the expected structures. The observed parent ion m/z values for these complexes are provided in Table 3.1. Due to low solubility of the dendritic complexes (**C3** and **C4**) in acetonitrile ESI-MS could not be done on these complexes. The formulated structures of all the complexes were confirmed by the means of elemental analysis. The elemental analysis data is shown in Table 3.1. Solvent inclusion was assumed for **C1** and this was confirmed from the ^1H NMR spectrum.

3.2.1.3 Characterization by means of ^1H NMR spectroscopy

In the ^1H NMR spectrum of the complexes, the protons of the carbon next to the N atom in the pyridine ring shifts by about 0.1 ppm on complexation. The ^1H NMR spectrum shows no shift of the proton of the imine functionality external to the ring. These complexes were found to be stable in the solid state under ambient conditions while in solution they tend to decompose rapidly. The latter was observed by the change of colour from dark orange-brown to green. Also from the ^1H NMR spectrum there were signs of hydrolysis of both the imine ligand and/or the benzylidene group to form an aldehydic species because over time a peak for an aldehyde proton appears rapidly around 10 ppm. The imine peak as well as the carbene peak disappear concomitantly. ^{31}P NMR spectroscopy was also used as an analytical technique in the characterization of complexes **C1-C2**. It confirmed the presence of the phosphorous atom and it was found to be in the range of 35 ppm - 37 ppm as a singlet for all the complexes. This is where one would expect the signal for a metal bound tricyclohexyl phosphine.

The ^1H NMR data for **C1-C4** are tabulated in Table 3.2. The significant proton peaks are that of the external imine group around 8.20 ppm which had not changed upon complexation. The signal for the protons of the C atom next to the pyridine N atom shift downfield giving evidence of complexation through the pyridine nitrogen. In addition the metal-carbene proton signal appears around 20 ppm. In the mononuclear complexes the metal-carbene proton peak appears as a doublet which is assumed to be due to coupling of its proton with the α -H on the pyridinyl ligand. Grubbs G1 catalysts modified with pyridine ligands have been reported [5, 14] previously and these reports claimed that two pyridine ligands coordinate to the metal and that the carbene proton appears as a doublet. In our studies, only one ligand complexed to the Ru center. This was confirmed by the integration of the signals in the ^1H NMR spectrum which only showed mole ratio of the ligand to the metal carbene of 1:1.

In the dendritic complexes the metal-carbene proton peak occurs as a singlet. This could be due to the rigidity of the dendrimer. The other important factor is that significant overlap of the signals occurs, especially in the aliphatic region between 1-2 ppm. Figure 3.6 shows the ^1H NMR spectrum of the crude complex **C3** before work-up. After the work-up, both dendritic complexes formed, have low solubility. This meant that ^{13}C NMR could not be done as it requires a long time to acquire the spectra, which would be a problem as these complexes (**C1-C4**) are unstable in solution. This limited the analytical techniques which could be employed to characterize these dendritic complexes.

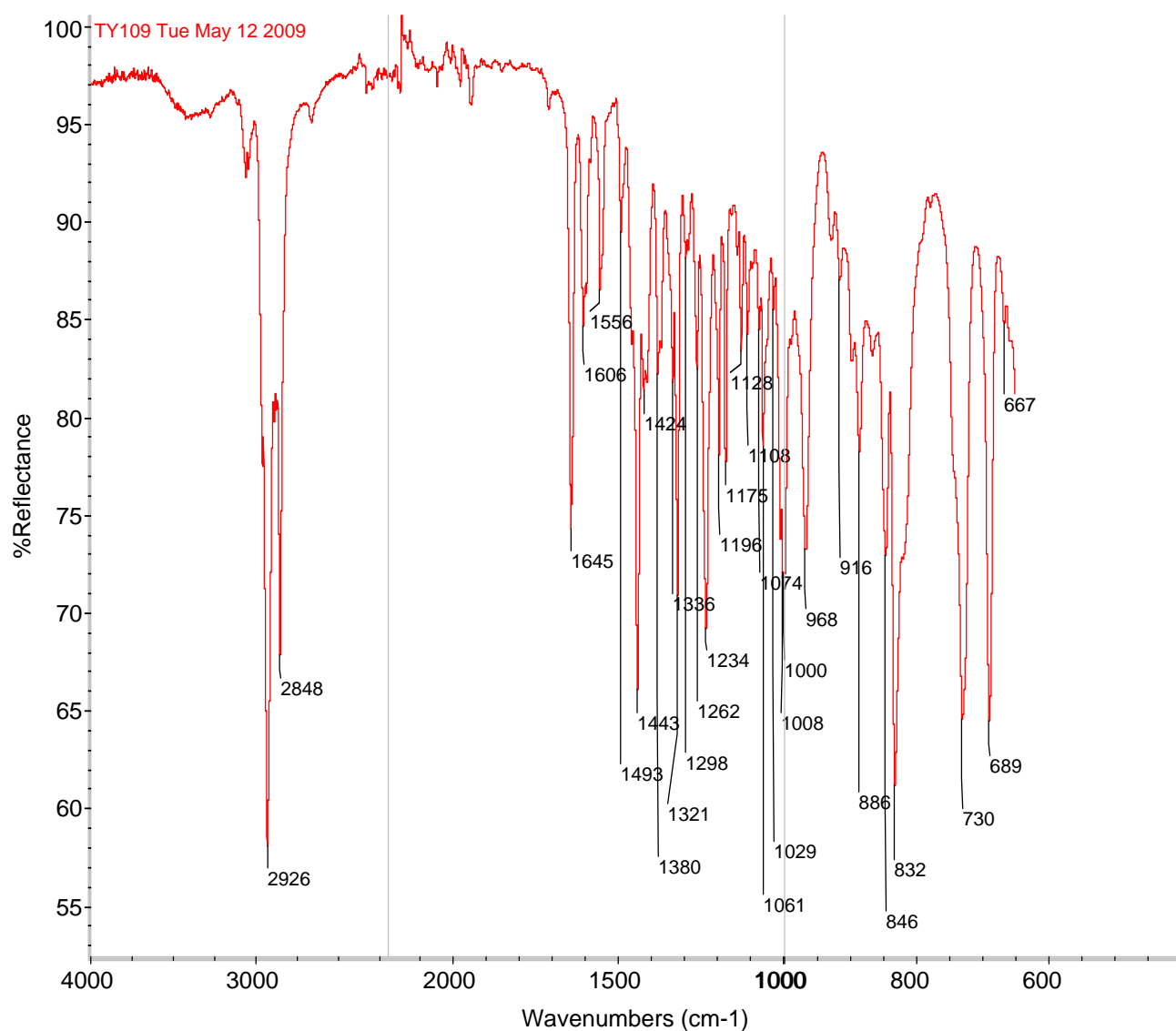


Figure 3.3 IR spectrum of the mononuclear complex **C1**, showing the mode of bonding in Grubbs G1 4-imino-pyridyl complexes.

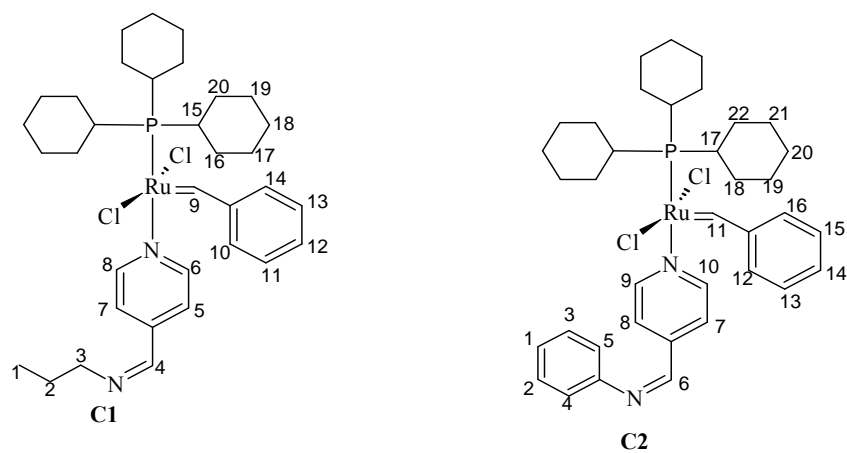


Figure 3.4 C-Atom labelling for mononuclear complexes, **C1** and **C2**

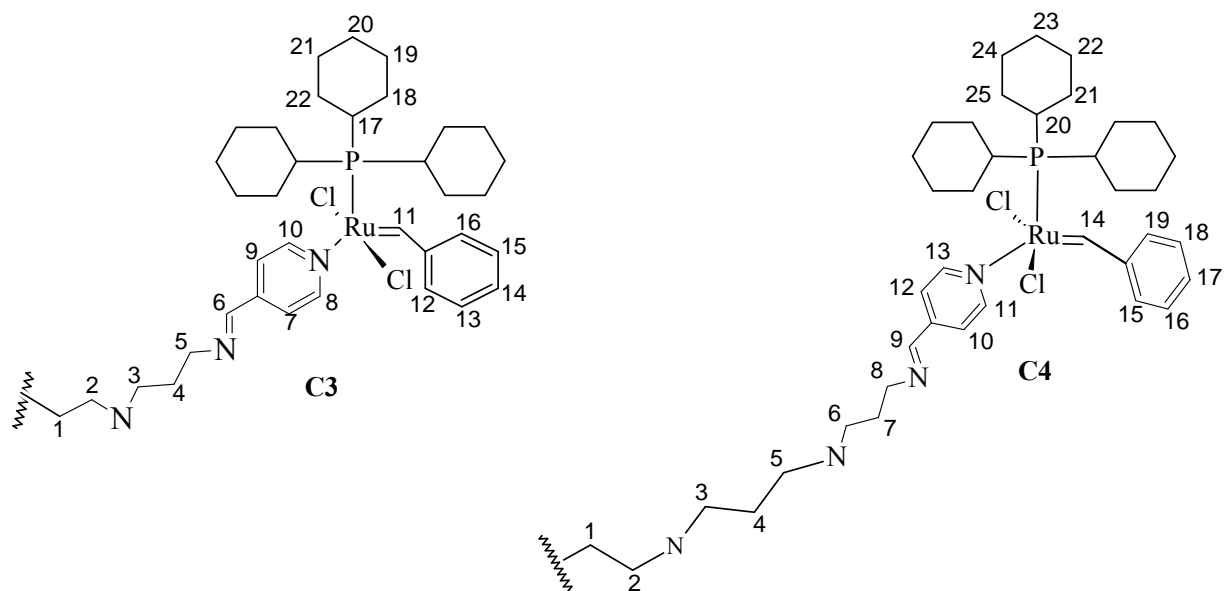


Figure 3.5 C-Atom labelling for dendritic complexes, **C3** and **C4**. (Note: only one arm of the dendrimer molecule is shown)

Table 3.2: ¹H NMR data for phosphine containing 4-imino-py Ru carbene complexes, C1-C4.

Complexes	Chemical shift (̈́- ppm)	Assignment
C1	0.96 t	H1
	^a 1.26 m	H2/15/18
	^a 1.79-1.62 m	H17/19
	^a 2.04 m	H16/20
	2.36 q	H15
	3.61 t	H3
	7.18 t	H11/13
	7.34 t	H12
	7.55 t	H5/7
	8.25 s	H4
	8.45 d	H10/14
	8.77 d	H6/8
	19.93-19.89 d	H9
C2	^a 1.25 m	H17/20
	^a 1.78-1.64 m	H19/21
	^a 2.03 m	H18/22
	2.36 q	H17
	7.19 t	H1
	7.29 t	H14
	7.43 t	H2/3
	7.54 t	H15/13
	7.78 d	H4/5
	7.98 d	H7/8
	8.47 s	H6
	8.76 s	H16/12
	8.92 s	H9/10
20.00 d	H11	

^a Signals overlap. Recorded in CDCl₃

Table 3.2 Cont.

C3	1.19 m	H (PCy ₃)
	^a 1.43 m	H1/19/21
	^a 1.78-1.68 m	H2/3/4/18/22
	2.61 t	H17
	3.66t	H5
	7.14 t	H14
	^a 7.53 t	H7/9
	7.32 t	H13/15
	8.27 s	H6
	8.45 d	H12/16
	8.69 d	H8/10
	19.98 s	H11
C4	1.18 t	H 1/(PCy ₃)
	^a 1.45 m	H4/7/20/23
	^a 1.78-1.68 m	H2/3/5/6/22/24
	2.62 t	H20
	3.66 t	H8
	7.16 t	H17
	^a 7.55 t	H12/10
	7.34 t	H16/18
	8.28 s	H9
	8.46 d	H15/19
	8.74 s	H11/13
20.00 s	H14	

^a Signals overlap.

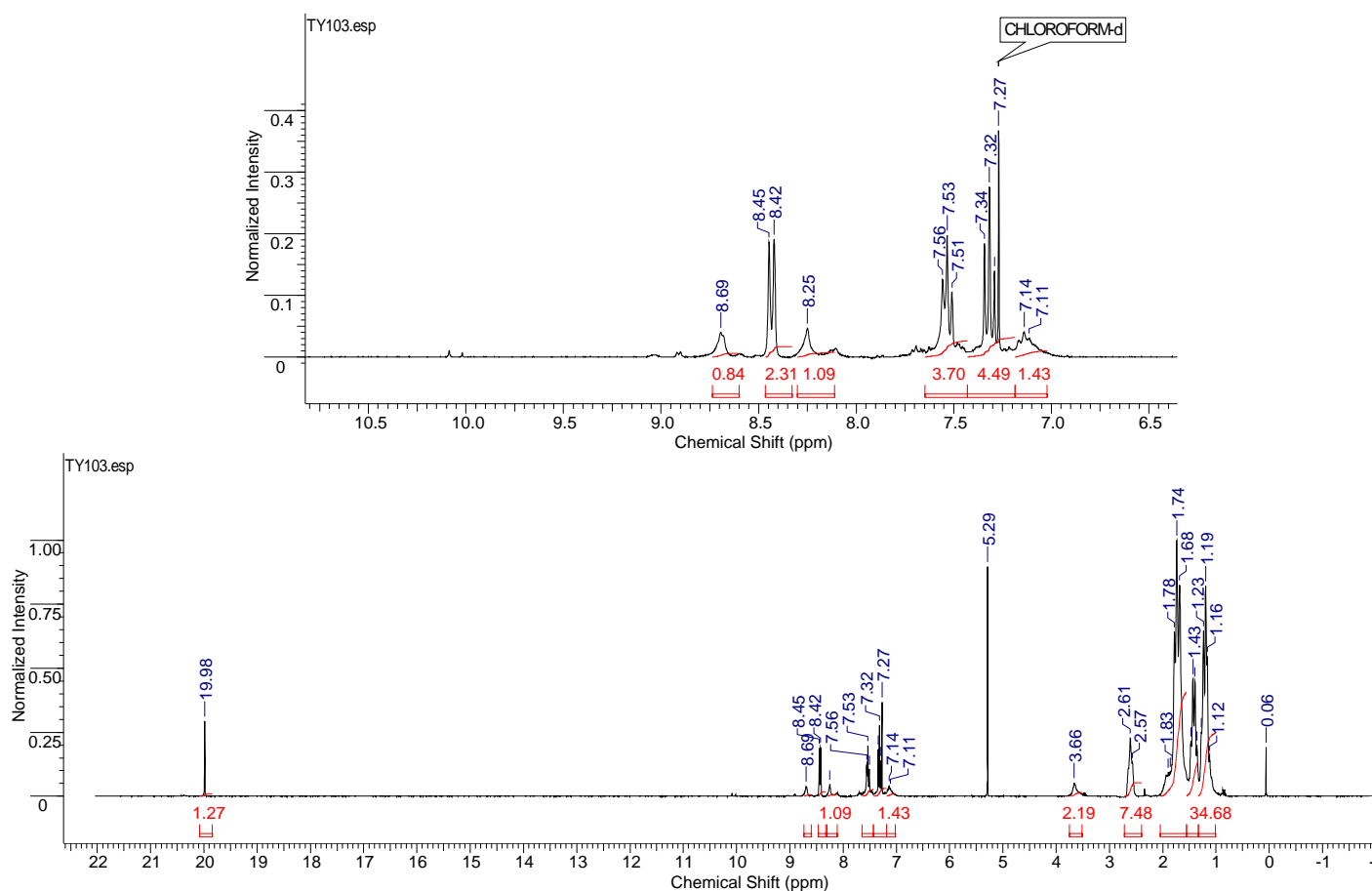


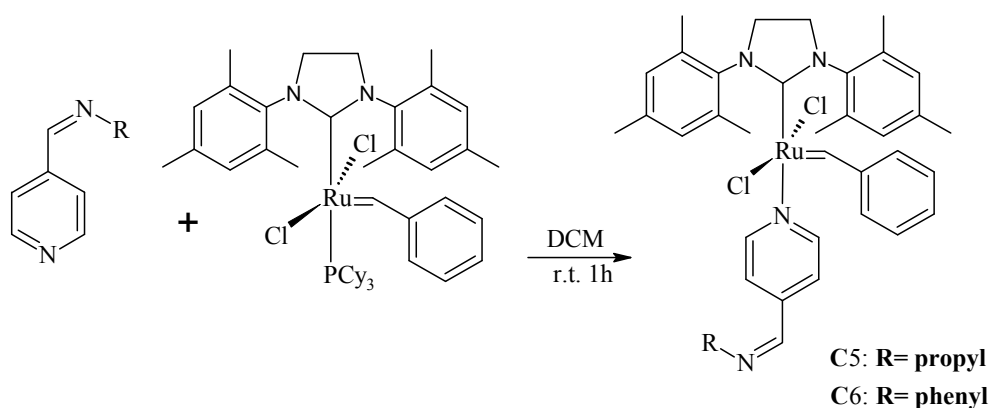
Figure 3.6 The ^1H NMR spectrum of the dendritic complex **C3** showing typical signals of phosphine substituted 4-imino-py-Ru carbene complexes.

3.2.2 Synthesis of model and dendritic 4-imino pyridine Ru NHC carbene complexes using Grubbs G2.

In this part we report on the reaction of the 4-imino-py ligands (**L1-L4**) directly with Grubbs G2 (**6**). This was after it was observed that the desired products were formed without the problem of trying to get rid of PCy_3 . The by-product was removed together with unreacted Grubbs 2 as well as other impurities by cooling the crude product in pentane solution to 0°C . The product precipitates out and the impurities are found in the mother liquor. The synthesis of this type of complex where the phosphine is replaced by the more stable NHC ligand was carried out under similar conditions used for **C1-C4**. However the yields of the Grubbs G2, 4-imino-pyridyl complexes were slightly lower than those of the Grubbs G1 complexes and

range between 50-53%. These complexes were purified following the same procedure described for the above mentioned phosphine complexes.

Complexes (**C5**, **C7** and **C8**) were found to be yellowish-brown in colour whereas **C6** was a red solid. These solids were found to be more stable than those with phosphine ligands in both solution and solid state. The general structures of the dendritic complexes are shown in Figures 3.7 and 3.8.



Scheme 3.2: Synthetic pathway for formation of imino-pyridyl Ru carbene complexes.

3.2.2.1 Characterization by means of Infrared spectroscopy

The mode of bonding was also established by IR spectroscopy which confirmed that also Grubbs G2 coordinate *via* the N atom in the pyridine ring. There was a shifting of $\nu(\text{C}=\text{N})$ of the pyridine ring to $\sim 1600\text{ cm}^{-1}$ whilst the imine external to the ring remained unchanged. The $\nu(\text{C}-\text{N})$ stretch due to NHC ligand is also observable around 1264 cm^{-1} which also confirms the nature of the complex formed. A stretch around 1200 cm^{-1} is not observed for phosphine containing Ru carbene complexes (**C1-C4**). In the dendritic complexes the shifting of $\nu(\text{C}=\text{N})$ of the pyridine ring was not as significant as that observed for the mononuclear complexes.

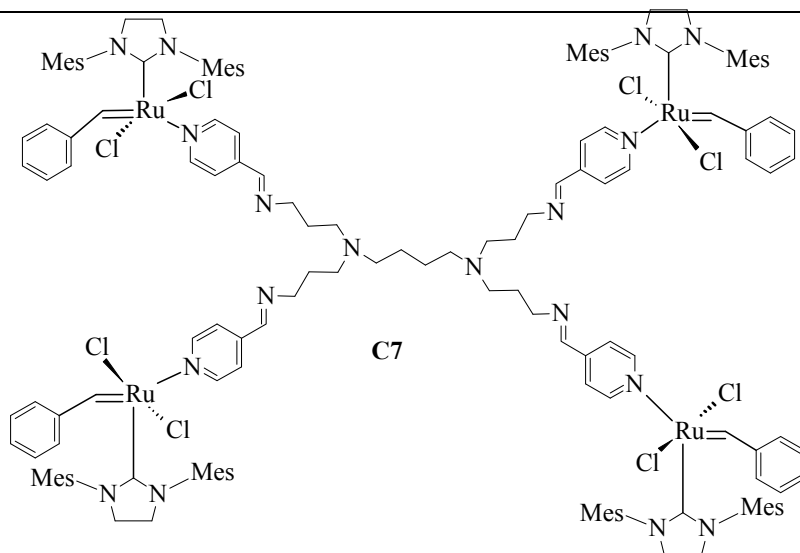


Figure 3.7 General structure for the G1 dendritic Ru carbene complex, **C7**.

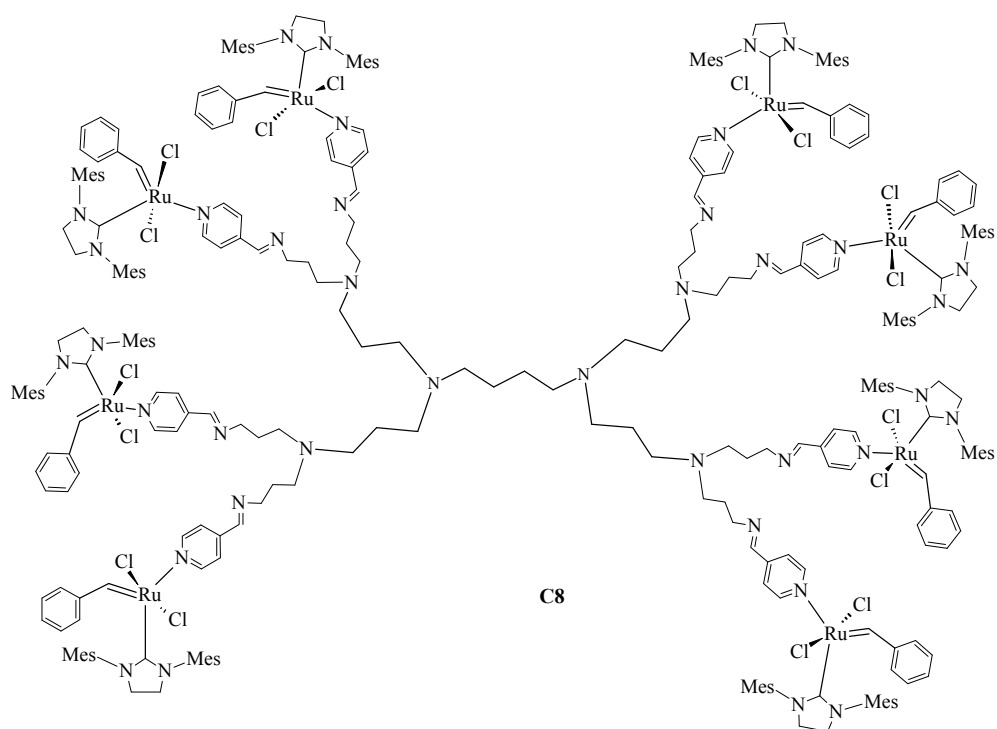


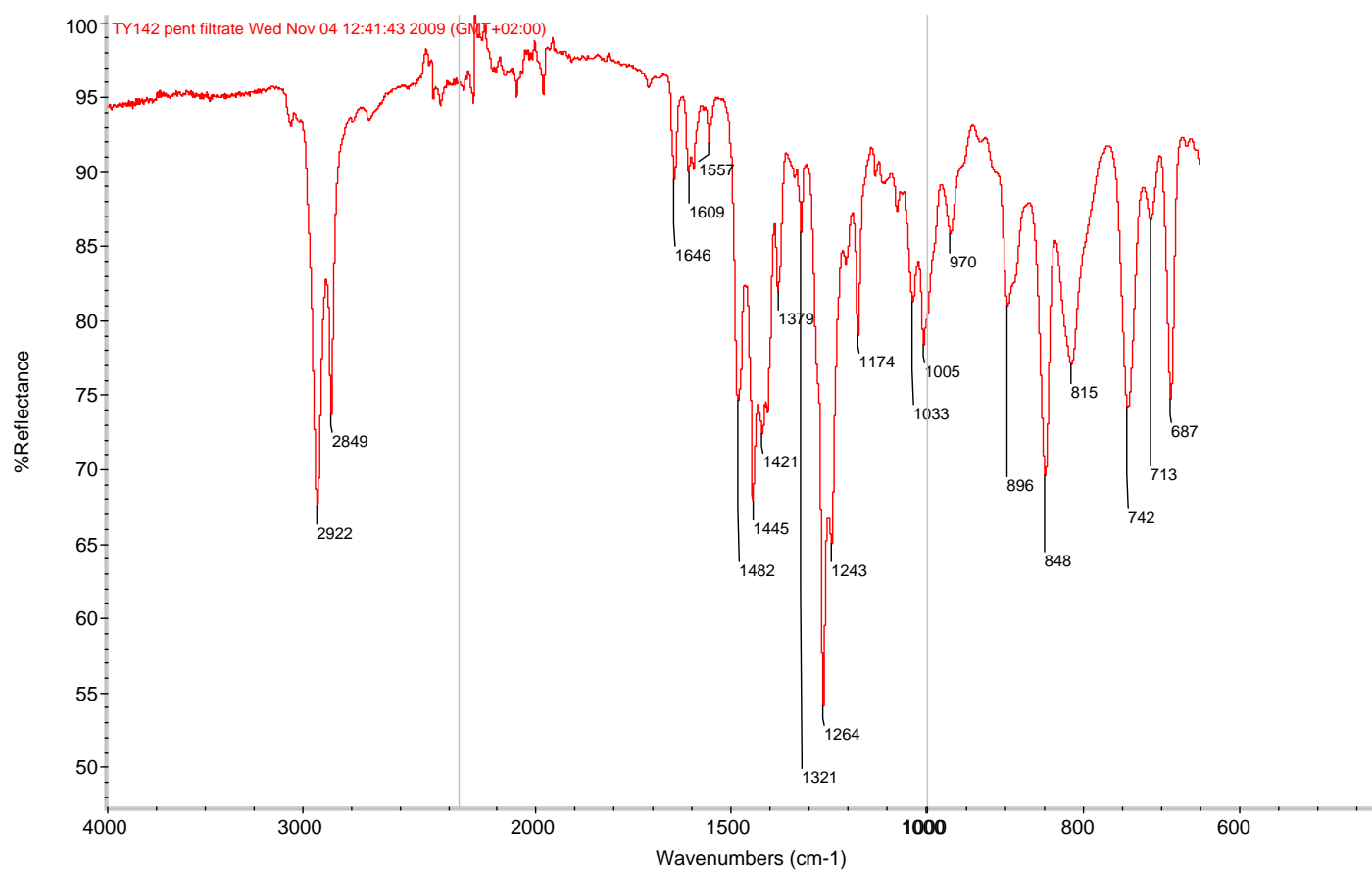
Figure 3.8 General structure for the G2 dendritic Ru carbene complex, **C8**.

Table 3.3 Selected IR, MS and microanalysis data for the 4-imino-py Ru NHC carbene complexes, **C5-C8**.

Complexes	IR		ESI-MS (m/z)	Elemental analysis % Found (calculated)		
	$\nu(\text{C=N})$	$\nu(\text{C=N})_{\text{py}}$		C	H	N
C5	1646	1609	717	58.90 (59.41)	7.01 (6.31)	6.48 (7.29)
C6	1625	1609	750			-
C7^c	1645	1599		56.68 (56.94) ^a	6.45(5.88) ^a	11.06(7.66) ^a
C8^c	1645	1600	-	58.19 (58.29) ^b	6.72(6.09) ^b	11.88(8.12) ^b

^a $\text{C}_{152}\text{H}_{184}\text{Cl}_8\text{N}_{18}\text{Ru}_4 \cdot 4 \text{CH}_2\text{Cl}_2$; ^b $\text{C}_{312}\text{H}_{284}\text{Cl}_{16}\text{N}_{38}\text{Ru}_8 \cdot 6 \text{CH}_2\text{Cl}_2$

^c No ESI-MS due to low solubility.

Figure 3.9 IR spectrum of the mononuclear 4-imino-py Ru NHC carbene complex, **C5**

3.2.2.2 Characterization by means of ESI-MS and elemental analysis

The elemental analysis data obtained for the modified 4-imino pyridine Grubbs G2 complexes are shown in Table 3.3. The mononuclear complexes **C5** and **C6** formulation were further confirmed by electron spray ionization mass spectrometry. Parent ions for both complexes were observed and are shown in Table 3.3. The ESI-MS spectra for both complexes had similar fragmentation patterns which showed the presence of the NHC ligand at m/z 307.2 as well as a fragment peak at m/z 597.4 due to a species formed as a result of the hydrolysis of both the benzylidene and imine functional groups. In addition to the parent ion, another significant fragment peak was observed at m/z 149 (**C5**) and at m/z 183 (**C6**) which are due to the 4-imino pyridine groups of each ligand.

In all cases for the mononuclear Ru-carbene complexes, it was found that these complexes do not melt but decompose between the temperatures 110°C-165°C. This was observed after these complexes changed colour to black. The dendritic complexes were exposed to temperatures as high as 285°C but did not show any sign of decomposition or melting.

3.2.2.3 Characterization by means of ^1H NMR spectroscopy

^1H NMR spectroscopy further confirmed the bonding mode of these types of complexes. The data tabulated in Table 3.4, give evidence of the mode of bonding in these complexes. This shows the shifting of the signal for the imino functionality of the pyridine ring to ~ 8.70 ppm. Figure 3.12 shows a typical spectrum of the Ru-NHC carbene complexes using **C8** as an example.

Another distinct observation from the spectra of these complexes is the presence of the signal for the NHC protons around 4 ppm as well as the metal-carbene signal at ~ 19.15 ppm for mononuclear and 19.24 ppm for the dendritic complexes. The metal-carbene signal of these

complexes appears upfield relative to that found in the phosphine counterparts (**C1-C4**). The signals for the mesityl protons were also observed for all complexes. In the dendritic complexes there is an overlap of signals of the DAB core protons with those of the mesityl protons in the NHC ligand.

The data obtained for these type of complexes are comparable with that of similar complexes reported in literature. There are a number of reports on Grubbs NHC complexes incorporating pyridines or functionalized pyridine units [6, 15]. The results we obtained, correlated well with those reported in terms of ^1H NMR results. Grubbs type catalysts tend to coordinate with the pyridine ring even when other coordination sites are present. The coordination of the pyridine ring to ruthenium leads to shifting of the pyridine protons to higher chemical shifts. The number of signals due to the presence of the NHC ligand was found to be similar to those reported in literature. There is evidence that the displacement of the PCy_3 ligand by pyridine ligands is facile as no signals of PCy_3 are observed.

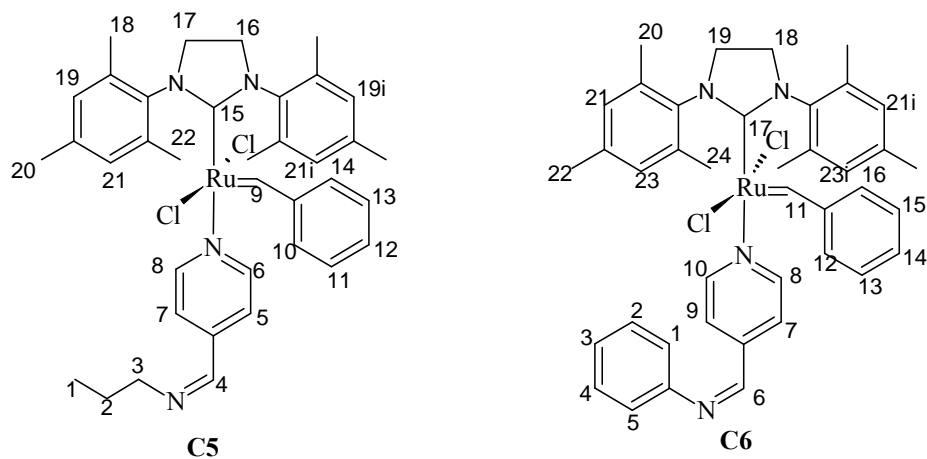


Figure 3.10 C-atom labelling of mononuclear complexes, C5 and C6

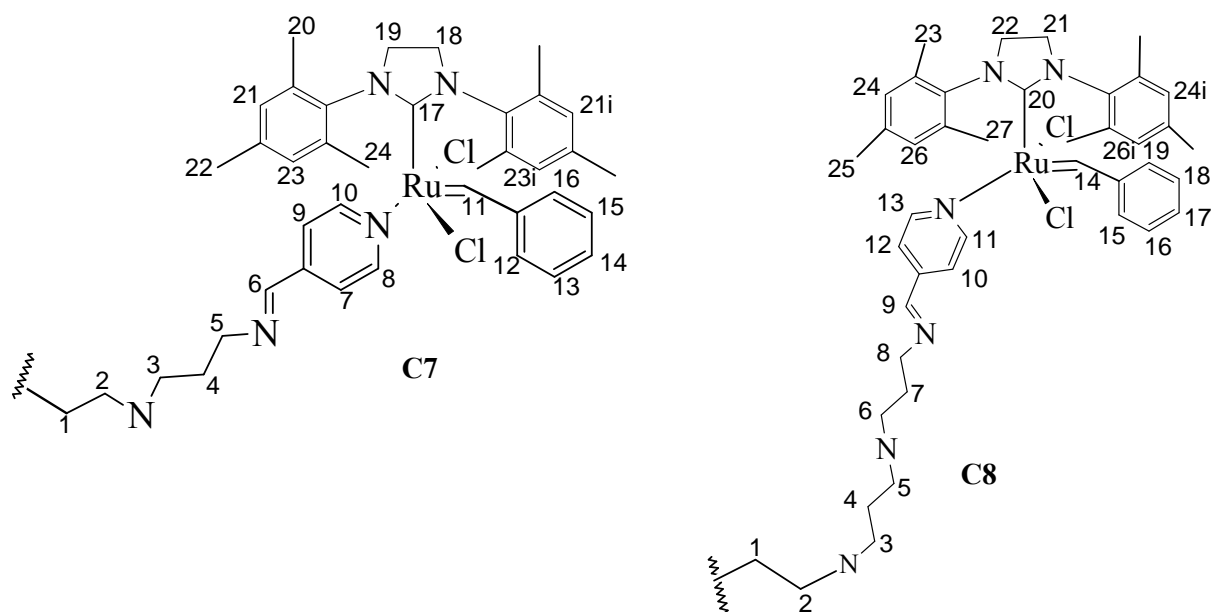


Figure 3.11 C-atom labelling of dendritic complexes, C7 and C8 showing only one arm of the dendrimer generation.

Table 3.4: ^1H NMR data for 4-imino-py Ru NHC carbene complexes, recorded in CDCl_3 , **C5-C8**.

Complexes	Chemical shift (δ - ppm)	Assignment
C5	0.97 t	H1
	1.00 d	H20
	1.51-1.46 m	H18/20
	1.74 m	H2
	1.92 s	H18
	2.32-2.26 s	H18/20/22
	2.65 s	H18/22
	3.64 t	H3
	4.01 t	H16/17
	6.77 s	H15
	7.02 s	H19
	7.21 s	H21
	7.06 t	H12
	7.48 t	H11/13
	7.58 d	H7/5
	7.64 d	H10/14
	7.90 s	H19i
	8.10 s	H21i
8.27 s	H4	
8.72 d	H6/8	
19.16 s	H9	
C6	1.02 d	H22
	1.51 t	H20/22
	1.92 s	H20
	2.32-2.26 s	H20/22/24
	2.66 s	H20/24
	4.08 t	H18/19

Table 3.4 Cont...

	6.78 s	H17
	7.03 s	H23
	7.20 s	H21
	7.09 t	H3
	7.24 d	H2/4
	7.37 d	H1/5
	7.49 t	H14
	7.64 d	H13/15
	7.70 s	H21/23
	7.97 d	H7/9
	8.24 s	H12/16
	8.46 s	H6
	8.80 d	H8/10
	19.16 s	H11
C7	1.28 s	H1
	1.67-1.51 s	H20/22/24
	2.25 s	H2/3
	2.31 s,	H20/24
	^b 2.54-2.44 m	H4/20/22/24
	3.66 t	H5
	3.98 d	H18/19
	6.68 s	H17
	6.92 s	H21
	6.99 t	H14
	7.20 s	H23
	7.34 s	H21i
	7.55 t	H13/15
	7.75 d	H7/9

^b Proton overlap

Table 3.4 Cont.

	7.89 d	H12/16
	8.08 s	H23i
	8.24 s	H6
	8.69 d	H8/10
	19.23 s	H11
C8	1.28 s	H1
	^b 1.65-1.51 s	H4/7/23/25/27
	2.11 s	H5/6
	2.31 s	H23/27
	^b 2.54-2.44 m	H2/3/23/25/27
	3.64 t	H8
	3.95 d	H21/22
	6.62 s	H20
	6.92 s	H24
	6.99 t	H17
	7.20 s	H26
	7.34 s	H24i
	7.55 t	H16/18
	7.62 s	H26i
	7.77 d	H10/12
	7.89 d	H15/19
	8.23 s	H9
	8.73 d	H11/13
	19.26 s	H14

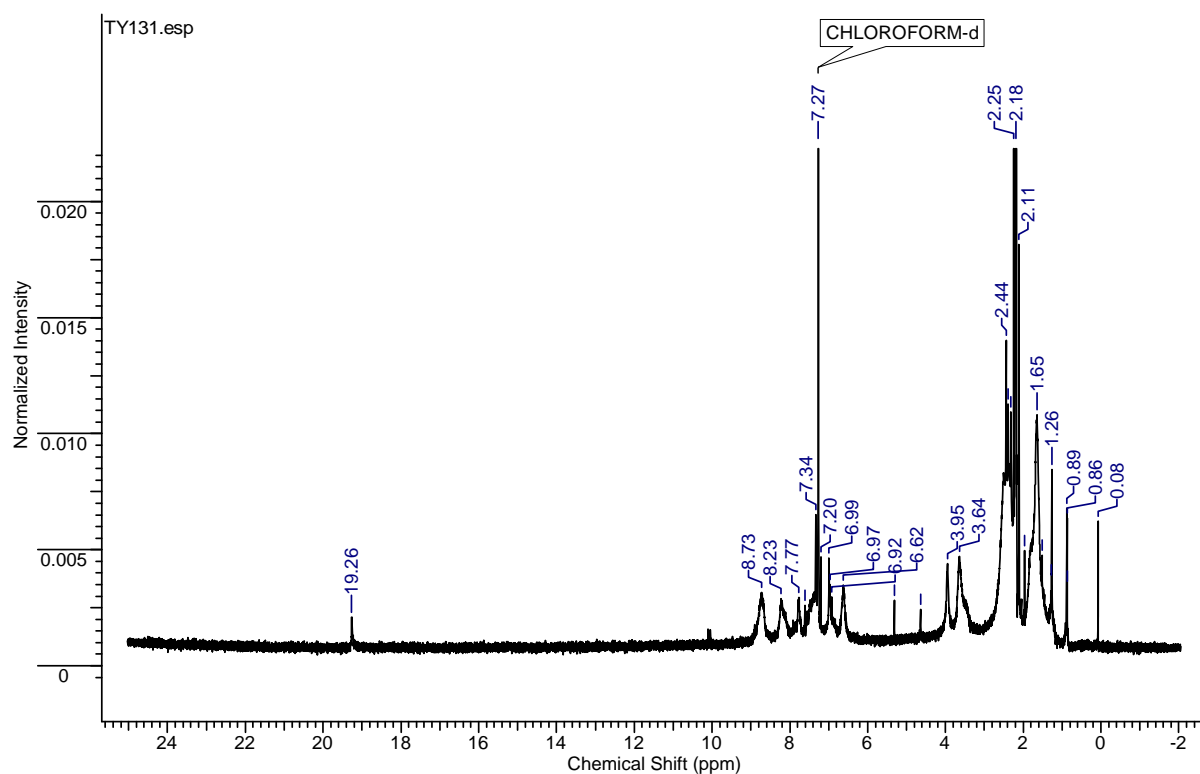


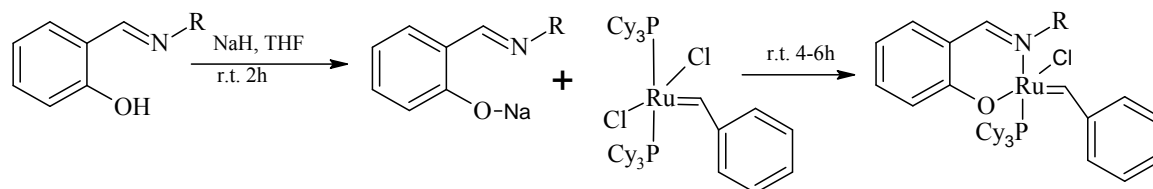
Figure 3.12 ^1H NMR spectrum of the G2 dendritic Ru NHC carbene complex, **C8**.

3.2.3 Attempted synthesis of model and dendritic salicylaldimine Ru carbene complexes.

Initially the aim of the project was to also extend the work to salicylaldimine ruthenium carbene catalyts by anchoring Ru carbene catalyts on salicylaldimine functionalized diaminobutane polypropyleneimine dendrimers. This was however found to be problematic.

The attempted synthesis of salicylaldimine Ru-carbene complexes in which Grubbs G1 was reacted with monofunctional and dendritic salicylaldimine ligands was undertaken. However the synthesis of the targeted complexes was not very successful. Initially we thought that deprotonation of the phenoxy group to form the sodium salt of the ligands was the problematic step leading to failure in forming the desired complex. Alternatively not completely dry solvents were also thought to be responsible for unsuccessful reactions. Different deprotonating agents were employed to try and overcome this problem. These deprotonating agents included the use of compounds such as TIOEt, *n*-BuLi, KOH and NaH. The deprotonating agents that proved to be the most efficient were NaH and *n*-BuLi. The

formation of the salts was confirmed by ^1H NMR spectroscopy where the hydroxy proton is not observed whilst the imine proton moves to a lower chemical shift and the aromatic protons are resolved into four distinct signals. After confirmation of anion formation, we then reacted it with Grubbs G1 as shown in Scheme 3.3. This reaction was also monitored by ^1H NMR. After several attempts there were only a few instances which showed some evidence of complexation occurring in the model complexes but giving very low yields, which made it difficult to work-up the resulting product. The target compounds were thus never isolated in pure form and were thus not fully characterized. Trying various reaction conditions did not improve the situation.



Scheme 3.3: Attempted synthesis of salicylaldimine Ru carbene complexes using Grubbs G1.

In case of the dendritic compounds the reaction also did not yield the desired product. The reaction resulted in formation of an unstable ruthenium species which was not characterized further. Many factors may have contributed to the failure of these reactions. As reported in literature, Grubbs catalysts need to be handled under extremely inert conditions when reacting them, as they tend to decompose in solution when exposed to moisture and air [17]. The target molecules themselves might also be unstable and could thus have decomposed before isolation.

Given the above results, an alternative approach involving a different ruthenium precursor, *i.e.* the ruthenium *p*-cymene dichloride dimer, $[\text{Ru}(\mu\text{-Cl})\text{Cy}(\text{Cl})_2]_2$ was investigated. This involved the reaction of the Na salts of dendritic salicylaldimine ligands with the *p*-cymene

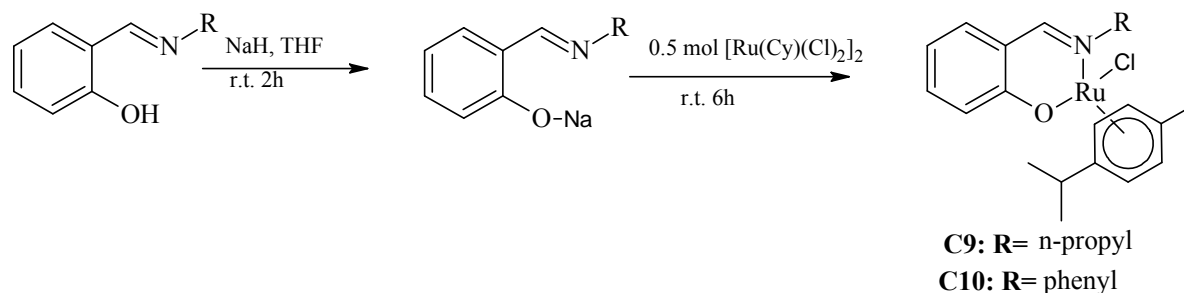
ruthenium chloride dimer. Some salicylaldimine Ru- η^6 coordinated *p*-cymene chloride complexes have been previously reported. The work done by Verpoort *et al.* [15] where they synthesized some of the above-mentioned complexes and used them in olefin metathesis reactions inspired us to extend this work to form dendritic complexes of this nature. Verpoort claimed that these type of complexes show high activity in the presence of an activator *viz.* trimethylsilyldiazomethane (TMSD) which is believed to initiate the formation of an active Ru carbene species in-situ. The second part of our investigation involved the preparation of monofunctional and dendritic salicylaldimine ruthenium *p*-cymene chloride complexes.

The *p*-cymene ruthenium dichloride dimer, $[\text{Ru}(\mu\text{-Cl})\text{Cy}(\text{Cl})_2]$ was prepared according to a reported method [17] and its purity was checked with IR and ^1H NMR spectroscopy. The reaction of this precursor with salicylaldimine salts yielded Ru complexes containing both the salicylaldimine and *p*-cymene ligands. Exploring the literature we found a report on this type of complexes being used in an olefin metathesis reaction, *viz.* ROMP of NBE [16]. We thus opted to study these complexes in some more detail. The following section describes the synthesis of salicylaldimine ruthenium *p*-cymene complexes as well as their full characterization.

3.2.4 Synthesis of model and dendritic salicylaldimine Ru *p*-cymene complexes.

Sodium salts were relatively easy to prepare compared to other possible salts. They were formed as light yellow crystalline materials and were subsequently used in the complexation reaction with the ruthenium *p*-cymene dimer as shown in Scheme 3.4. The ruthenium cymene dimer precursor was prepared following the procedure reported in the literature [18]. Both model and dendritic complexes were formed as orange brown solids in reasonable yields ranging from 60-68%. The general G1 and G2 dendritic structures are shown in Figures 3.13 and 3.14 respectively. These complexes were found to be stable in both solution and the solid

state. A range of analytical techniques was used to characterize the complexes. This included ^1H , ^{13}C NMR, IR spectroscopy and ESI-MS. Melting points of the complexes were also recorded. The mononuclear complexes **C9** and **C10** show sharp melting points whilst the dendritic complexes showed signs of decomposition between 170-180°C before they start to melt above 200°C.



Scheme 3.4: Synthesis of salicylaldimine Ru *p*-cymene complexes

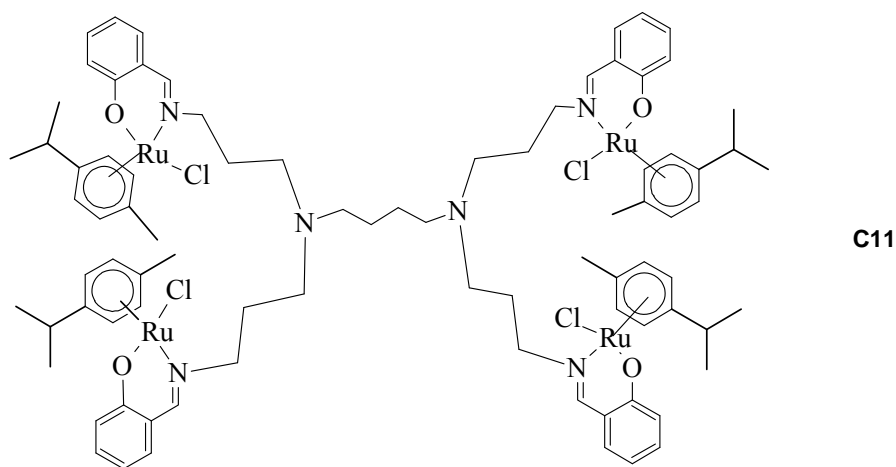


Figure 3.13 Dendritic G1 salicylaldimine Ru chloro *p*-cymene complex.

3.2.4.1 Characterization by means of infrared spectroscopy

Complexation was confirmed by various analytical techniques. Using FTIR spectroscopy, the spectra showed a clear shifting of both the peaks for the imine and aryloxy functionalities. The imine band $\nu(\text{C}=\text{N})$ shifted from 1631cm^{-1} to 1621cm^{-1} and the $\nu(\text{C}-\text{O})$ band was found

around 1149cm^{-1} . The results for all complexes are shown in Table 3.5. This is also supported by the $^{13}\text{C}\{^1\text{H}\}$ NMR where the carbon of the C-O functionality shifts from 160 ppm to 165 ppm whereas the imine C does not show any significant shift and occurs at 164 ppm.

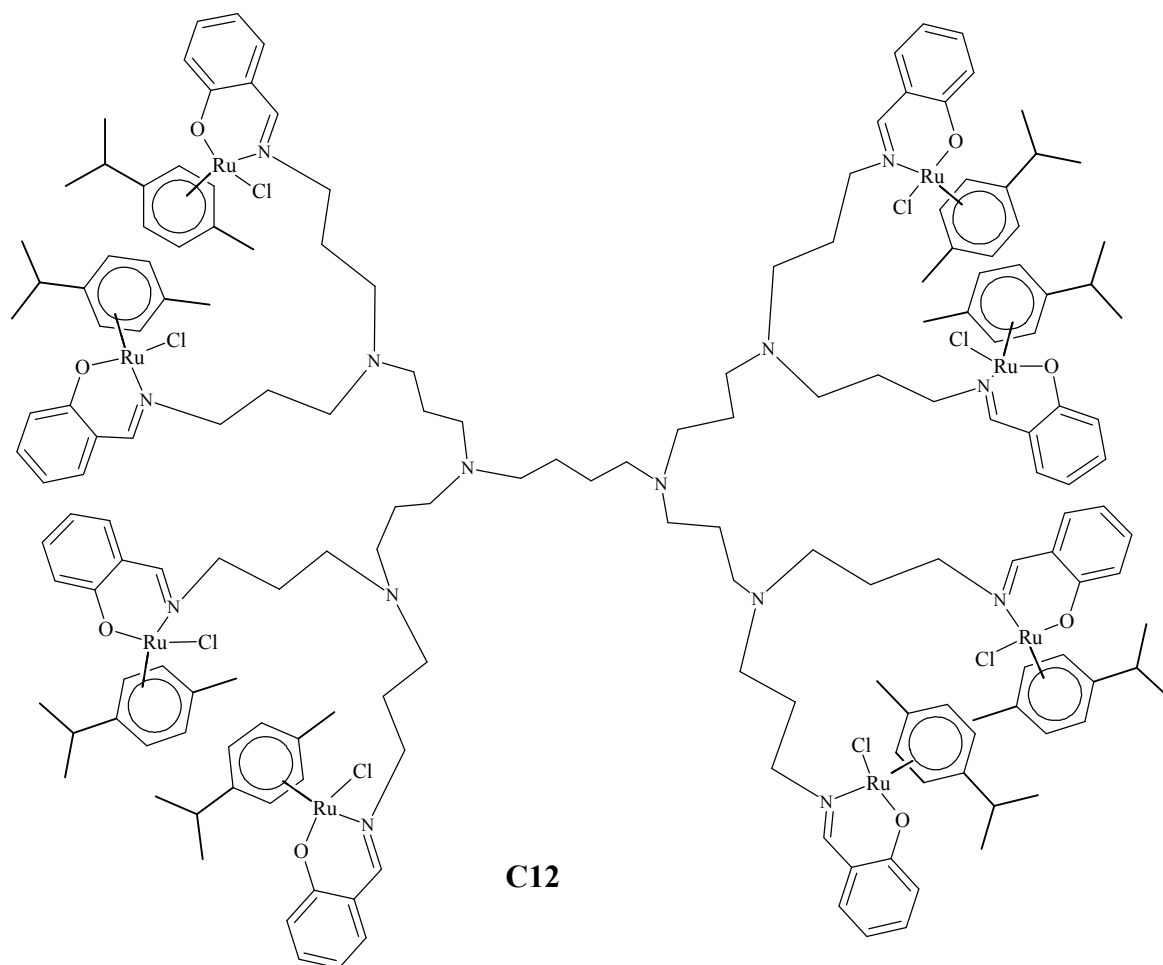


Figure 3.14 G2 dendritic salicylaldimine Ru chloro *p*-cymene complex.

3.2.4.2 Characterization by means of ESI-MS and elemental analysis

The ESI mass spectra of the mononuclear complexes (**C9** and **C10**) gave peaks at m/z 396 (**C9**) and at m/z 423 (**C10**) which are assigned as $[\text{M}-\text{Cl}]^+$. Similar results were also observed for analogous complexes reported in the literature [19] and analyzed *via* ESI mass spectrometry in which loss of chloride ligands is observed during ionization. For the dendritic complexes, multi-charged species are observed. In G1 complex (**C11**) there is a triply charged fragment peak at m/z 604.16 and is the highest mass peak observed. Ionization of the Cl^- ion results in the fragmentation peak at m/z 569.09. The fragment peak at m/z 534.10 is the result

of the second Cl⁻ ion being lost. Hydrolysis of the imine bond was shown to have occurred under the conditions used to run the mass spectra and the peak of the hydrolysis product is at *m/z* 519.07. The symmetrical nature of the dendrimers is also noted from the ESI mass spectra of these complexes as **C11** and **C12** have very similar fragmentation patterns.

Elemental analysis data shown in Table 3.5 confirmed the purity and formulated structures of **C10-C12**. In the case of **C9**, we were unable to obtain satisfactory elemental analysis due to the sensitive nature of the material.

Table 3.5 Analytical data for salicylaldimine Ru *p*-cymene complexes, **C9-C12**.

Complexes	IR		MS (<i>m/z</i>)	M.P.(°C)	Elemental analysis % Found (calculated)		
	<i>i</i> (C=N)	<i>i</i> (C-O)			C	H	N
C9	1622	1149	^a 396	100-110			-
C10	1606	1147	^a 432	160-165	53.22(52.23) ^b	5.36(4.75) ^b	2.27(2.54) ^b
C11^b	1620	1148	604	190-195	51.39(52.12) ^c	5.79(5.85) ^c	3.82(4.43) ^c
C12^b	1621	1148	518	210-222	53.05(53.50) ^d	5.85(5.97) ^d	4.35(4.88) ^d

^aion peak as [M-Cl]⁺

^b C₂₃H₂₄ClNORu.1CH₂Cl₂; ^c C₈₄H₁₀₈Cl₄N₆O₄Ru₄.2CH₂Cl₂; ^d C₁₇₆H₂₃₂Cl₈N₁₄O₈Ru₈.3CH₂Cl₂

3.2.4.3 Characterization by means of ¹H NMR spectroscopy

The ¹H NMR spectra showed shifting of the imine proton upfield from around 8.8 ppm to around 7.9 ppm with the aromatic proton peaks of the aldimine splitting into four signals. The other observations were the presence of the *p*-cymene signals around 5.4 ppm as well as the alkyl moieties in the range of 1.1-2.9 ppm.

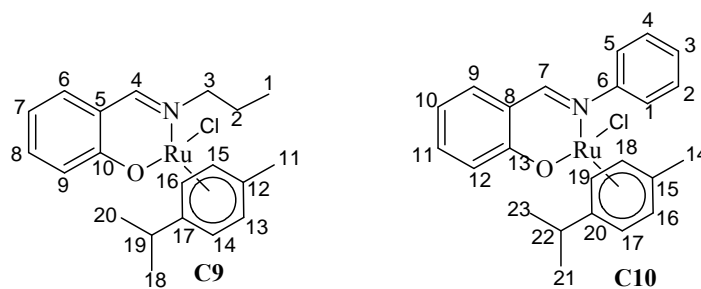


Figure 3.15 Atoms labelling for mononuclear salicylaldimine Ru-p-cymene complexes, C9 and C10.

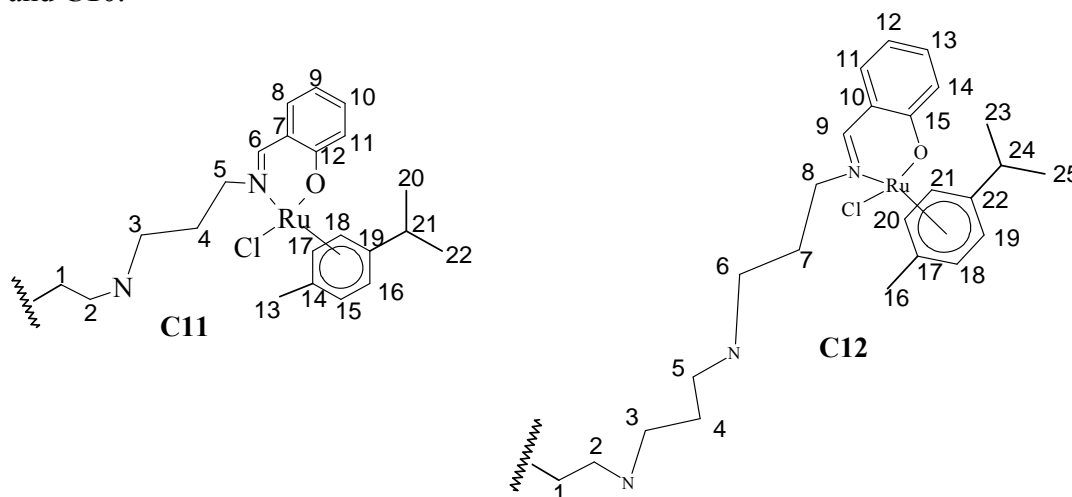


Figure 3.16 Atoms labelling for dendritic salicylaldimine Ru chloro *p*-cymene complex, C11 and C12. (NB: only one of the dendrimer arms shown).

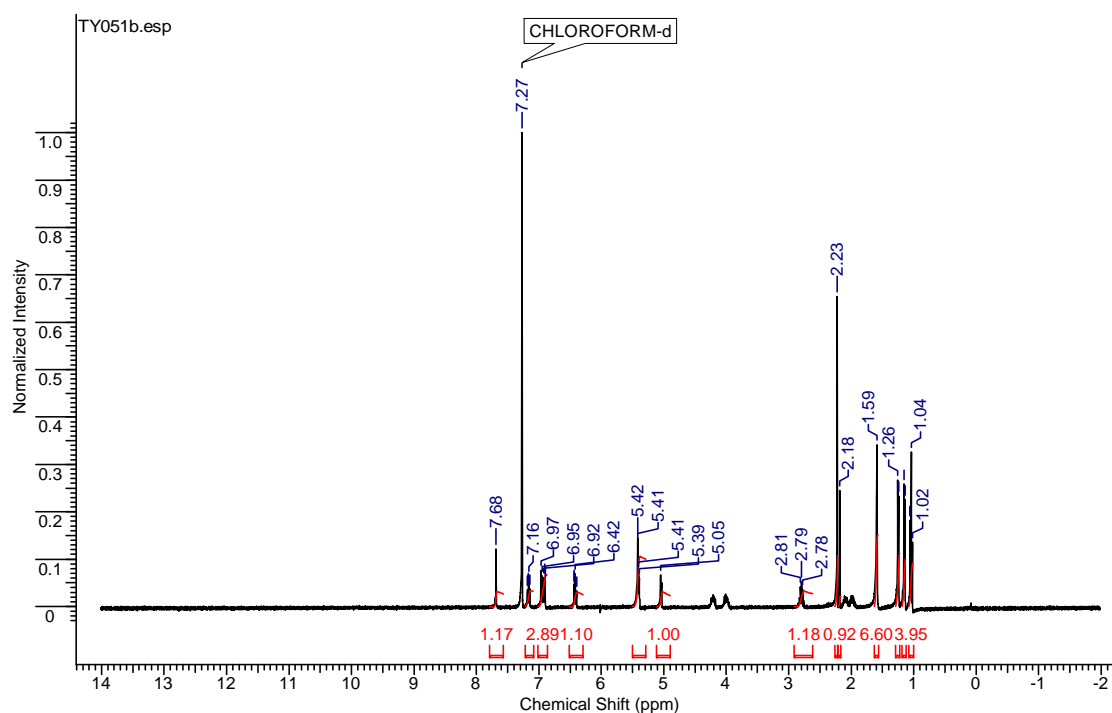


Figure 3.17 A typical ¹H NMR spectrum of salicylaldimine Ru chloro *p*-cymene complex, C9.

Table 3.6: ^1H NMR data for salicylaldimine Ru *p*-cymene complexes, **C9-C12** recorded in CDCl_3

Complexes	Chemical shift (δ - ppm)	Assignment
C9	1.04 t	H1
	1.16 d	H20
	1.26 d	H18
	1.59 s	H11/18
	2.06-1.96 m	H2
	2.23 s	H11
	2.79 q	H19
	4.20-4.00 m	H3
	5.05 d	H13/14
	5.42 d	H15/16
	6.41 t	H7
	6.94 d	H9
	6.96 d	H8
7.16 t	H6	
7.68 s	H4	
C10	1.14 d	H21
	1.19 d	H23
	1.78 d	H14/21
	2.17 s	H14
	2.63 q	H22
	4.21d	H16
	4.99 d	H17
	5.26 d	H18
	5.35 d	H19
	6.42 t	H3
	6.99 d	H9
	7.01 d	H1/5
	7.22 t	H11

Table 3.6: Cont.

	7.35 t	H10
	7.45 t	H2/4
	7.64 d	H12
	7.75 s	H7
C11	1.10 d	H20
	1.20 d	H22
	1.65 s, br	H1
	2.10 m	H6
	2.24 s	H13
	2.53 m	H2/3
	2.72 sp	H21
	4.20 m	H5
	5.12 d	H15/16
	5.39 d	H18/19
	6.40 t	H10
	6.94 t	H9
	7.19 d	H8/11
	7.70-7.77 s	H6
C12	1.07 d	H23
	1.27 d	H25
	1.47 s	H1
	1.77 t	H2/3/5/6
	2.13 m	H1/4/7
	2.23 s	H16
	2.50 m	H4/7
	2.71 sp	H24
	4.20 m	H8
	5.12 d	H18/19
	5.30 d	H21/22
	6.91 m	H12
	7.17 m	H11/14
	7.70 s	H4

3.2.4.4 $^{13}\text{C}\{^1\text{H}\}$ NMR characterization

The $^{13}\text{C}\{^1\text{H}\}$ NMR spectra of these type of complexes confirmed the complexation of salicylaldimine ligands with Ru chloro *p*-cymene dimer. This is seen from the presence of all the C atoms signals found in the complexes.

Table 3.7 $^{13}\text{C}\{^1\text{H}\}$ NMR data for salicylaldimine Ru *p*-cymene complexes, **C9-C12**

Complexes	Chemical shift (δ - ppm) ^a	Assignment
C9	11.60	C1
	18.57	C11
	22.55	C18
	22.75	C20
	24.41	C2
	30.52	C19
	71.10	C3
	80.18	C13
	81.89	C14
	83.15	C15
	85.85	C16
	97.40	C12
	101.55	C17
	114.07	C8
	119.26	C7
	122.31	C9
134.31	C6	
134.55	C5	
163.49	C10	
164.95	C4	

Table 3.7 Cont.

C10	18.42	C14
	21.57	C21
	22.74	C23
	30.30	C22
	80.24	C16
	83.48	C17
	86.46	C15
	97.83	C18
	101.39	C19
	114.18	C1
	118.09	C0
	122.62	C2
	123.65	C4
	126.88	C5
	128.78	C9
	135.32	C12
	135.32	C6
	158.50	C8
	164.16	C13
	165.14	C7
C11	18.68	C13
	21.75	C1
	22.67	C20
	22.82	C22
	28.39	C4
	30.51	C21
	51.08	C2
	67.94	C3
	75.50	C5
	80.27	C15
	82.44	C16
	83.42	C17

Table 3.7 Cont.

	85.55	C18
	96.94	C14
	101.33	C19
	113.87	C8
	119.36	C9
	122.23	C11
	134.28	C10
	134.54	C7
	163.46	C12
	164.85	C6
C12	14.03	C1
	18.83	C16
	22.06	C23
	22.77	C25
	24.00	C4
	25.41	C7
	30.43	C24
	30.54	C5
	31.48	C6
	51.10	C2
	67.94	C3
	76.49	C8
	80.72	C18
	81.22	C19
	83.14	C20
	87.62	C21
	98.47	C17
	100.03	C22
	114.06	C11
	118.96	C12
	121.77	C14
	126.16	C13
	128.86	C10
	164.48	C15
	164.69	C9

3.2.4.5 Thermogravimetric analysis

The salicylaldimine *p*-cymene ruthenium complexes (**C10-C12**) were examined by thermogravimetric analysis (TGA). Figure 3.18-3.20 shows the TG plots for **C10** which is a phenyl substituted mononuclear *p*-cymene complex, **C11** which is a G1 metallodendrimer and **C12** which is a G2 metallodendrimer respectively.

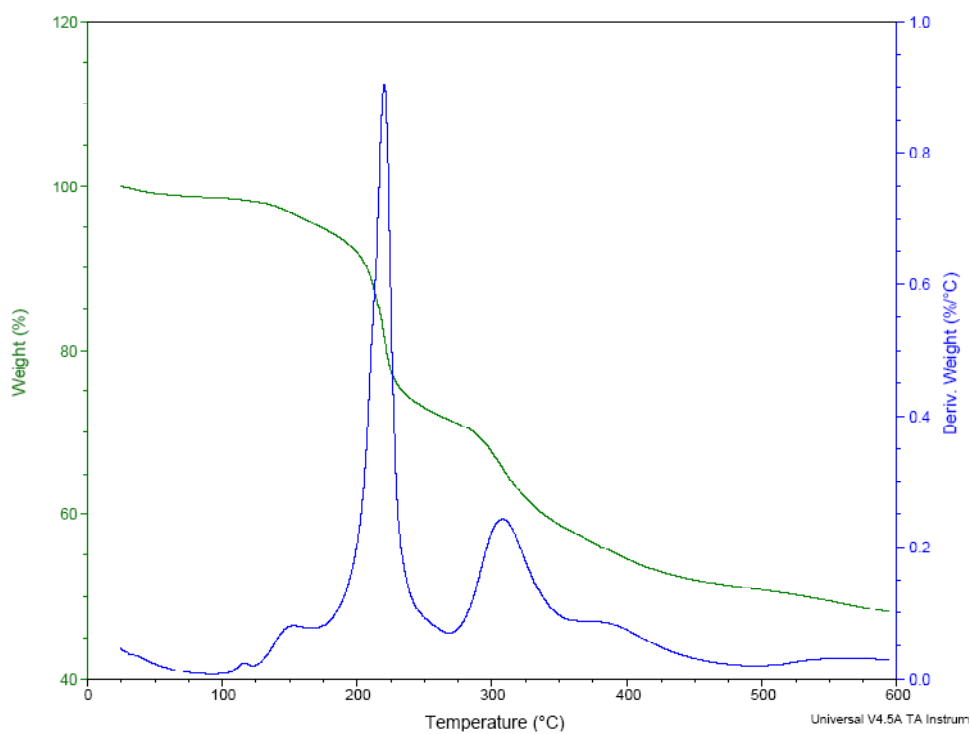


Figure 3.18 TG plot and its derivative for the mononuclear complex, **C10**

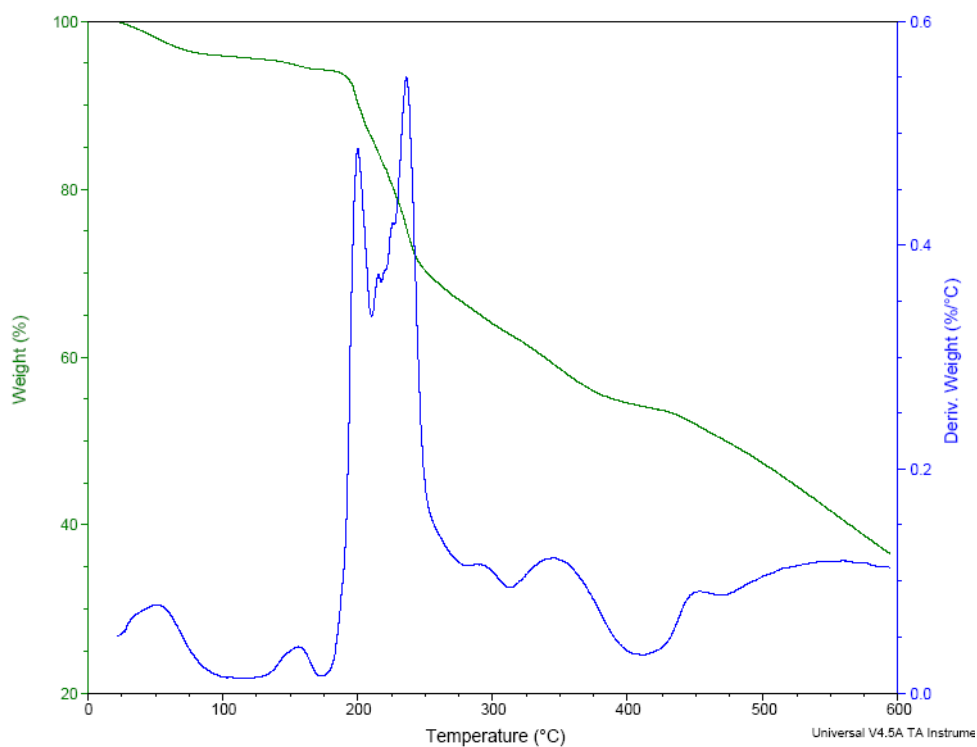


Figure 3.19 TG plot with its derivative for the G1 dendrimer complex **C11**.

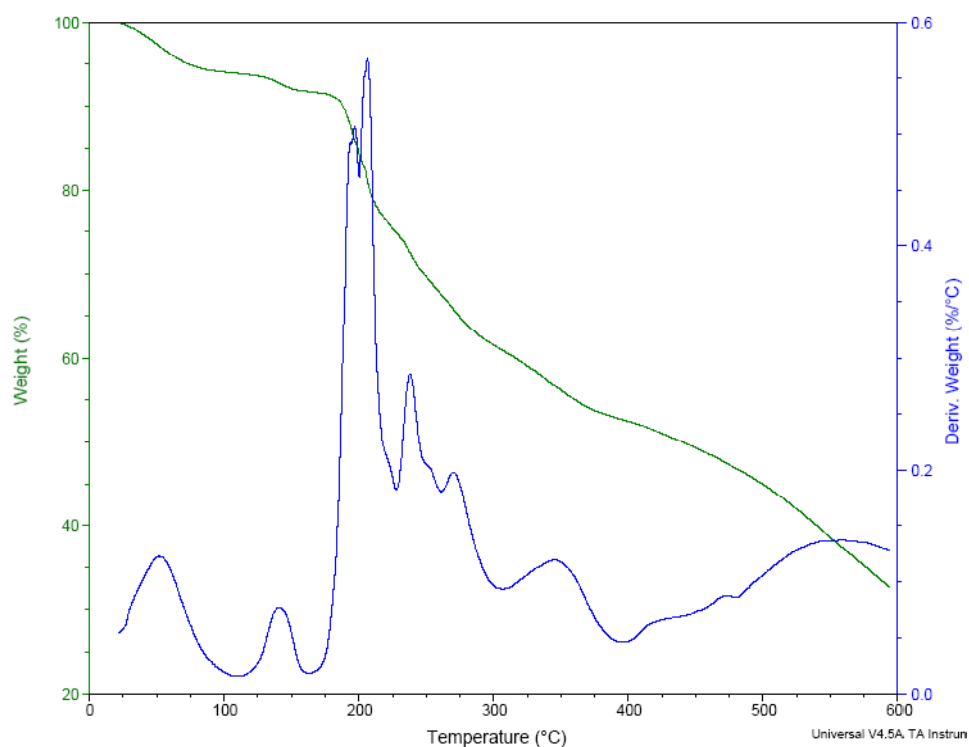


Figure 3.20 TG analysis of G2 dendritic complex, **C12**.

The plots show the weight loss (%) as a function of increasing temperature. For dendritic complexes, the small weight loss (~5% in **C11**) and (~7% in **C12**) just below 190°C are due

to the loss of included solvent molecules which were also observed from the elemental analysis results as well as from ^1H NMR spectra. PPI dendrimers have a tendency of encapsulating solvent molecules within their structure. It has been reported that decomposition of PPI dendrimers only starts slightly above 190°C [20]. The first stage of decomposition in **C10** occurs in the temperature range 150°C - 250°C . For metallodendrimers the initial significant decomposition occurs in the temperature range 190°C - 275°C . This decomposition in all cases reflects a weight loss of approximately 25%, which is due to the loss of *p*-cymene units. From the derivative graphs it is clear that in dendritic complexes more than one *p*-cymene units dissociates. In the case of the **C11** complex we expect 4 *p*-cymene units to dissociate whilst in **C12**, 8 *p*-cymene units are expected to dissociate but due to symmetrical nature of these complexes the derivative plots only reflect half the number of *p*-cymene units expected. Analogous complexes to **C10** synthesized by Verpoort *et al.* showed similar behavior [21] where *p*-cymene was observed to be displaced at this temperature. A final stage of the decomposition above 300°C is also noted for **C10** ($\sim 350^\circ\text{C}$), **C11** and **C12** ($\sim 380^\circ\text{C}$) reflecting a weight loss of approximately 43% responding to the loss of the remaining organic fragments. During the final stage the metal fragment is oxidized to form RuO. This is to be expected as the TGA's were recorded under aerobic conditions.

3.3 Conclusion:

All the Ru dendritic complexes were found to exist as stable brown solids in the solid state whereas the monofunctionalized complexes were found to have colours influenced by the use of a different precursor. The half-sandwich Ru-arene dendritic complexes are by far the most stable in solution than the Ru-carbene complexes. For Ru carbene complexes, complexation takes place *via* the N atom in the pyridine ring whereas in Ru-arene complexes coordination takes place *via* the imine bond functionality as well as the O donor site. It is known that

pyridine is a very labile ligand. This will be a major factor in catalytic testing of these complexes.

3.4 Experimental:

3.4.1 General

All manipulations were performed using standard Schlenk techniques under a nitrogen or argon atmosphere. Solvents were dried by distillation prior to use, and all reagents were employed as obtained. NMR (^1H ; ^{13}C and ^{31}P) spectra were recorded on Varian VNMRs 300 MHz; Varian Unity Inova (400 MHz and 600 MHz) spectrometers and chemical shifts were reported in ppm relative to TMS (^1H and ^{13}C) and H_3PO_4 (^{31}P) as internal standards. ESI-MS (ESI+/-) analyses were performed on a Waters API Quattro Micro or a Waters API Q-TOF Ultima instrument by direct injection of sample. FT-IR analysis was done on a Thermo Nicolet AVATAR 330 instrument, and was recorded as neat spectra using an ATR accessory unless specified. TG analysis was done in an open space.

3.4.2 : Synthesis of complexes

Synthesis of CI

A Schlenk tube was charged with the *pyridine* modified Grubbs G1 complex (0.120 g, 0.913 mmol) dissolved in dichloromethane (1 ml). To this solution was added a solution of **L1** (0.029 g) in 4 ml of dichloromethane. The reaction was stirred without a noticeable colour change at first but as it proceeded, the reaction mixture became greenish-brown in colour. The reaction was done under inert atmosphere for 1 hour. The solvent was removed under vacuum and this yielded a sticky greenish-brown residue. Neat pentane was then added upon which a dark orange brown solid formed. The filtrate was syringed off and the residue washed further with dry pentane (3×10 ml). The resulting dark brown solid was vacuum dried. Yield, 0.071 g (54%).

Synthesis of C2

A Schlenk tube was charged with the *pyridine* modified Grubbs G1 complex (0.108 g, 0.913 mmol) dissolved in dichloromethane (1 ml). To this solution was added a solution of **L2** (0.032 g) in 4 ml of dichloromethane. The reaction was stirred without an immediate colour change but as it proceeded it became greenish brown. The reaction was continued under inert atmosphere for 1 hour. The solvent was removed under vacuum and the resulting residue was a sticky greenish-brown material. Neat pentane was then added resulting in the residue solidifying. The mother liquor was syringed off and the residue washed further with dry pentane (3×10 ml). The resulting dark brown solid was vacuum dried. Yield, 0.078 g (61.9 %).

Synthesis of C3

Grubbs G1 catalyst (0.197 g, 0.239 mmol) was weighed into a Schlenk tube, and **L3** (0.043 g, 0.0291 mmol) dissolved in 10 ml dichloromethane was added to it. Immediately the colour changed to a dark brown solution that was stirred for an hour at room temperature. The solvent was removed under vacuum leaving a dark greenish-brown solid. The residue was then redissolved in dichloromethane after which pentane was added slowly upon which a brown solid precipitated out of the solution. The solid was washed repeatedly with pentane until the washings were colourless. The solid was then vacuum dried resulting in an amorphous brown solid. Yield, 0.075 g (66 %)

Synthesis of C4

The same procedure as that used for **C3** was employed but the mole ratio of the precursor was 8:1 to the ligand (**L4**). Yield, 0.079 g (68 %)

Synthesis of C5

Into a clean Schlenk tube containing a stirrer bar, Grubbs G2 catalyst (0.126 g; 0.148 mmol) was weighed and an equimolar amount of ligand **L1** (0.022 g) dissolved in dichloromethane (5 ml) was added and then stirred for an hour. The reaction solution became pinkish brown but as the reaction progressed it changed to orange brown. The volume of the reaction mixture was then reduced and pentane was added with the aim of precipitating the product but it redissolved most of the residue. The solvents were then removed under vacuum which resulted in the formation of an orange brown solid. Yield, 0.039 g (53 %)

Synthesis of C6

Into a clean Schlenk tube containing a stirrer bar, Grubbs G2 (0.022 g; 0.026 mmol) was added. An equimolar amount of ligand **L2** (0.005 g) dissolved in dichloromethane (5 ml) was added and the reaction mixture stirred for an hour. The reaction solution became orange during this time. The solvent was removed and hexane added in an attempt to precipitate most of the product while cooling the mixture at 0°C. A red solid precipitated out of the solution and the solvent was siphoned off and the solid dried under vacuum. Yield, 0.049 g (54%)

Synthesis of C7

The dendritic ligand (**L3**) (0.012 g, 0.018 mmol) in 6ml dichloromethane was added to Grubbs G2 (0.061 g, 0.072 mmol) in a Schlenk flask. The colour of the reaction mixture changed to dark yellowish-brown. This mixture was stirred for an hour. After this the volume of the reaction mixture was reduced to ~2 ml and then 20 ml pentane was added to precipitate the desired product. A dark brown solid precipitated out and was washed with pentane to get rid of un-reacted precursor and other impurities. Yield, 0.016 g (59 %)

Synthesis of C8

A similar reaction was also carried out for the G2 dendritic ligand (**L4**) whereby it is reacted with Grubbs G2. The product was also purified using a similar procedure. The product of this reaction was recovered as a dark brown amorphous solid. Yield, 0.015 g (52 %)

Synthesis of C9

To a Schlenk flask charged with (0.495 g, 0.838 mmol) $[\text{Ru}(\mu\text{-Cl})\text{Cy}(\text{Cl})_2]$ in THF (20 ml) and the salt of **L5** 1.676 mmol in 5 ml THF was added. The colour of the reaction mixture became deep red. It was then stirred for 4 hours at room temperature under N_2 gas. After 4 hrs the reaction mixture was filtered into a clean Schlenk through celite to remove excess NaH. The solvent was removed by vacuum. The dark red residue was re-dissolved in toluene and then placed in the freezer overnight. This resulted in a red-brown crystalline solid which was washed with cold toluene. Yield, 0.213 g (59 %)

Synthesis of C10

The sodium salt of the ligand (**L6**) was prepared successfully recovering (0.163 g, 0.745 mmol) of the yellow solid. It was dissolved in THF (5 ml) and added to a solution of *p*-cymene chloro Ru dimer (0.228 g, 0.373 mmol) in 10 ml THF. The reaction mixture was stirred for 6 hrs. After this time the solvent was removed and an orange solid was recovered. It was then dissolved in toluene and cooled to 0°C . This resulted in the formation of an orange-brown solid. Yield, 0.271 g (78 %)

Synthesis of C11

The sodium salt of the ligand (**L7**) was prepared using Schlenk techniques. **L7** (0.473 g, 2.902 mmol) in THF (10 ml) was added slowly to NaH (0.14 g) and the evolution of H_2 gas was observed. The reaction mixture was stirred for an hour and its colour became pale

yellow. The solvent was removed and the solid residue dried under vacuum. The Na salt (0.22 g, 0.268 mmol) was recovered and was used in the complexation reaction. To a Schlenk flask charged with (0.146 g, 0.24 mmol) $[\text{Ru}(\mu\text{-Cl})\text{Cy}(\text{Cl})_2]$ dissolved in THF, salt of **L7** (0.1 g; 0.06 mmol) dissolved in THF (5 ml) was added. The colour of the reaction mixture became deep red. It was then stirred for 6 hours at room temperature under N_2 gas. After 6 hrs it was filtered into a clean Schlenk tube through celite to remove the excess of NaH and the solvent removed from the filtrate by vacuum. A reddish brown solid was obtained which was recrystallized by dissolving the product in a minimum volume of dichloromethane and then layered with hexane. An orange-brown solid was recovered and was dried under vacuum. Yield, 0.078 g (72 %)

Synthesis of C12

The same approach was followed for preparing the anionic salt of the ligand of **C11**. In a Schlenk flask charged with the *p*-cymene chloro Ru dimer (0.152 g, 0.252 mmol) in THF (7 ml), **L8** salt 0.1 g; 0.126 mmol dissolved in 5 ml THF was added to this solution. The reaction mixture became red-brown. Upon completion of the reaction, the reaction mixture was filtered through celite. From the red brown filtrate the solvent was removed and a dark brown residue obtained. The work-up was similar to that done for **C11**. The complex was recovered as a dark brown solid. Yield, 0.0298 g (64 %)

3.5 References:

1. Thornback, J. R.; Wilkinson, G., *J. Chem. Soc.*, **1978**, 110.
2. (a) Nakajima, K.; Ando, Y.; Mano, H.; Kojima, M., *Inorg. Chim. Acta*, **1998**, 274, 184. (b) Nakajima, K.; Isibashi, S.; Inamo, M.; Kojima, M., *Inorg. Chim. Acta*, **2001**, 325, 36.
3. Sanford, M.S.; Henling, L.M.; Grubbs, R.H., *Organometallics*, **1998**, 17, 5384.
4. De Clercq, B.; Verpoort, F., *Tetrahedron Lett*, **2002**, 43, 4687.
5. Trnka, T.M.; Dias, E.L.; Day, M.W.; Grubbs, R.H., *ARKIVOC*, **2002**, xiii, 28.
6. Sanford, M.S., Love, J.A., Grubbs, R.H., *J. Am. Chem. Soc.*, **2001**, 123, 6543.
7. Denk, K.; Fridgen, J.; Herrman, W.A., *Adv. Synth. Catal.*, **2002**, 344, 666.
8. Van der Schaaf, P.A.; Kolly, R.; Kirner, H.-J.; Rime, F.; Mühlebach, A.; Hafner, A., *J. Organomet. Chem.*, **2000**, 606, 65.
9. Nguyen, S.T.; Grubbs, R.H., *J. Organomet. Chem.*, **1995**, 497, 195.
10. Ahmed M.; Barrett, A.G.M.; Braddock, D.C.; Cramp S.M.; Procopiou, P., *Tetrahedron Lett.*, **1999**, 40(49), 8657.
11. Varray, S.; Lazaro R.; Marinez, J.; Lamaty, F., *Organometallics*, **2003**, 22, 2426.
12. (a) Garber, B.S.; Kingsbury, J.S.; Gray, B.L.; Hoveyda, A.H., *J. Am. Chem. Soc.*, **2000**, 122, 8168. (b) Beerens, H.; Verpoort, F.; Verdonck, L., *J. Am. Chem. Soc.*, **2000**, 159, 197. (c) Wijkens, P.; van Koten, G., *Org. Lett.*, **2000**, 11, 1621.
13. (a) Astruc, D., *Oil and Gas Science and Technology-Rev.*, **2007**, 62, 787.
(b) Astruc, D.; Hauzé, K.; Gatard, S.; Méry, D.; Nlate, S.; Plault, L., *Adv. Synth. Catal.*, **2005**, 347, 329. (c) Gatard, S.; Kahlal, S.; Méry, D.; Nlate, S.; Cloutet, E.; Saillard, J.-Y. Astruc, D. *Organometallics*, **2004**, 23, 1313. (d) Gatard, S.; Nlate, S.; Cloutet, E.; Bravic, G.; Blais, J.-C. Astruc, D., *Angew. Chem. Int. Ed.*, **2003**, 42, 452

14. (a) Clavier, H.; Petersen, J. L.; Nolan, S.P., *J. Organomet. Chem.*, **2006**, 691, 5444.
(b) P'Pool, J. S.; Schanz, H-J., *J. Am. Chem. Soc.*, **2007**, 129, 14200.
15. (a) Monsaert, S.; Drozdak, R.; Dragutan, V.; Dragutan, I.; Vepoort, F., *Eur. J. Inorg. Chem.*, **2008**, 3, 432. (b) Love, J. A.; Morgan, J. P.; Trnka, T. M.; Grubbs, R. H., *Angew. Chem. Int. Ed.*, **2002**, 41, 21. (c) Samanta, D.; Kratz, K.; Zhang, X.; Emrick, T., *Macromolecules*, **2008**, 41, 530.
16. De Clerq, B.; Verpoort, F., *J. Mol. Catal. A: Chem.*, **2002**, 180, 67.
17. (a) Dinger, M.B.; Mol, J.C., *Organometallics*, **2003**, 22, 1089. (b) Mieock, K.; Eum, M.; Jin, M.J.; Jun, K.; Lee, C. W.; Kyoung, K.A.; Kim, C.H.; Chin, C.S., *Organometallics*, **2004**, 23, 3535.
18. Bennet, M. A.; Smith, A. K., *J. Chem. Soc. Dalton Trans.*, **1974**, 233.
19. (a) Kumar, A.; Agarwal, M.; Singh, A. K.; Butcher, R., *J. Inorg. Chim. Acta*, **2009**, 362, 3208. (b) Kumar, A.; Agarwal, M.; Singh, A. K., *J. Organomet. Chem.*, **2008**, 693, 3533.
20. (a) Newkome, G. R.; Yoo, K. S.; Hwang, S.-H.; Moorefield, C. N., *Tetrahedron*, **2003**, 59, 3955. (b) Hwang, S.-H.; Yoo, K. S.; Moorefield, C. N.; Lee, S.-W.; Newkome, G. R., *J. Polym. Sci: Pt B Polym. Phys.*, **2004**, 42, 1487.
21. Van Craenenbroeck, J.; Van Isterdael, K.; Vercaemst, C; Verpoort, F., *New J. Chem.*, **2005**, 29, 942.

CHAPTER 4
PRELIMINARY TESTING OF SOME COMPLEXES IN OLEFIN METATHESIS
REACTIONS

CONTENT

4.1 Introduction	119
4.2 Results and Discussion	121
4.2.1 Self Metathesis of 1-octene	121
4.2.1.1 Activity and Conversion	122
4.2.1.2 Stability	132
4.2.2 Ring-Closing Metathesis of diethyl diallylmalonate	137
4.2.3 Ring-Opening Metathesis Polymerization of norbornene	142
4.3 Conclusion	145
4.4 Experimental	146
4.5 References	148

4.1 Introduction

Amongst the organic and organometallic reactions involving the formation of C-C double bonds, olefin metathesis is one of the most powerful and is becoming more widely used in organic transformations both from a fine chemical and polymer industry point of view. It is now accepted that olefin metathesis reactions are initiated by metal-carbene complexes in particularly the neutral ruthenium carbene complexes developed by Grubbs and co-workers shown in Figure 4.1. These complexes were modified to be active, tolerant to harsh reaction conditions and are extremely compatible with various functional groups. Through mechanistic studies of metathesis reactions using these complexes, it was found that the ancillary ligands affect dramatically the rate of the initiation and propagation steps in the process. This has resulted in an ongoing effort focussing on modification of the ligand environment of Grubbs-type complexes to improve stability, activity, selectivity and functional group tolerance. Furthermore search for commercially relevant and alternative metathesis initiators with improved accessibility that have comparable performance to that of Grubbs catalysts is an ongoing process.

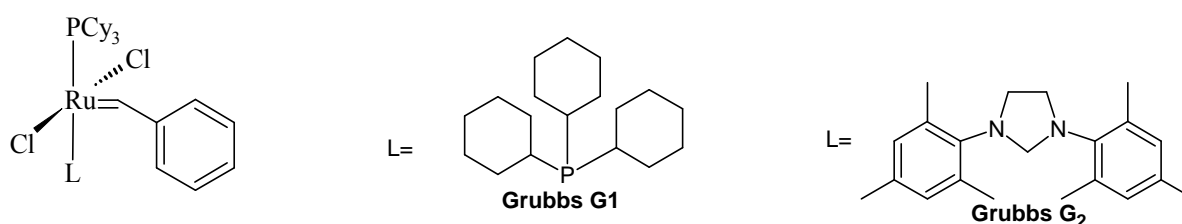
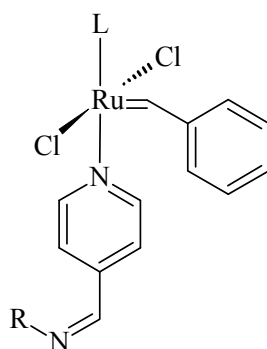


Figure 4.1 Neutral ruthenium carbene complexes developed by Grubbs and co-workers

Earlier in Chapter 3, we reported the synthesis of modified Grubbs-type complexes, including pyridyl modified Grubbs complexes. Simple pyridine substituted Grubbs complexes have already been reported to be active in metathesis but were found to be unstable in solution. In this Chapter we report on the evaluation of the 4-pyridylimine carbene complexes **C1**, **C2**, **C5**

and **C6** (Figure 4.2) in the metathesis of 1-octene. In addition, analogues of these complexes immobilized on dendrimers were also tested. In this regard we employed the dendritic catalysts **C3**, **C4**, **C7** and **C8**, see Figure 4.3. A ^1H NMR study of the mononuclear complexes **C1** and **C5** was also done in order to evaluate the stability and reactivity of these complexes in self metathesis of 1-octene. The mononuclear complexes **C1** and **C5** were further tested in ring closing metathesis of diethyl diallylmalonate for their catalytic capabilities. This was done by monitoring the reactions using ^1H NMR spectroscopy.

In addition to these metathesis reactions, ring opening metathesis polymerization (ROMP) of norbornene was also done using the *p*-cymene salicylaldimine chloro ruthenium complexes (**C10-C12**) as catalyst precursors. In this type of metathesis reaction, the metal carbene species, active for metathesis is generated *in-situ*. The generation of the carbene is promoted by the use of a co-catalyst. This work is later discussed in more detail.



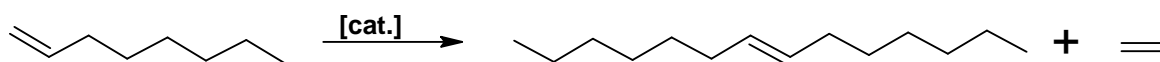
- C1:** R= propyl, L= PCy₃
C2: R= phenyl, L= PCy₃
C5: R= propyl, L= NHC
C6: R= phenyl, L= NHC

Figure 4.2 Model complexes used in the testing of the catalytic activity for the metathesis of 1-octene.

4.2 Results and discussion

4.2.1 Self Metathesis of 1-octene

The metathesis reactions were carried out using standard Schlenk techniques under nitrogen, at room temperature and in the absence of a solvent. The metal concentration was kept constant irrespective of the catalyst precursor employed. Thus for example in the case of dendritic complex **C3**, only a quarter of the amount of the metallodendrimer was employed relative to what was used in the case of the mononuclear complex. The process was monitored by gas chromatography (GC) and in some cases ^1H NMR. Scheme 4.1 shows the metathesis of 1-octene (C-8) to form primary products, 7-tetradecene (C-14) either *cis* or *trans* as well as ethylene which is formed as a gas.



Scheme 4.1: Metathesis of 1-octene to 7-tetradecene in the presence of a catalyst.

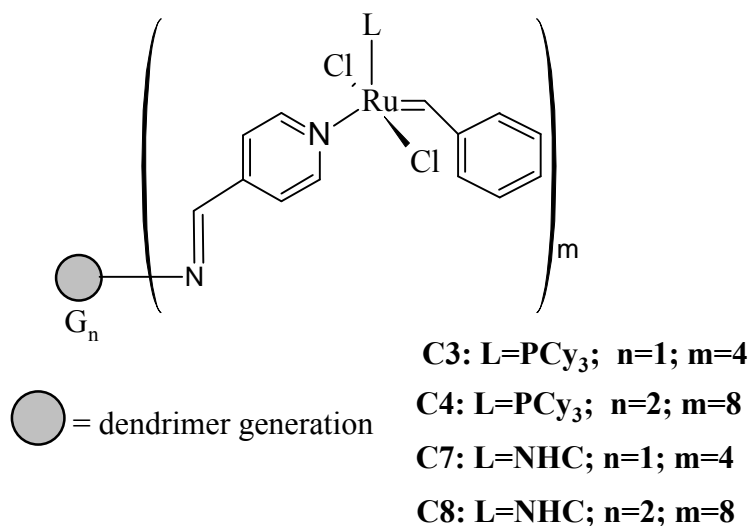


Figure 4.3 Dendritic complexes employed in the metathesis of 1-octene.

4.2.1.1 Activity and Conversion

^1H NMR studies for complexes **C1** and **C5** were conducted to investigate the reactivity of these metal carbene complexes in 1-octene metathesis. Their dendritic analogues were not monitored by NMR spectroscopy due to their low solubility in NMR solvents. The study was conducted under ambient conditions. The catalysts were weighed into a vial and then dissolved in CDCl_3 . Into this solution, the substrate (1-octene) was then injected. The substrate to metal concentration ratio was 1000: 1.

Figure 4.5 shows an array of ^1H NMR scans done over 5minute intervals for an initial period of 30 minutes for **C1**. The signals in the alkyl region (1 ppm-3 ppm) show the methylene groups that are found in both 1-octene and 7-tetradecene. The olefinic protons for 1-octene are found at 4.95 ppm and 5.81 ppm whilst the olefinic protons of 7-tetradecene appear at 5.41 ppm. These signals are comparable to that of authentic standards of 1-octene and *trans* 7-tetradecene. A significant observation was that, immediately after the addition of the substrate the product *trans* 7-tetradecene started forming. The reaction also shows 100% selectivity to only *trans* 7-tetradecene and this was observed from GC results. The monitoring was continued over a 16h period and no significant changes occurred thereafter. The complex **C1** behaves in a similar way to the *pyridine* modified Grubbs G1 catalyst in terms of showing high initial rate but with very little subsequent propagation of the active species. The reported activity of the *pyridine* modified Grubbs G1 catalyst was previously tested in ring-closing metathesis reactions [1]. This implies that these type of complexes tend to reach equilibrium within a short period of time after which decomposition occurs forming unstable and inactive species.

Vosloo *et al.* followed the behaviour of Grubbs G1 catalyst in 1-octene metathesis using ^1H NMR and found it to show regeneration of catalytic active ruthenium intermediates [2].

Unlike the Grubbs G1 catalyst, which showed the propagation of other carbene species during the metathesis of 1-octene, **C1** does not exhibit this phenomenon.

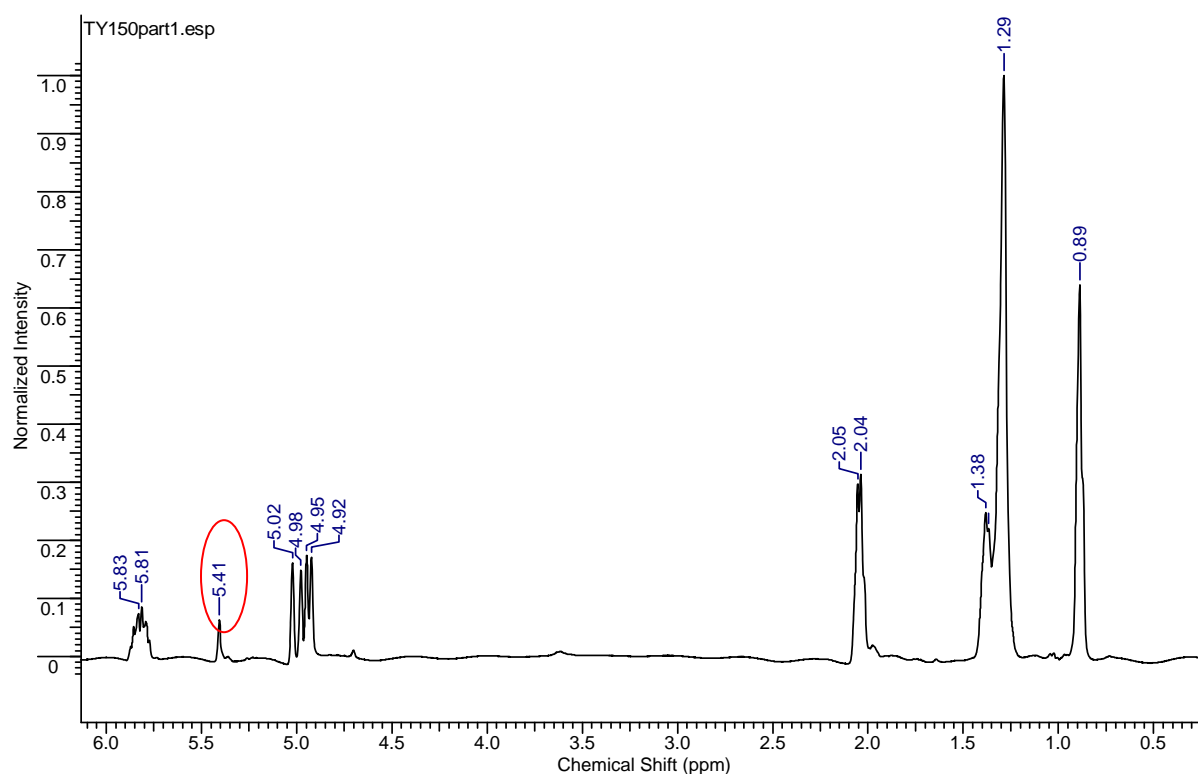


Figure 4.4 ^1H NMR spectrum showing the catalysis by **C1** immediately after addition of 1-octene.

In order to see the progression of the reaction, some spectra were isolated from the ^1H NMR array of this reaction. In Figure 4.5, ^1H NMR spectra at different reaction times are shown and they give an idea of the progression of the catalytic process. We clearly observe an immediate formation of the product and as time continues the intensity of the peaks show very little change. Figure 4.8 confirms the fast initiation of the complex, which then reaches a steady state over time.

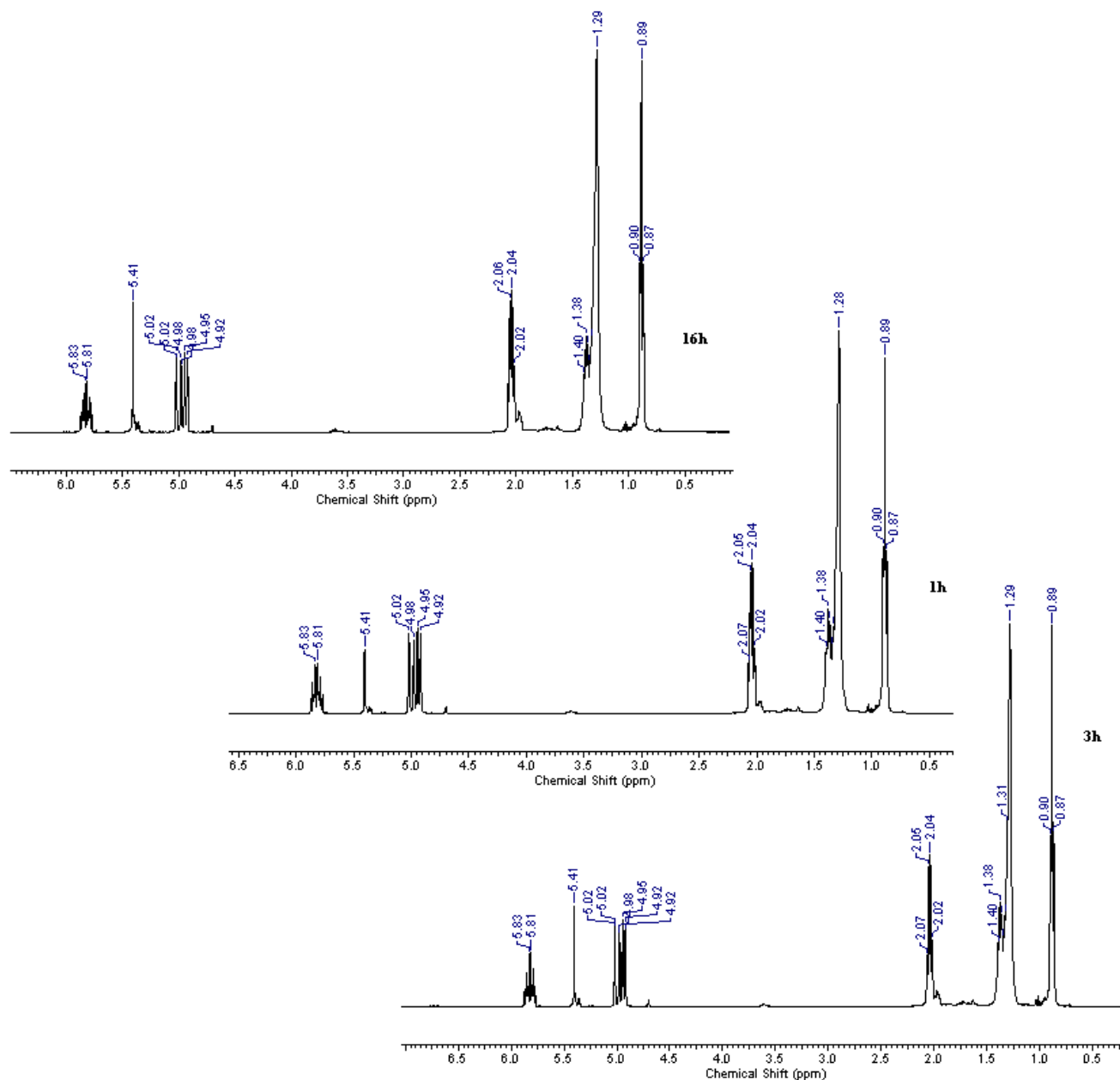


Figure 4.5 Selected ^1H NMR spectra of the **C1** catalysis of 1-octene.

In a similar way we monitored the behaviour of complex **C5**, the Grubbs G2 analogue of **C1** in the self-metathesis of 1-octene. What was observed in this case was a slow initiation rate to form the desired product. Figure 4.6, shows the monitoring of the reaction *via* ^1H NMR over a 30 minutes period. The spectra were collected at 5 minute intervals. There is little indication of peaks for both the carbene and the 7-tetradecene after the addition of the substrate. This is evidence of the low activity of the complex. After several hours signs of a peak resonance at

5.43 ppm due to the formation of 7-tetradecene can be seen. Figure 4.7 shows the selected spectra as the reaction progresses. What is clearly observed is the growth in the intensity of the peak signalling product formation with time. Once again we were unable to study the corresponding dendritic complexes *via* NMR spectroscopy due to their low solubility in the NMR solvents.

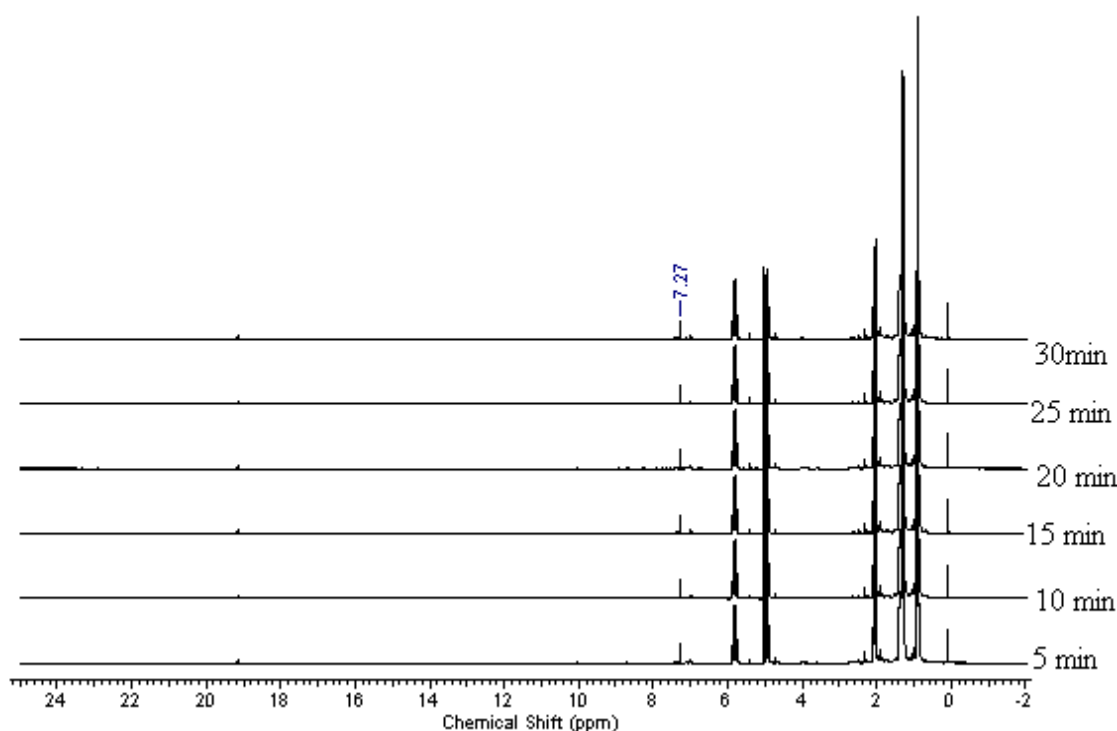


Figure 4.6 ^1H NMR monitoring of 1-octene metathesis using **C5** as a catalyst.

From the NMR results we extrapolated data to find out how much of the product forms over time. This was done by integrating the peak area of the olefinic proton of the product (C-14) relative to that of C-8. Figure 4.8 shows the rate of product (C-14) formation over time. It is observed that after an hour **C1** slowly becomes inactive, thereby reaching equilibrium. For **C5** complex, the initiation step is slow, only after a 4h period does the rate of the reaction actually increase. After 6h the reaction reaches a steady state. It can be concluded that **C1** is more active than **C5** in self metathesis of 1-octene under ambient conditions.

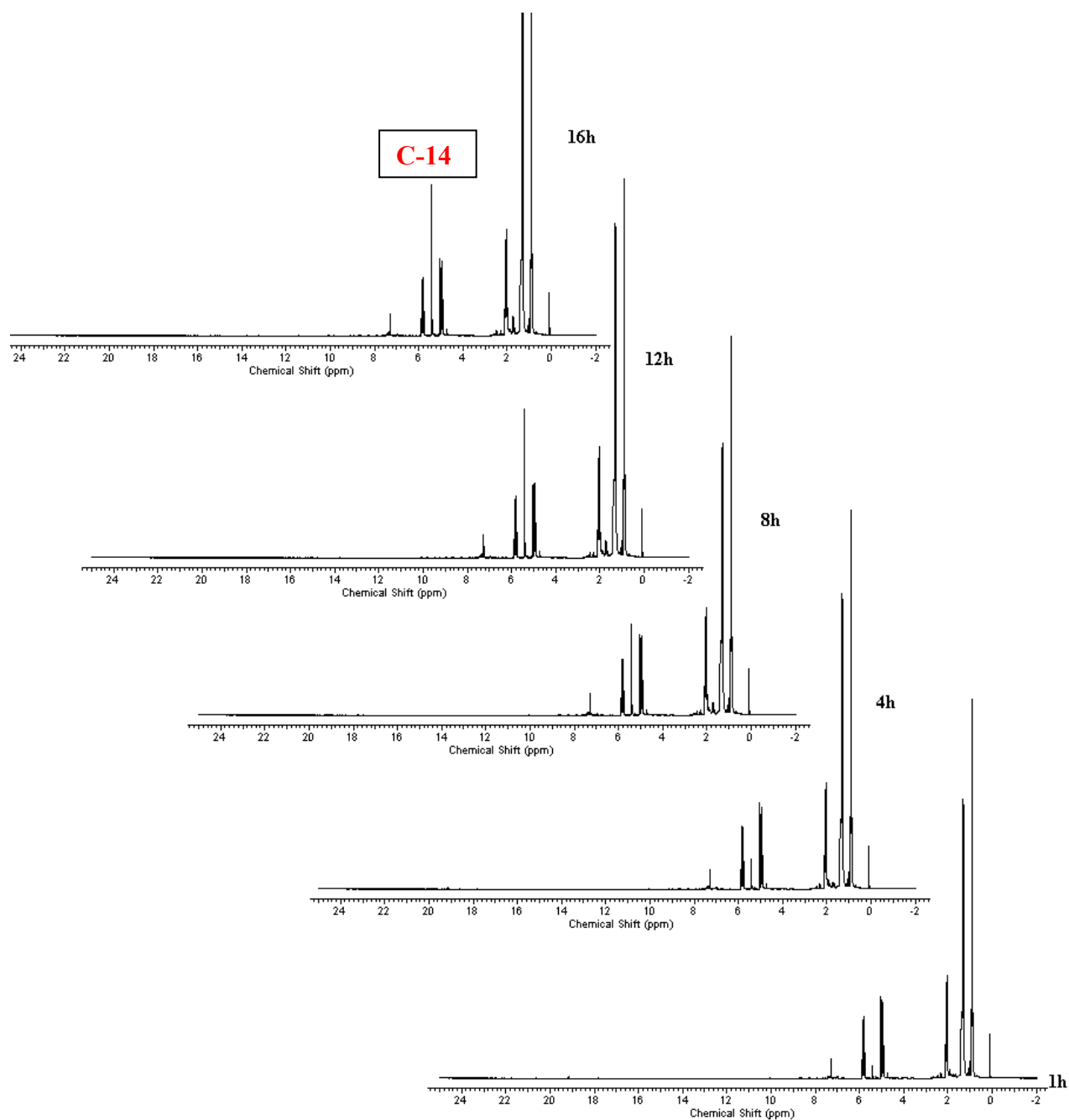


Figure 4.7 ^1H NMR monitoring of 1-octene metathesis for longer period using **C5** as a catalyst.

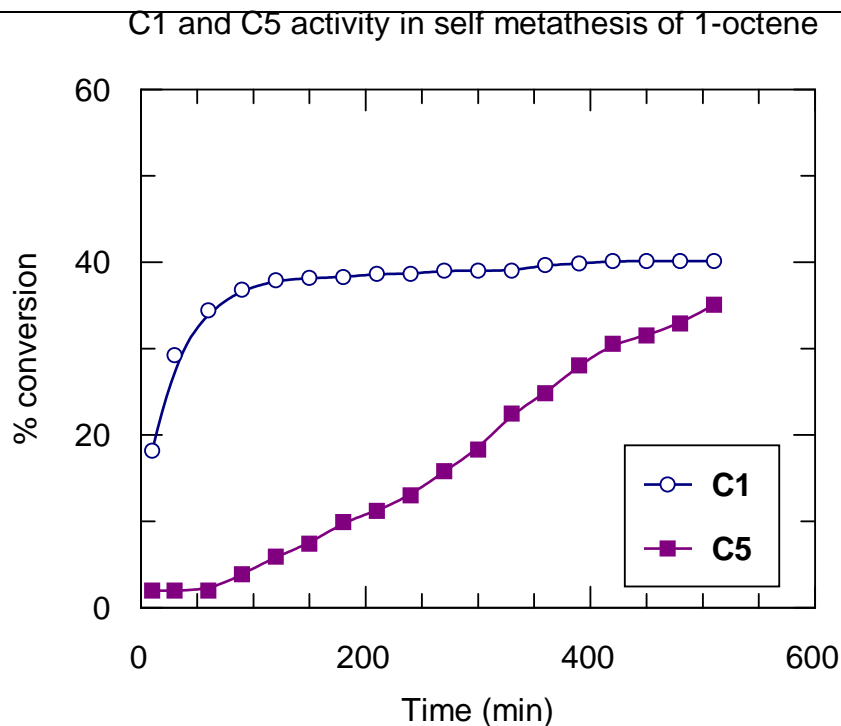


Figure 4.8 A graph showing the relative formation of the product in a reaction mixture over time.

After it was observed from the NMR study that the 4-imino pyridine Grubbs type complexes show catalytic behaviour towards 1-octene metathesis, all the complexes were used as catalysts in the metathesis of 1-octene. The 1-octene metathesis reactions using the various catalysts were monitored by gas chromatography. As mentioned earlier all reactions were done in neat 1-octene. Figure 4.9 shows the conversions obtained using modified Grubbs G1 complexes (C1-C4) whilst Figure 4.10 depicts conversion data for modified Grubbs G2 complexes (C5-C8).

The plots show that the unmodified Grubbs G1 catalyst and Grubbs G2 catalysts maintain higher overall activity even for reactions over extended periods. On the other hand complexes C1-C4 show that they reach equilibrium within a short period of time and exhibit a similar range of the conversion. The conversion plots for all complexes tested indicated similar conversions for the different catalysts. This could possibly be explained by looking at the

metathesis mechanism. Scheme 4.2 depicts a possible mechanism that these complexes might follow to catalyze 1-octene, using modified Grubbs G1 catalyst type complexes as an example. In metathesis, an active species such as (1) must be generated *via* the dissociation of one of the neutral ligands. During the initial analysis of the catalysis mixtures, it was observed that all complexes including Grubbs G1 catalyst had a similar conversion for 1-octene. This can be explained by the fact that a similar active species must have been generated for the different catalysts precursors. For this to be the case, the 4-imino pyridine ligand must be the species that dissociates to allow the generation of the active species. This is suggested as a result of the fact that regardless of the complexes used as precursors, it appears that the same active species is generated. After dissociation, the coordination of the olefin occurs (a) which subsequently forms the metallocyclobutane (3), followed by bond breakage to form the desired product and in some instances a new metal carbene species. Hypothetically, a new carbene species *i.e.* heptylidene (4) must first be formed and styrene released for the formation of *trans/cis* 7-tetradecene to occur. The regenerated active carbene species then reacts with excess substrate. Once the 1-octene has coordinated to the metal carbene, the metallocyclobutane species will be formed and subsequently collapses to form either *cis* or *trans* 7-tetradecene (6). After this there are several species in the reaction mixture several of which might not favour regeneration of the active species. It is assumed that this is what happens in the case of C1-C4 since there is no increase in conversion of 1-octene after 3h period. In the case of Grubbs G1 complex, it has been proven that regeneration of an active carbene species occurs within the reaction mixture [1, 3]. This could explain why the conversion of 1-octene using Grubbs G1 catalyst reaches over 70% after 24h reaction time. Another significant observation from the conversion plots of 1-octene under the above mentioned reaction conditions, is that the incorporation of the Grubbs type complexes onto dendrimers does not seem to have a major role in terms of reactivity. This can be seen from the observations that they do not show any enhanced reactivity when compared to the

mononuclear analogues. Higher reactivity of dendritic complexes was expected due to the fact that more than one active site is available within the same molecule. The low solubility of these dendritic complexes **C3-C4** in 1-octene, might have an effect on their reactivity.

The mononuclear *pyridine* modified Grubbs G1 catalyst showed the lowest percentage conversion in the self metathesis of 1-octene. This allows us to conclude that the use of 4-imino-pyridine ligands brings about a slight enhancement of the catalytic activity as compared to the simple *pyridine* modified system.

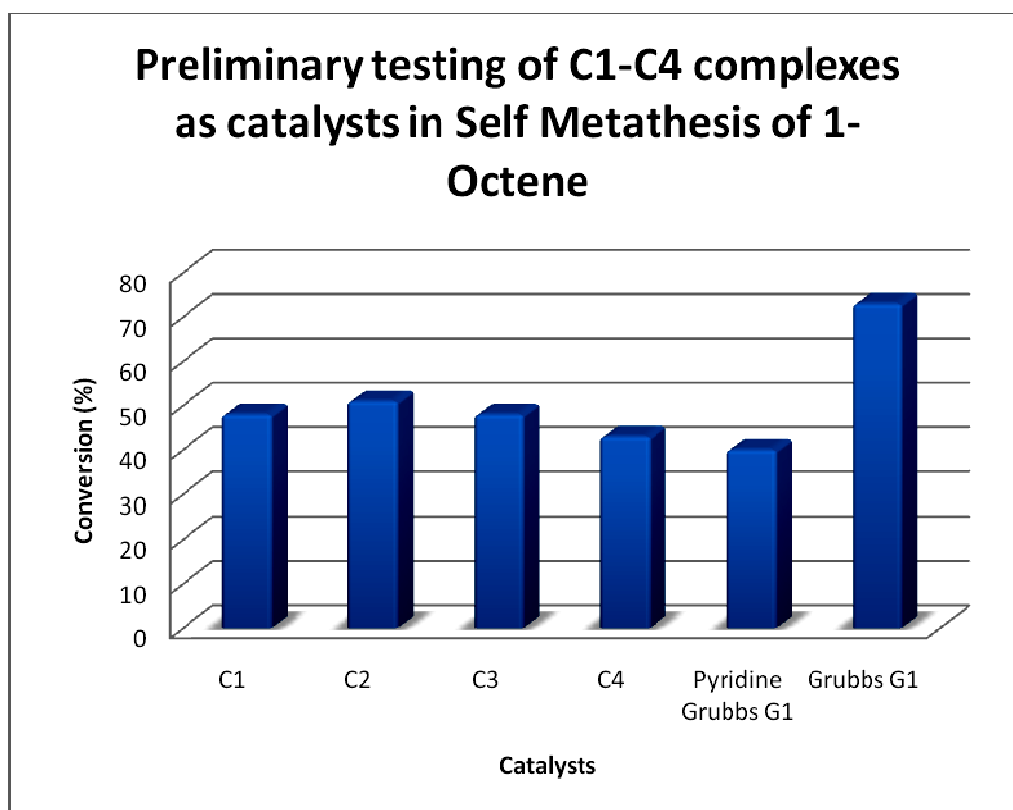
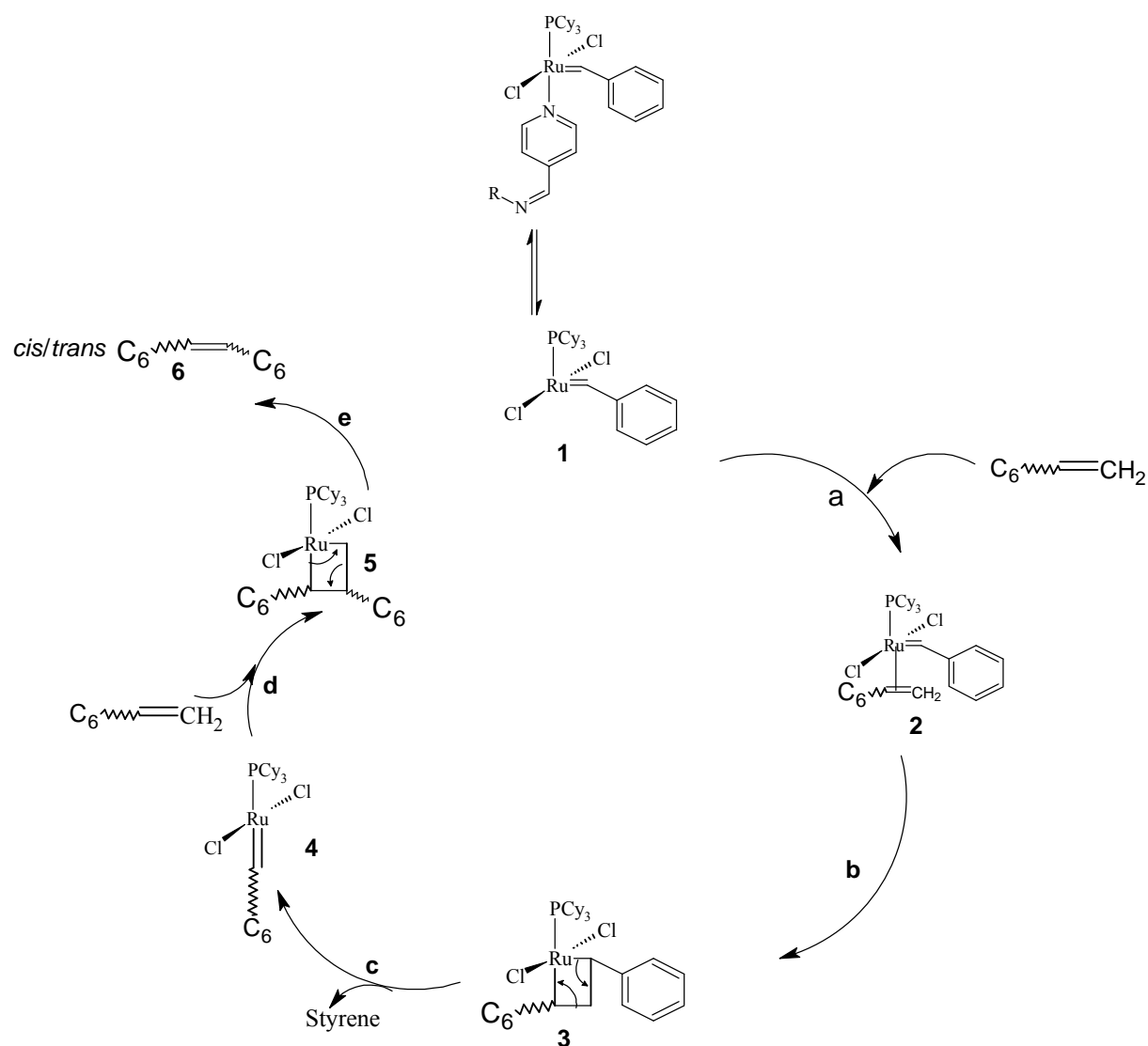


Figure 4.9 1-octene conversion using **C1-C4** and Grubbs G1 catalyst (24h).



Scheme 4.2 A possible mechanism for the metathesis of 1-octene using 4-imino pyridine Grubbs type complexes.

It is well known that the Grubbs G2 catalysts generally show higher catalyst activity when compared to Grubbs G1 catalyst [3]. Our observations were also in agreement with this. In our hands modified Grubbs G2 catalysts were found to form octene isomerization products as well as both isomers of 7-tetradecene within an hour as seen from GC analysis. However after 24h only the 7-tetradecene was detected in the reaction solution. From this we can assume that the catalyst must be converting the isomerization products to 7-tetradecene, which is why we do not observe any significant changes in terms of 1-octene conversion after 24h.

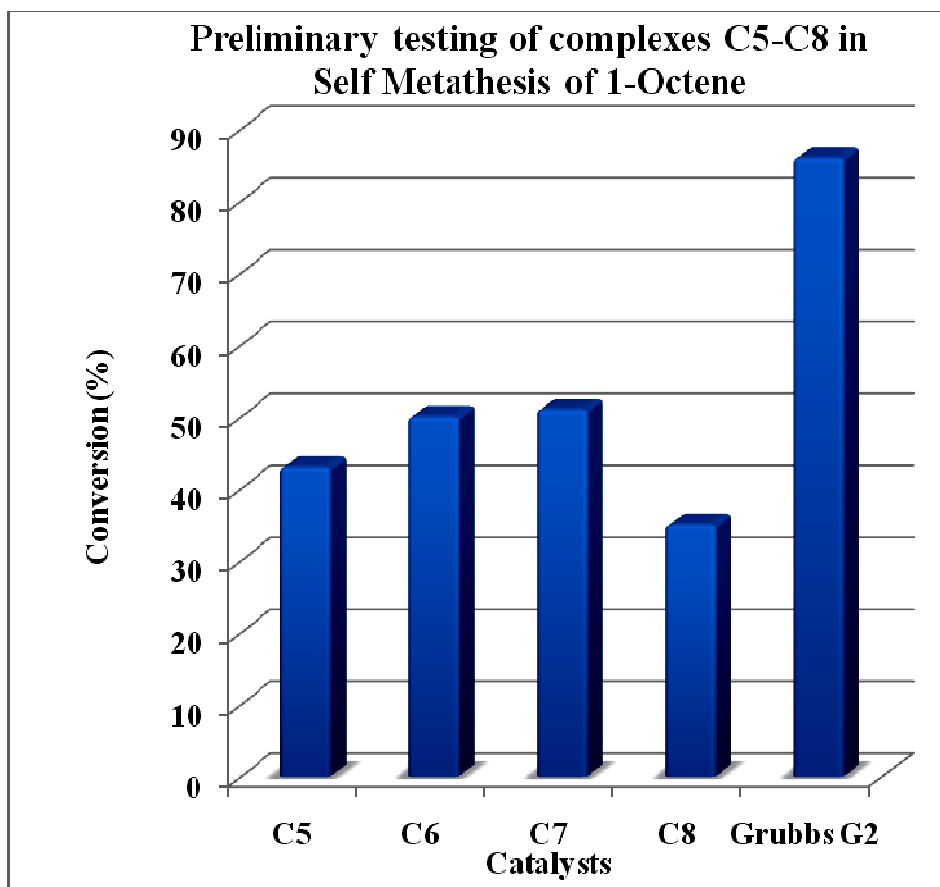


Figure 4.10 Grubbs G2 modified complexes (C5-C8) as catalysts in the metathesis of 1-octene (24h).

The 4-imino pyridine modified Grubbs G2 type complexes showed a different behaviour from its Grubbs G1 analogues. The reactivity of the complexes (C5-C8) was slightly different in that C7 (Grubbs G2 anchored on G1 dendrimer) was found to be the most reactive whilst C8 (Grubbs G2 anchored on G2 dendrimer) was the least reactive. The possible explanations are the solubility problems and that the anchoring of the Grubbs-type complex on a higher generation of the dendrimer does not necessarily enhance the reactivity of these complexes. It should be noted that the G2 dendrimer complex is less soluble than G1 analogue. Therefore the higher the dendrimer generation the slower the activity of the anchored system. This phenomenon was also observed by Astruc *et al.* [5] who suggested that the low activity of their dendritic ruthenium carbene complexes on higher generation dendrimers was due to low

solubility. The higher reactivity of **C7** as compared to its Grubbs G1 analogue (**C3**) is not unexpected since previously it has been found that all Grubbs G2 systems exhibit higher activity than Grubbs G1 catalyst systems. The higher activity of unmodified Grubbs G2 catalysts compared to its Grubbs G1 catalyst analogue in the self metathesis of 1-octene has also previously been reported [4]. However on our hands the slow initiation rate observed from the ^1H NMR study of **C5** gives evidence for the low reactivity of these type of complexes.

4.2.1.2 Stability

Complex **C1** was taken as a model catalyst to study the solution stability of these N,N' type complexes in comparison with the Grubbs G1 catalysts and *pyridine* modified Grubbs G1 catalysts. This study was carried out to determine why there is such a big difference in 1-octene conversion between the unmodified Grubbs G1 catalyst and N,N' 4-imino pyridine modified Grubbs G1 type catalysts. Indeed this study gave some insight into the catalytic results obtained. The stability of these catalysts was monitored using ^1H NMR. Figure 4.11 shows explicitly that the unmodified Grubbs G1 catalyst is more stable in solution than the two modified ruthenium carbene complexes. In the literature there are also some reports on the monitoring of the stability of Grubbs G1 catalyst using ^1H NMR. Mol *et al.* [6] for example showed that Grubbs G1 catalyst in solution remains intact for several days. There are some signs of hydrolysis but not as extensive as observed for other carbene complexes. This report correlates well with what we also observed in our experiments. This further shows the overall stability of the Grubbs type catalysts and the effects that are brought about when the ligand environment is changed. The higher stability in solution accounts for the higher overall activity of Grubbs G1 catalyst *versus* **C1** over extended times.

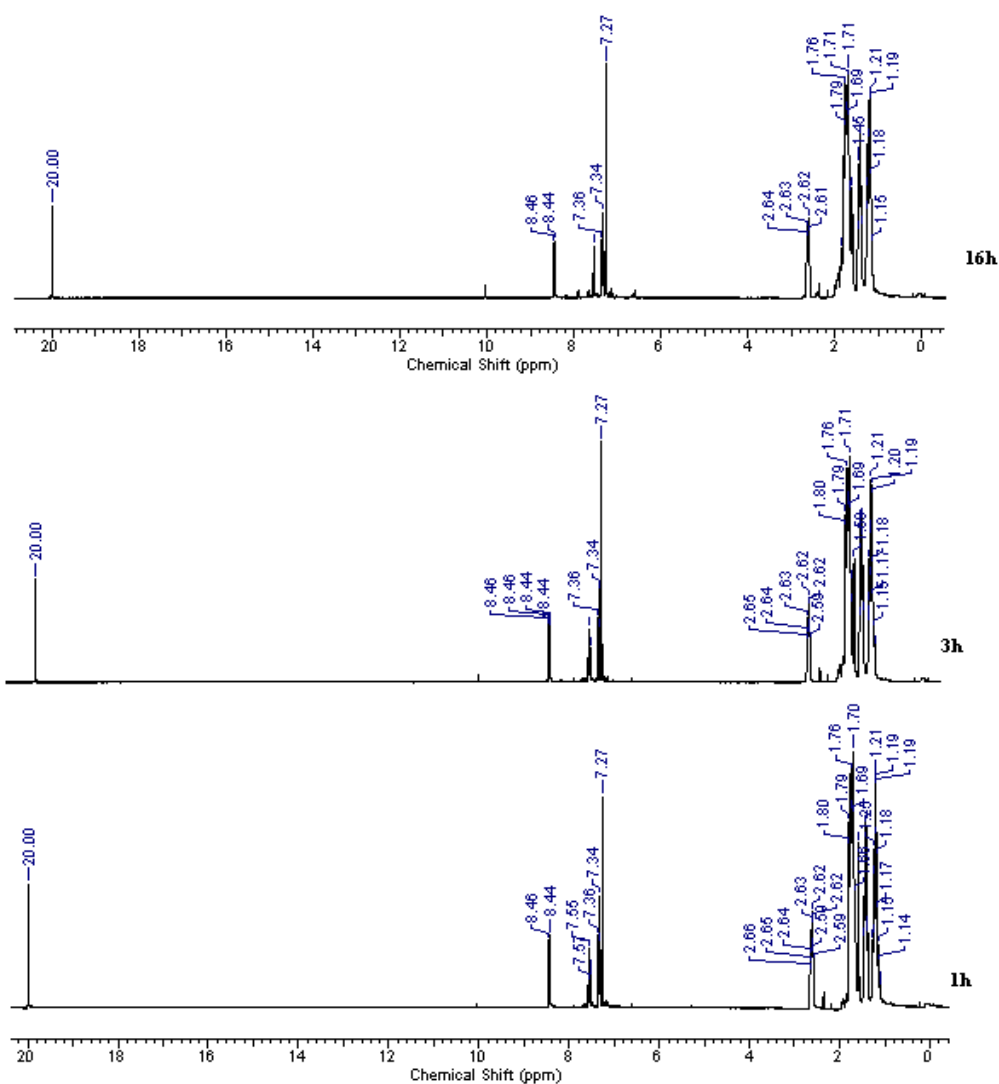


Figure 4.11 ^1H NMR (CDCl_3) spectra of the Grubbs G1 catalyst in solution within 16 hours.

The substantial decomposition of **C1** within an hour accounts for the **C1** concentration being depleted within a short period of time. A similar situation is observed for the *pyridine* modified Grubbs G1 catalyst (Figure 4.13). The difference between the pyridine modified and the 4-imino pyridine modified Grubbs G1 complexes is that the latter shows very little signs of the carbene protons after 16 hours whereas the former still shows no significant decomposition of the carbene peak. Another significant observation from monitoring of the Grubbs type complexes in solution was the indication of the formation of an aldehydic proton found around 10 ppm. In the case of **C1**, the aldehyde forms concurrently with the depletion of the carbene peak signal. Figure 4.12 shows the spectra while monitoring the stability of **C1**

in solution. Close examination of the spectra of **C1** in solution also reveals that not only does the carbene group seem to undergo hydrolysis but also the free imine signalled at 8.23 ppm. This is clearly seen by the growing aldehyde peak around 10.04 ppm. The instability of the Grubbs type complexes in solution has previously been reported to be due to hydrolysis of the carbene functionality as a result of small amounts of moisture in the reaction mixture [7]. The hydrolysis of the imine is believed to be metal-mediated because the ligand on its own in solution does not show any signs of hydrolysis even over extended periods. Even for the *pyridine* modified Grubbs G1 complex, the hydrolysis of the carbene in solution is observed but the rate is much slower since the carbene signal does not disappear completely unlike the case for **C1**.

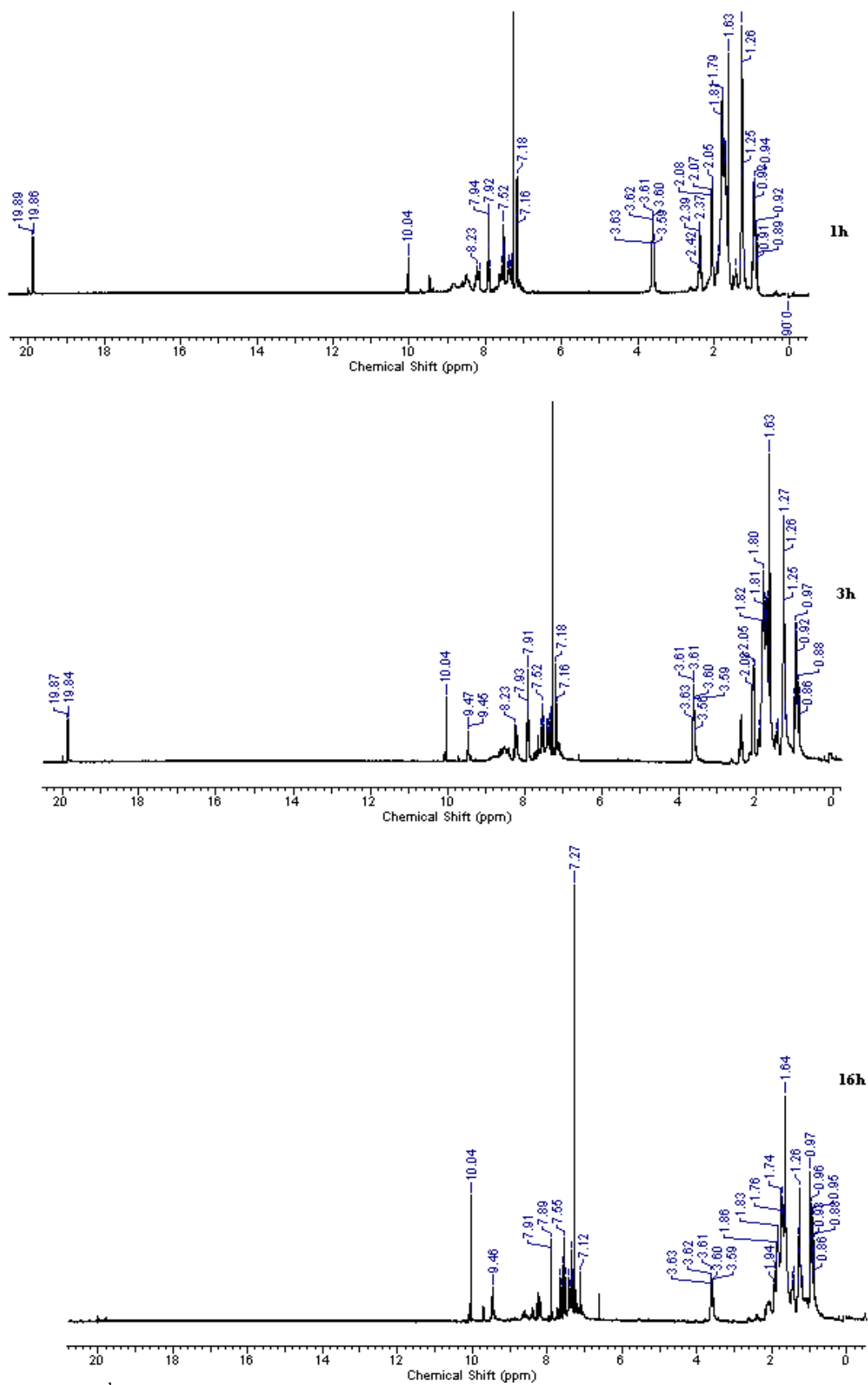


Figure 4.12 ^1H NMR (CDCl₃) spectra of C1 in solution for a maximum period of 16h.

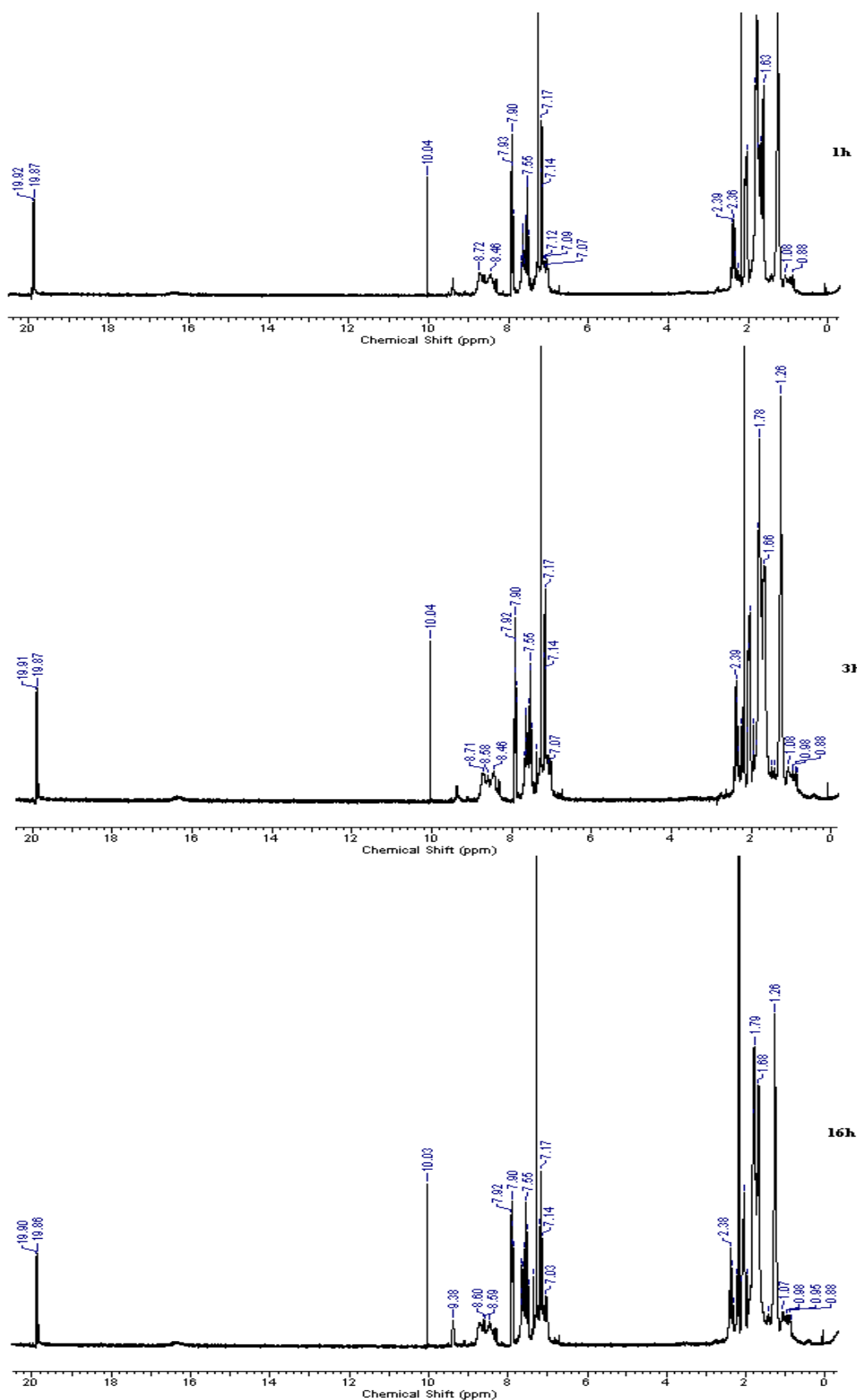
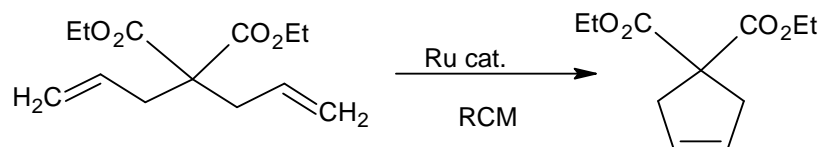


Figure 4.13 ^1H NMR (CDCl₃) spectra of the pyridine modified Grubbs G1 catalyst.

4.2.2 Ring-closing metathesis of diethyl diallylmalonate

The catalytic activity of complexes **C1** and **C5** in a different metathesis reaction was also investigated. The process involved ring-closing metathesis of diethyl diallylmalonate to form diethyl cyclopentene dicarboxylate, see Scheme 4.3. The reaction was monitored by ^1H NMR spectroscopy.



Scheme 4.3 Ring-closing metathesis of diethyl diallylmalonate catalyzed by a ruthenium carbene complex.

In the NMR experiments, we monitored the disappearance of the methylene proton in the starting material at δ 2.6 ppm and the olefinic protons at 5.1 ppm and 5.6 ppm together with concomitant growth of signals in the product around 3 ppm and 5.3 ppm. Indeed the expected changes were clearly seen from the ^1H NMR spectra, indicating the presence of both diethyl diallylmalonate and 3-cyclopentene-1,1-dicarboxylic acid, 1-diethyl ester. Figures 4.14 and 4.15 clearly show the methylene protons of diethyl diallylmalonate at 2.51 ppm, 4.96 and 5.5 ppm as well as those of diethyl cyclopentene dicarboxylate resonating at 5.37 ppm and 2.99 ppm in both **C1** and **C5** catalysed reactions. The spectra shown are that of the reaction mixture immediately after the addition of the substrate. This further proves the highly active nature of both **C1** and **C5** in ring closing metathesis. We also observed that allowing the reaction for longer periods, until a maximum of 16 h showed growth of the product peak. However only a slight increase in product formation is observed over longer times with both systems appearing to reach steady state.

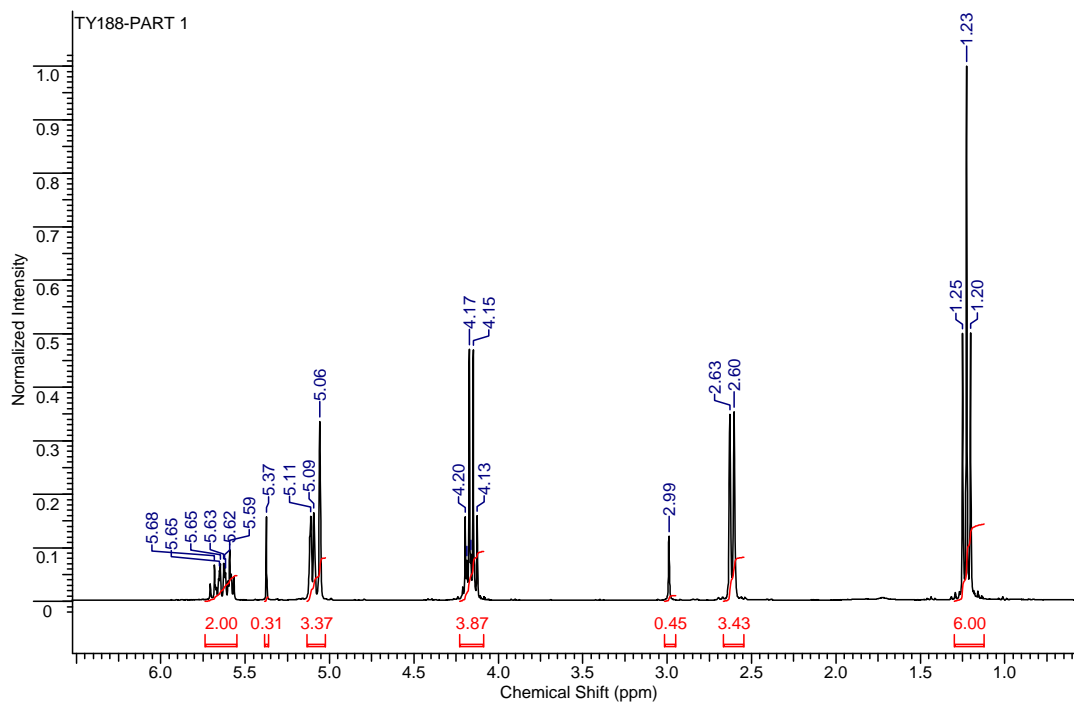


Figure 4.14 ^1H NMR spectrum (CDCl_3) immediately after the addition of substrate, catalyzed by **C1**.

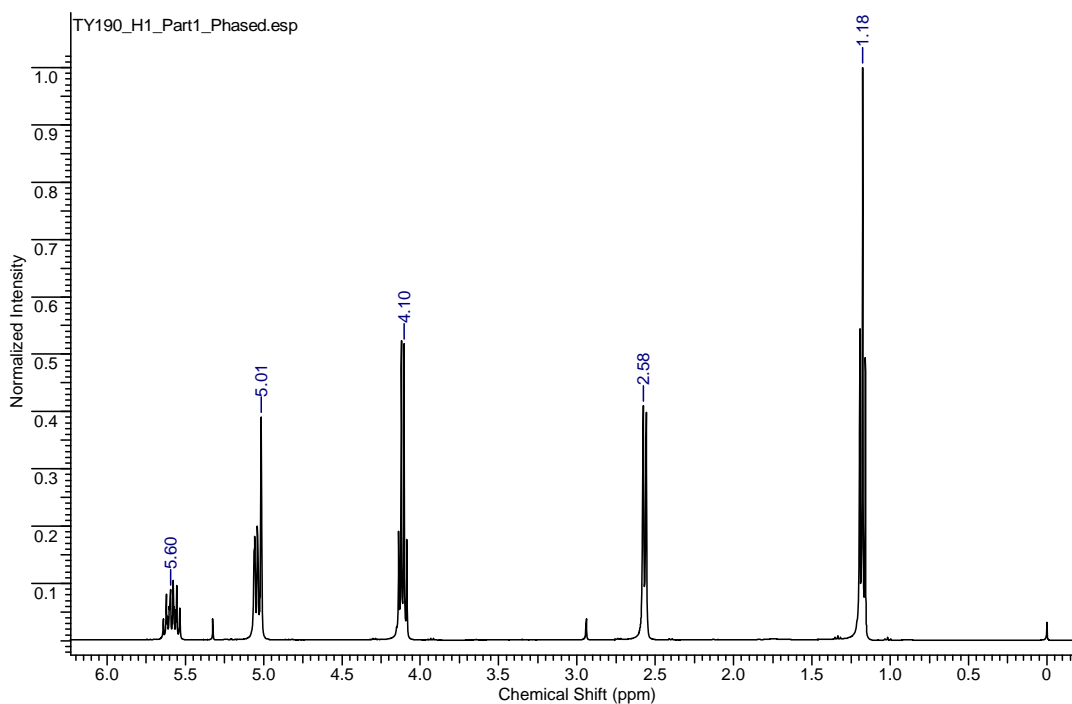


Figure 4.15 ^1H NMR spectrum (CDCl_3) immediately after the addition of substrate, catalyzed by **C5**.

Figure 4.16 and 4.17 depicts the reactions catalysed by **C1** and **C5** respectively for several hours. An NMR study for ring closing metathesis of diethyl diallylmalonate using *pyridine* modified Grubbs G1 type complexes has been reported [1].

In our hands the catalytic behaviour of the pyridyl modified Grubbs type complexes seem to follow the same trend regardless of the metathesis type of reaction. This is confirmed from the observation of a fast initiation step and then very slow progress of the reaction after catalysis has been initiated.

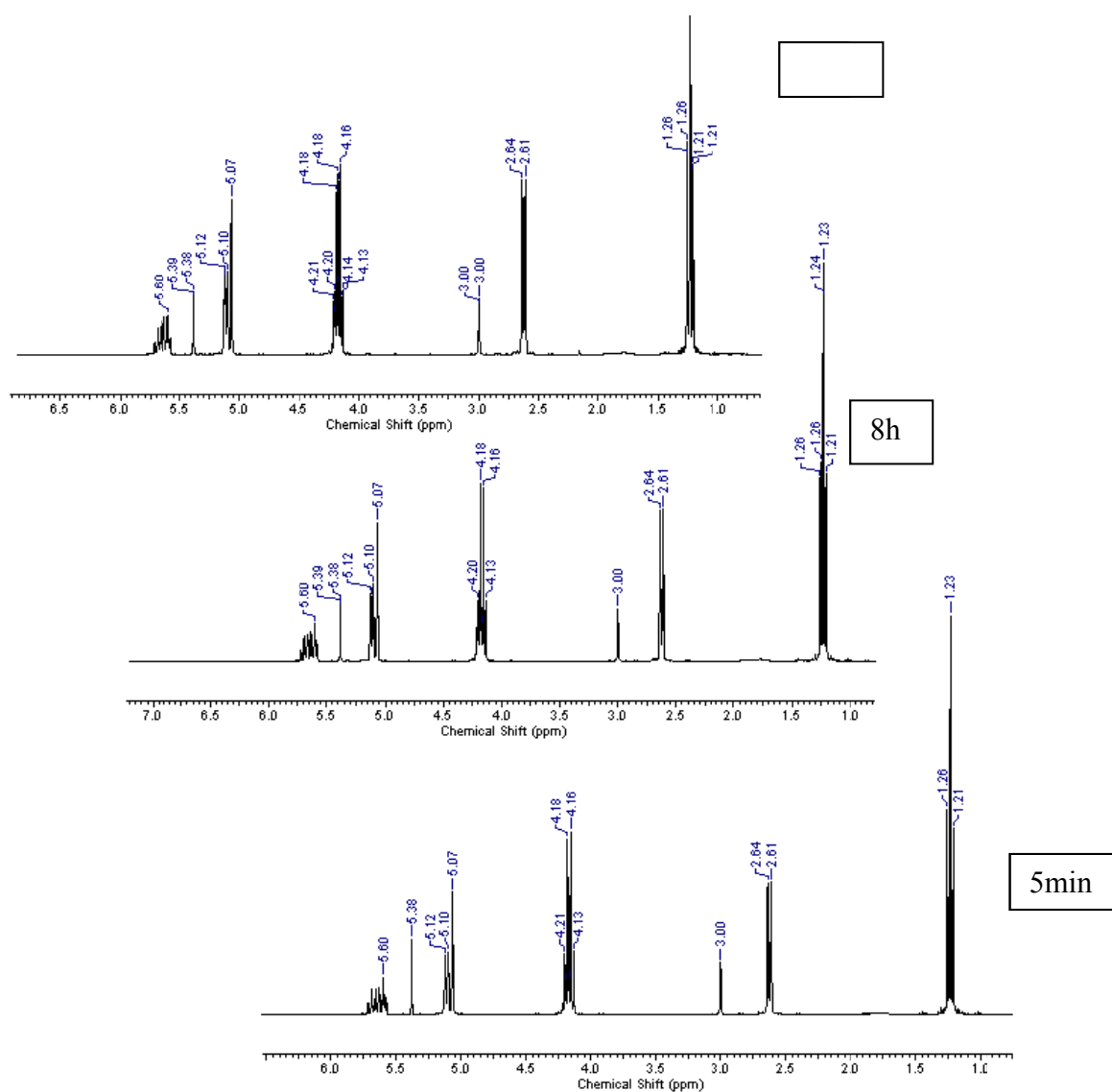


Figure 4.16 ^1H NMR spectra monitoring **C1** activity in RCM of diethyl diallylmalonate.

Figure 4.18 shows the amount of product formed within the presence of the substrate. The data is extracted from the ^1H NMR study of activity of **C1** and **C5**. Both complexes were found to be good initiators of the ring closing metathesis reaction. **C5** is however a better catalyst than **C1** in ring closing metathesis of diethyl diallylmalonate.

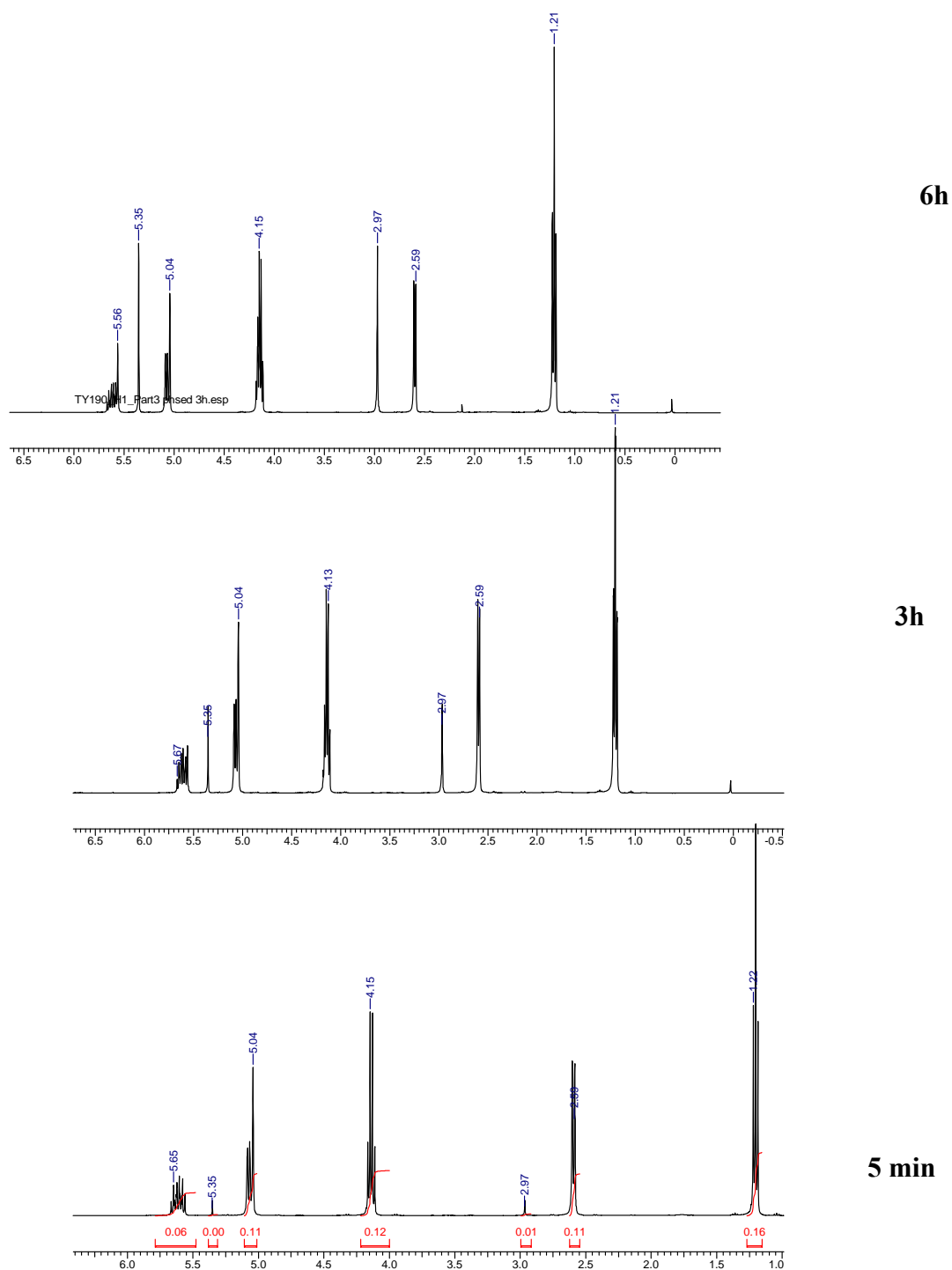


Figure 4.17 ^1H NMR spectra monitoring **C5** activity in RCM reaction of diethyl diallylmalonate.

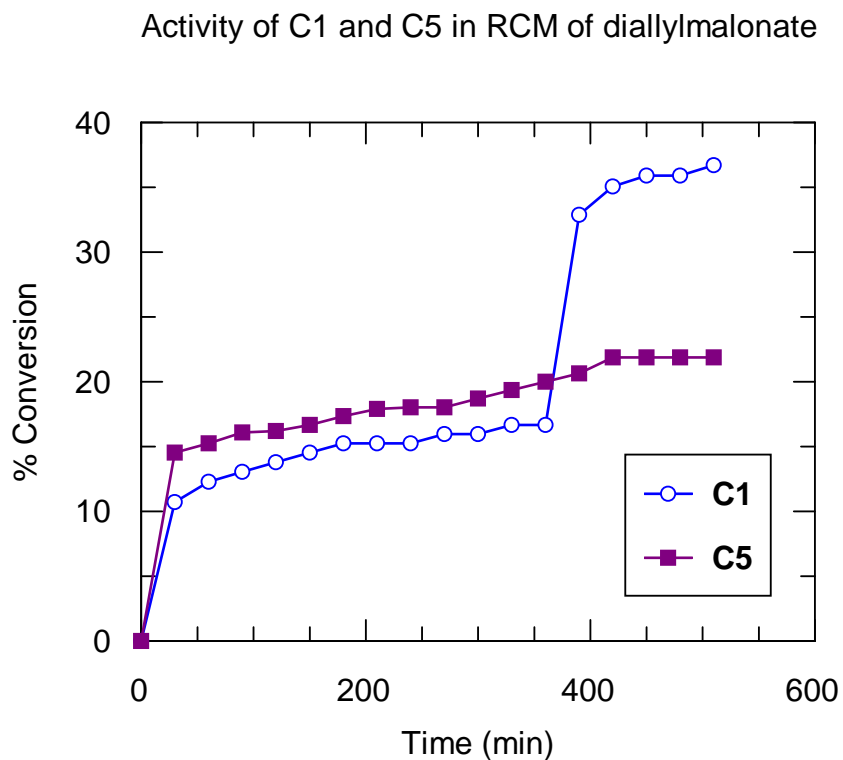


Figure 4.18 A graph showing the relative formation of the product in the RCM reaction mixture over time.

Due to low solubility of dendritic complexes in the NMR solvents these could not be monitored by NMR. However reactions were carried out using a suspension of the catalyst. We opted to use **C3** as the model for the dendritic complexes and set-up a reaction to test its catalytic behaviour in ring closing metathesis of diethyldiallyl malonate. The reaction was set-up using Schlenk techniques. The reaction was done under ambient conditions for 16h and dichloromethane was used as the solvent. After work-up, the product was isolated as a red-brown oil which was analysed by ^1H NMR. Figure 4.19 shows the ^1H NMR spectrum of the isolated product. What is evident is that only a small amount of the substrate had been converted.

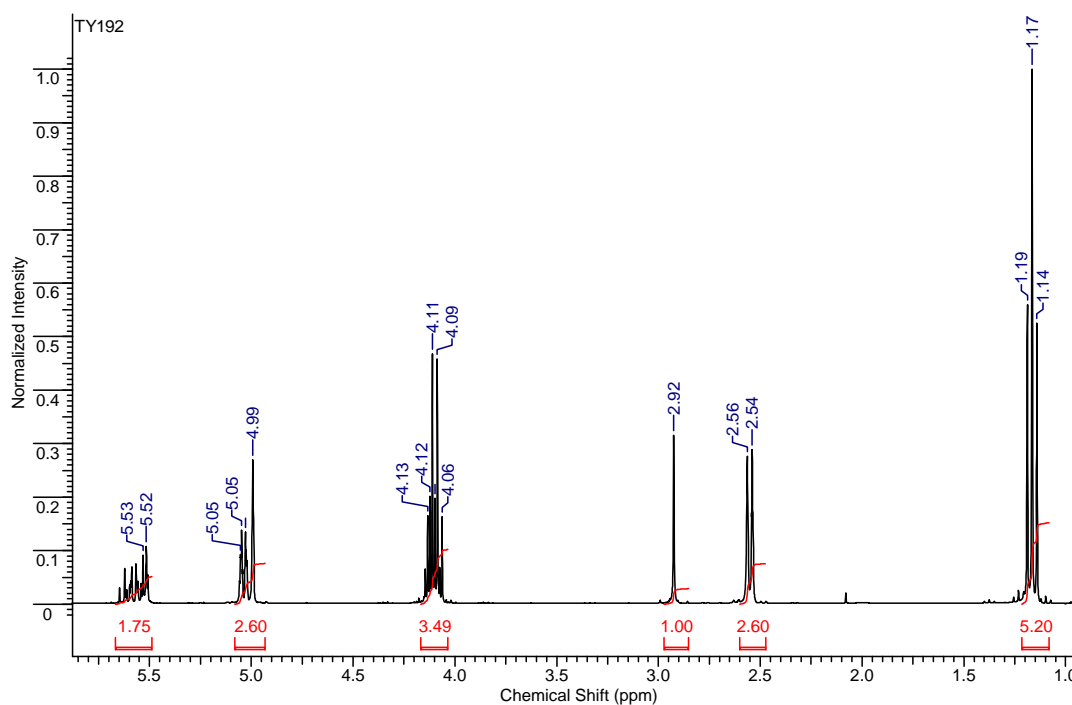
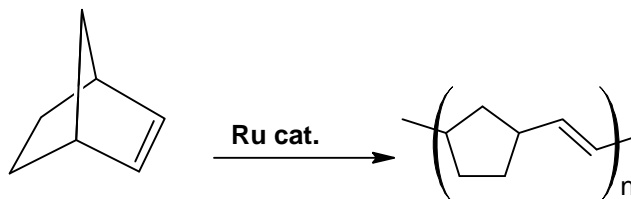


Figure 4.19 ^1H NMR spectrum of the product formed from the reaction catalysed by **C3**.

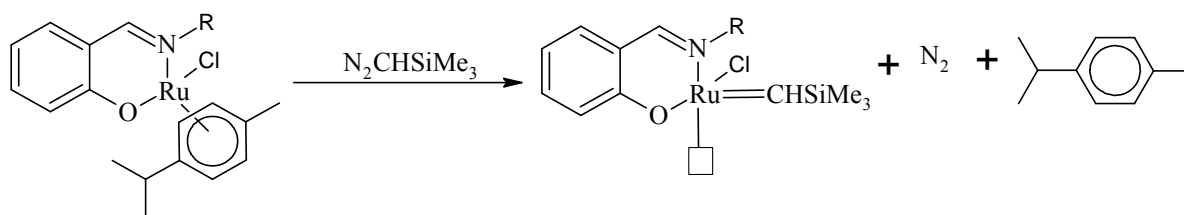
4.4 Ring-opening metathesis polymerization of norbornene

Some of the complexes prepared were also tested in ROMP of norbornene. In particular the *p*-cymene complexes. These type of complexes have been found to be precursors for active ROMP catalysts which are normally generated in situ. The method used here is similar to the process reported by Verpoort and co-workers [8]. It involves the use of co-catalysts which promote the formation of the active metal carbene. The complexes which were tested for ROMP are the mononuclear complex, **C10** as well as the dendritic analogues **C11** and **C12** shown in Figure 4.20. The activator or co-catalyst used was trimethylsilyldiazomethane (TMSD).



Scheme 4.4 Typical ROMP reaction of norbornene to form polynorbornene.

In a typical ROMP experiment the metal content in all reactions were the same irrespective of the ruthenium complexes (**C10-12**) employed. 5 μmol of Ru was used whilst TMSD was employed using a range of TMSD: Ru ratios. The monomer to metal ratio was kept constant at 800:1. The first step is the reaction of the complex with TMSD for half an hour before addition of the monomer to allow for the formation of the active species. Scheme 4.5 shows a possible reaction for the formation of the active species. The reaction was carried out at 85°C.



Scheme 4.5 A possible mechanism for activation of *p*-cymene Ru salicylaldimine complexes in ROMP reactions.

The only complexes that were found to polymerize norbornene were **C10** and **C12**. In the case of **C10**, when using an activator to metal ratio of 50:1, the polymer forms with a yield of only 11%. At lower ratios, *i.e.* 2:1 or 10:1 activator to metal ratio, only traces of polymer was observed. The polymer was found to be soluble in chloroform, dichloromethane, tetrahydrofuran and chlorobenzene at room temperature. It was characterized using FT-IR, ^1H NMR and gel permeation chromatography (GPC). From all these techniques it was confirmed that polynorbornene had formed. In the IR spectrum, depicted in Figure 4.21, the typical signals of the polynorbornene were observed. These signals include the broad band around 2900cm^{-1} due to the C-H stretch, a band at 1700cm^{-1} , 1650cm^{-1} as well as bands at 964cm^{-1} and 732cm^{-1} which are C-H bending modes for *trans* and *cis* disubstituted C=C double bonds. These observations agree with several reports [9] that have examined polynorbornenes by means of FTIR. The ^1H NMR spectrum in Figure 4.22 clearly shows that the product is a mixture of *cis/trans* polynorbornene. The presence of the olefinic protons (=CH) found at 5.35 ppm (*trans*) and 5.22 ppm (*cis*) as well as the α -olefinic protons observed at 2.80 ppm

for a *cis* polymer and at 2.44 ppm for the *trans* polymer [10]. The GPC analysis revealed that the molecular weight is 1.83×10^5 and the molecular weight distribution is 4.05. These results are similar to that reported by Verpoort *et al.* [8]. He explained the broad polydispersities as being indicative of not well controlled polymerization as a result of backbiting and chain transfer reactions taking place.

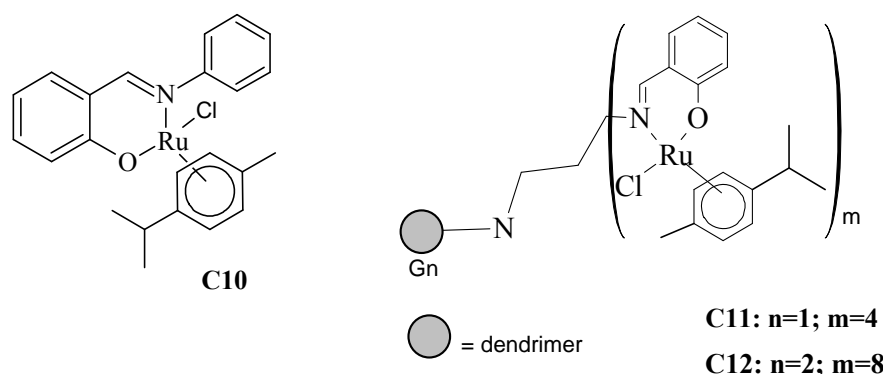


Figure 4.20 Complexes used in evaluating catalytic activity for ROMP, showing only one arm of the dendritic complexes.

In the case of the dendritic complexes **C11** and **C12**, up to 500:1 activator to metal ratios were used. In the case of **C11**, only traces of the product are observed at 500:1 ratio. At lower ratios no polymer formation was observed. **C12** polymer was formed in better yields than was found for the mononuclear complex **C10**. The activator ratio was ten times more for the dendrimer complex and the reaction was allowed to run overnight. The yield obtained was 37%. The polymer isolated from this reaction was also characterized by the same analytical techniques used for the product obtained from the mononuclear catalyst. Similar results were obtained using FTIR and ^1H NMR spectroscopy. GPC analysis showed a molecular weight distribution of 9.22 ($M_w=3.35 \times 10^5$) signalling that the process does not go *via* single site polymerization and that the polymerization is essentially uncontrolled. The molecular weight (M_w) was slightly higher than obtained for **C10**. The results obtained were in agreement with those for similar complexes used in ROMP of norbornene [7]. The molecular weight of the polynorbornene formed from the use of *p*-cymene salicylaldimine ruthenium complexes have

been reported to be around 10^5 Da. In the case of analogous mononuclear complexes that have been previously reported, the PDI is in the region of 3.

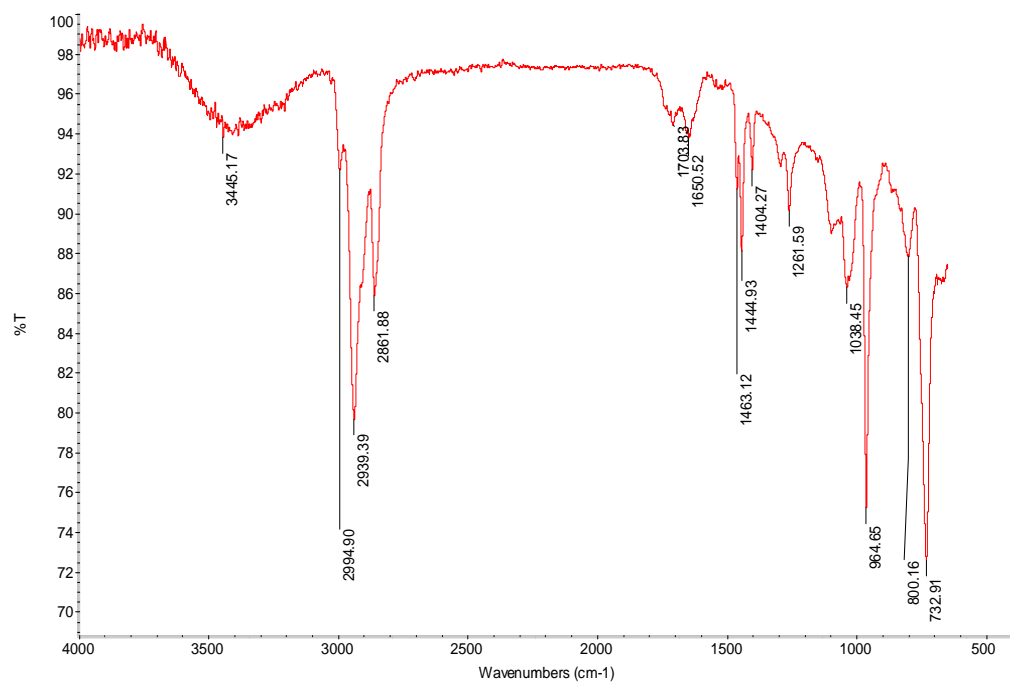


Figure 4.21 IR spectrum of polynorbornene, produced using Ru *p*-cymene catalysts.

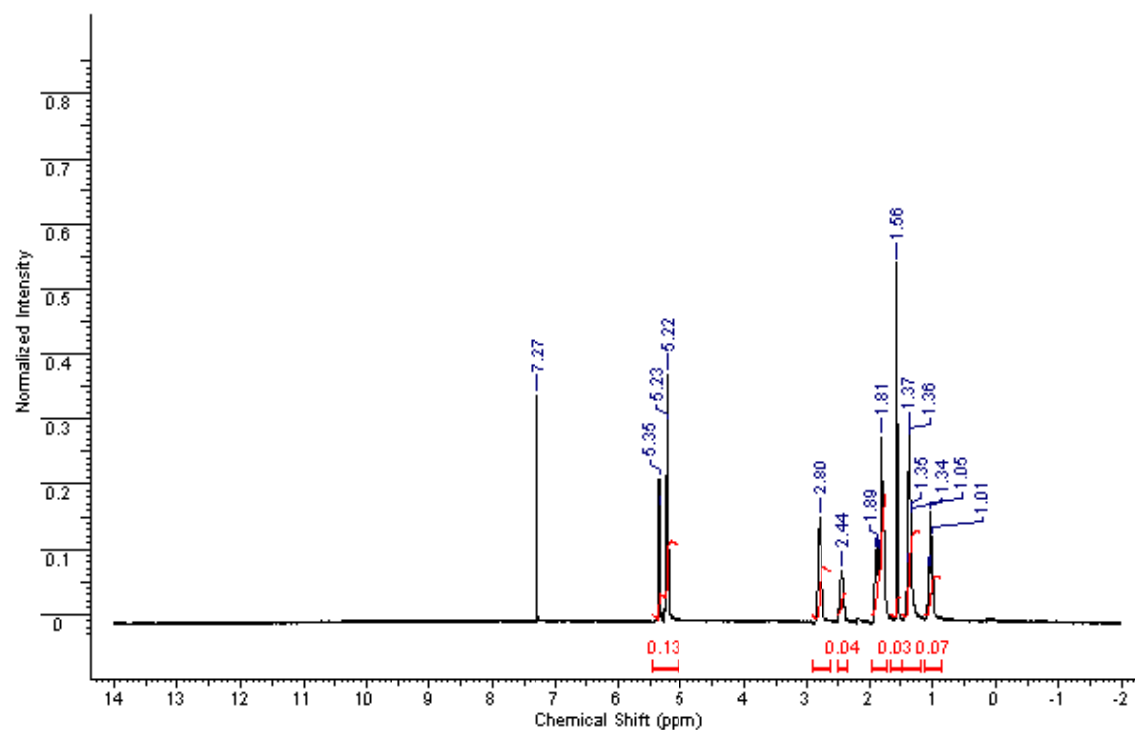


Figure 4.22 ¹H NMR spectrum of a polynorbornene sample.

4.3 Conclusion

Complexes **C1-C12** with the exception of **C9** were found to be catalytically active in olefin metathesis reactions. Even though preliminary testing showed **C1-C12** to be active, the drawback unfortunately was the low conversion of the substrates used under the reaction conditions employed.

In terms of stability, the Ru carbene complex **C1** was found to be the least stable in solution compared to the Grubbs G1 catalyst and the *pyridine* modified Grubbs G1 catalyst. ¹H NMR monitoring of the mononuclear complexes, **C1** and **C5** showed that regardless of the metathesis reaction they are tested in, they seem to follow the same trend of high initiation followed by rapid decomposition. In terms of the amount of the product formed relative to time as well as the conversion of substrates, **C1** seem to be a better catalyst in the self metathesis of 1-octene than **C5**.

C10 and **C12** showed activity in norbornene polymerization albeit at moderate rates. In addition, polymers obtained from these reactions are polydispersed. This is evident from the molar mass distribution which is far higher than the usually obtained for controlled polymerization.

4.4 Experimental

1-Octene, chlorobenzene, Grubbs G1 catalyst and Grubbs G2 catalysts were used without further purification. Norbornene was dried over calcium hydride before being distilled. A 5M norbornene stock solution in toluene was prepared. Toluene was dried by refluxing over sodium/benzophenone. Trimethylsilyldiazomethane (TMSD), a 2M solution in ethyl ether, was used without any further purification. All chemicals were obtained from Sigma Aldrich Ltd. The GC analyses were done using a Varian CP-3800 with a HP PONA column. GPC analysis was done on a GPC2006 using GPC-im-UV254-320 method. ¹H NMR spectra were

recorded on Varian 400MHz and 300MHz spectrometers. Infrared spectra were recorded on a Nicolet Avator 330 FTIR spectrophotometer using an ATR accessory.

General procedure in metathesis of 1-octene

1-octene (5ml, 0.0319 mol) was added to a Schlenk flask containing 7mg of the catalyst precursor. The reaction was carried out without the use of a solvent at room temperature. Aliquots of 1ml of the reaction mixture were sampled at different times for GC analysis. The internal standard used was chlorobenzene (0.05 ml) which was added after sampling from the reaction mixture.

¹H NMR study of C1 and C5 in metathesis of 1-octene.

A mass of 0.01g of Grubbs G1 catalyst, *pyridine* Grubbs G1 catalyst and **C1** were weighed in separate vial was of. The complexes were then dissolved in CDCl₃ and the solution transferred to a NMR tube. This was for testing stability of these complexes in solution. For catalysis reaction using **C1** and **C5**, (0.004g, 5μmol) of the complexes was dissolved in 0.75ml CDCl₃. A thousand equivalents of 1-octene (0.8ml, 5mmol) were then added. The reaction was monitored under ambient conditions.

¹H NMR study of C1 and C5 in metathesis of diethyl diallylmalonate.

A similar procedure was followed. For catalysis reaction using **C1** and **C5**, (0.004g, 5μmol) of the complexes was dissolved in 0.75ml CDCl₃. A thousand equivalents of the diethyl diallylmalonate (5M, 0.1ml) were then added.

General procedure in ROMP of norbornene

The reactions were run at 85°C using a parallel reactor. 5μmol of the catalyst was weighed into reaction tube, dissolved in 0.5ml of toluene followed by the addition of the activator. This

reaction mixture was allowed to stir for half an hour under nitrogen. After this time the 5M solution of the monomer in toluene (0.8ml) was then added. The reaction mixture was allowed to stir for a prescribed time. On completion of reaction, the solution is allowed to cool at room temperature. The reaction mixture was poured into methanol (50ml) and the polymer was allowed to precipitate out of the solution. The precipitate was filtered off and dried under vacuum.

4.5 References:

1. (a) Trnka, T. M.; Dias, E. L.; Day, M. W.; Grubbs, R. H., *ARKIVOC*, **2002**, *xiii*, 28.
(b) Clavier, H.; Petersen, J. L.; Nolan, S. P., *J. Organomet. Chem.*, **2006**, *691*, 5444.
2. Jordaan, M.; van Helden, P.; van Sittert, C. G. C. E.; Vosloo, H. C. M., *J. Mol. Catal. A: Chem.*, **2006**, *254*, 145.
3. (a) Scholl, M.; Trnka, T. M.; Morgan, J. P.; Grubbs, R. H., *Tetrahedron Lett.*, **1999**, *40*, 2247. (b) Huang, J.; Schanz, H.-J.; Stevens, E. D.; Nolan, S. P., *Organometallics*, **1999**, *18*, 5375. (c) Weskamp, T.; Kohl, F. J.; Hieringer, W.; Gleich, D.; Herrmann, W. A., *Angew. Chem. Int. Ed.*, **1999**, *38*, 2416. (d) Bielawski, C. W.; Grubbs, R. H., *Angew. Chem. Int. Ed.*, **2000**, *39*, 2903. (e) Sanford, M. S.; Love, J. A.; Grubbs, R. H., *Organometallics*, **2001**, *20*, 5314. (f) Conrad, J. C.; Yap, G. P. A.; Fogg, D. E., *Organometallics*, **2003**, *22*, 1986.
4. (a) Dinger, M. B.; Mol, J. C., *Adv. Synth. Catal.*, **2002**, *344*, 671. (b) Stark, A.; Ajam, M.; Green, M.; Raubenheimer, H. G.; Ranwell, A.; Ondruschka, B., *Adv. Synth. Catal.*, **2006**, *348*, 1934. (c) Jordaan, M.; Vosloo, H. C. M., *Adv. Synth. Catal.*, **2007**, *349*, 184.

-
5. (a) Astruc, D.; Hauzé, K.; Gatard, S.; Méry, D.; Nlate, S.; Plault, L., *Adv. Synth. Catal.*, **2005**, 347, 329. (b) Gatard, S.; Kahlal, S.; Méry, D.; Nlate, S.; Cloutet, E.; Saillard, J.-Y. Astruc, D., *Organometallics*, **2004**, 23, 1313.
 6. Buchowicz, W.; Mol, J. C., *J. Mol. Catal. A: Chem.*, **1999**, 97, 103.
 7. (a) Dinger, M.B.; Mol, J.C., *Organometallics*, **2003**, 22, 1089-1095. (b) Mieock, K.; Eum, M.; Jin, M. J.; Jun, K.; Lee, C. W.; Kucn, K. A.; Kim, C. H.; Chin, C. S., *Organometallics*, **2004**, 689, 3535.
 8. (a) De Clerq, B.; Verpoort, F., *J. Mol. Catal. A: Chem.*, **2002**, 180, 67. (b) Opstal, T.; Couchez, K.; Verpoort, F., *Adv. Synth. Catal.*, **2003**, 345, 393.
 9. (a) Brumaghim, J. L.; Girolami, G. S., *Organometallics*, **1999**, 18, 1923. (b) Meng, X.; Tang, G.-R.; Jin, G.-X., *Chem. Commun.*, **2008**, 3178.
 10. (a) Fitzgerald, R. P.; Rooney, A. D., *J. Mol. Catal. A: Chem.*, **2007**, 261, 24. (b) Düz, B.; Elbistan, C. K.; Ece, A.; Sevin, F., *Appl. Organometal. Chem.*, **2009**, 23, 359. (c) Galletti, A. M. R.; Pampaloni, G.; D'Alessio, A.; Patil, Y.; Renili, F.; Giaiacopi, S., *Macromol. Rapid Commun.*, **2009**, 30, 1762.

CHAPTER 5
SUMMARY AND FUTURE WORK

CONTENT

5.1 Summary	151
5.2 Future Work	152

5.1 Summary

The thesis covers synthesis and application of the novel ruthenium carbene complexes in olefin metathesis reactions. The first chapter reviews the development of ruthenium carbene complexes and the wide application of these complexes as olefin metathesis catalysts. The Grubbs type catalysts have been elaborated in attempts to enhance their application. This has resulted in joint ventures of both academics and industrialists to embark on studying and applying these catalytic systems.

Chapter one highlights the achievements reported thus far and highlights further potential for application of these complexes. Due to the fact that the ligand environment of Grubbs catalysts plays a significant role in terms of their applications, we set out to focus on this aspect. We opted to first synthesize ligands that could be used in modifying Grubbs generation 1 and 2 catalysts. Chapter 2 covers the synthesis and characterization of both monofunctional and dendritic ligands of the salicylaldimine type and 4-imino-pyridine type. The purity of these ligands was confirmed by a series of analytical techniques that include ^1H and ^{13}C NMR as well as FTIR spectroscopy, mass spectrometry (ESI and MALDI-TOF) and elemental analysis. These ligands were subsequently complexed to Grubbs G1 and G2.

Chapter 3 gives a detailed procedure followed in synthesizing 4-imino pyridine modified Grubbs G1 and Grubbs G2 complexes. These include both monofunctional and dendritic complexes. In addition salicylaldimine *p*-cymene ruthenium chloride complexes were also prepared. The formulation and purity of these complexes were confirmed by elemental analysis and by similar techniques employed for the ligands. Some of the metal complexes were also studied by thermal gravimetric analysis.

The complexes were tested in various olefin metathesis reactions. These reactions include cross metathesis of 1-octene using **C1-C8** complexes. Reactions were monitored by ^1H NMR and gas chromatography. The results showed that high overall activity is achieved by unmodified Grubbs G1 and G2. The complexes **C1-C8** showed moderate activity. Another catalytic reaction studied was ring closing metathesis of diethyl diallylmalonate. Only the mononuclear complexes **C1** and **C5** were tested and monitored by ^1H NMR spectroscopy. Data from ^1H NMR studies together with GC analysis revealed that complexes **C1** and **C5** initiate catalysis fast but also reach equilibrium quite rapidly. The last catalytic studies involved the use of *p*-cymene salicylaldimine ruthenium complexes (**C10-C12**) in ring opening polymerization. The active ruthenium carbene species was generated *in-situ* before the addition of norbornene. Polynorbonenes formed were characterized using ^1H NMR, FTIR and GPC techniques. The polymers were found to be polydispersed indicating that the polymerization process lacked control.

5.2 Future Work

The instability of the 4-imino pyridine Grubbs type complexes in solution proved to be the limiting factor in the application of these complexes. This suggests that the first challenge is to get a less labile ligand in order to make the catalyst less susceptible to decomposition. Seeing that the imine in the 4-position does not take part in complexation, it could be modified to alter electronic and steric properties of the system. This would allow us to study the impact of these changes on the catalytic performance. Another modification could be the reduction of the imine to a secondary amine. This should prevent ligand break down due to hydrolysis.

It does not seem to be advantageous to anchor Grubbs G1 and G2 catalysts on dendrimers in terms of activity of the catalysts especially on a higher generation dendrimers but this needs further exploration as other reports using different dendrimer rather than the PPI dendrimers have reported good activity.

In terms of catalysis, more work needs to be done as we have only reported preliminary work. The effect brought about by temperature changes was not explored. Different catalysts to substrate ratios were also not explored entirely and use of solvents or additives were not tested. This also leaves a range of catalytic condition that could be explored using the synthesized complexes.